Spatial Spectral Efficiency Analysis for Wireless Communications

by

Lei Zhang
B. Eng., Shandong University, 2005
M. Sc., Nanjing University of Posts and Telecommunications, 2008

A Dissertation Submitted in Partial Fulfillment of the
Requirements for the Degree of

DOCTOR OF PHILOSOPHY

in the Department of Electrical and Computer Engineering

© Lei Zhang, 2014
University of Victoria

All rights reserved. This dissertation may not be reproduced in whole or in part, by photocopying or other means, without the permission of the author.

Spatial Spectral Efficiency Analysis for Wireless Communications

by

Lei Zhang
B. Eng., Shandong University, 2005
M. Sc., Nanjing University of Posts and Telecommunications, 2008

Supervisory Committee

Dr. Hong-Chuan Yang, Supervisor
(Department of Electrical and Computer Engineering, University of Victoria)

Dr. Mazen O. Hasna, Co-supervisor
(Department of Electrical and Computer Engineering, University of Victoria)

Dr. Xiaodai Dong, Academic Unit Member
(Department of Electrical and Computer Engineering, University of Victoria)

Dr. Jianping Pan, UVic Non-unit Member
(Department of Computer Science, University of Victoria)

Supervisory Committee

Dr. Hong-Chuan Yang, Supervisor
(Department of Electrical and Computer Engineering, University of Victoria)

Dr. Mazen O. Hasna, Co-supervisor
(Department of Electrical and Computer Engineering, University of Victoria)

Dr. Xiaodai Dong, Academic Unit Member
(Department of Electrical and Computer Engineering, University of Victoria)

Dr. Jianping Pan, UVic Non-unit Member
(Department of Computer Science, University of Victoria)

ABSTRACT

Spectrum utilization efficiency is one of the primary concerns in the design of future wireless communication systems. Most performance metrics for wireless communication systems focus on either link level capacity or network throughput while ignore the spatial property of wireless transmissions. In this dissertation, we focus on the spatial spectral utilization efficiency of wireless transmissions. We first study the spatial spectral efficiency of single-cell and multi-cell wireless relay systems using area spectral efficiency (ASE) performance metric. We then generalize the performance metric, termed as generalized area spectral efficiency (GASE), to measure the spatial spectral utilization efficiency of arbitrary wireless transmissions. In particular, we first introduce the definition of GASE by illustrating its evaluation for conventional point-to-point transmission. Then we extend the analysis to four different transmission scenarios, namely dual-hop relay transmission, three-node cooperative relay transmission, two-user X channels, and underlay cognitive radio transmission. Finally, we apply the GASE performance metric to investigate the spatial spectral

efficiency of wireless network with Poisson distributed nodes and quantify the spatial spectral opportunities that could be explored with secondary cognitive systems. Our research on the spatial spectral utilization efficiency provides a new perspective on the designing of wireless communication systems, especially on the transmission power optimization and space-spectrum resource exploitation.

Contents

List of Tables

List of Figures

ACKNOWLEDGEMENTS

My deepest gratitude goes first and foremost to Prof. Hong-Chuan Yang, my supervisor, for his professional academic supervision and constant encouragement. Without his consistent and illuminating instructions, I could not have finished this dissertation.

Second, I would like to express my deepest gratitude to Prof. Mazen O. Hasna, my co-supervisor, who inspired me on this research topic during my visiting to Qatar University.

Last but not the least, I should thank Qatar Telecom and NSERC for their financial support on my Ph. D. program.

Chapter 1

Introduction

Current and future wireless communication systems are carrying more and more traffics to satisfy the growing demands for wireless data services. However, the radio spectrum available for wireless communication is extremely scarce and strictly regulated. Therefore, spectrum utilization efficiency is one of the primary concerns in the design of future wireless communication systems. Previously, most performance metrics focus on either link level capacity or network throughput. Seldom do they consider the spatial property of wireless transmissions. In my dissertation, we study the spatial spectral efficiency of various scenarios.

1.1 Cellular Networks

In Chapter 2 and Chapter 3, we investigate the spatial spectral utilization efficiency of single-cell and multi-cell wireless relay systems and provide their accurate quantifications. Recent researches show that relay transmission is a cost and power efficient approach to increase the spectral efficiency of cellular systems for high data rate services [1–3]. Various emerging wireless standards are incorporating relay transmissions into network-level design by introducing infrastructure relay stations (RSs) [4]. For example, IEEE 802.16j Task Group is developing new standards with infrastructure relaying capacity integrating into IEEE 802.16 systems. Another example is the wireless media system (WMS), which is a new wireless network architecture using infrastructure relays to improve cell-edge or shadowed area coverage [2]. The infrastructure RSs can usually be installed to enjoy favorable, likely line of sight (LoS), connections with BS, which greatly reduces their installation and maintenance cost.

Previous works have shown that relay transmission can achieve higher spectral efficiency than direct transmission only if the direct source to destination link experiences much poorer fading condition than the relay links [5]. The capacity and spectral efficiency of relay enhanced and conventional systems are compared in [6] for different cell topologies through simulation study. These results have, as such, generated considerable interest in opportunistic relaying systems [7]. In general, relay transmissions are carried out in two steps, i.e. i) source to relay step and ii) relay to destination step, because of the half-duplexing constraint [8]. Both steps will require appropriate time/spectral resource allocation, which leads to a certain penalty to the overall link spectral efficiency. We would like to note, however, previous analysis of relay transmission focused on the end-to-end spectral efficiency and neglected the fact that the two steps of relay transmission will affect much smaller areas than direct one-hop transmission. Specifically, the source to relay transmission needs only to reach the RSs, instead of the cell-edge users. In addition, RSs are used to cover a small near-cell-edge area. The smaller affected areas (or "spatial footprint") of relay transmissions can be exploited to achieve more efficient spectrum reuse and higher overall spectral efficiency. Specifically, the same spectrum can be used for other transmission outside the affected area using appropriate technologies, such as dynamic spectrum allocation and cognitive radios [9].

However, these research focused on either capacity increase or link reliability, seldom did they consider the actual smaller "footprint" of relay transmissions. As such, the important spatial property of relay transmission was ignored. To combat this deficiency, we adopt the performance metric of area spectral efficiency (ASE) in the analysis of infrastructure relay enhanced cellular networks. ASE performance metric was introduced in [10] to quantify the spectrum utilization efficiency of cellular wireless systems. In cellular systems, the radio spectrum is systematically reused at different geometrical areas, i.e. co-channel cells [11]. Specifically, the co-channel cells will be separated by a minimum reuse distance of D such that their transmission will not seriously interfere with one another. As such, the same spectrum will be used only once over an area of the size of $\pi D^2/4$. The ASE of cellular systems was therefore defined as the maximum data rate per unit bandwidth of an user randomly located in cell coverage area, over the area of $\pi D^2/4$, with unit being $bps/(Hz \cdot m^2)$. This performance metric captures the tradeoff between spectral efficiency and reuse distance in cellular systems. Note that the regular frequency reuse based on typical hexagon cell structure greatly facilitates the ASE analysis [5, 12]. Recently, the ASE

metric was intensively applied to characterizing the performance of two-tier heterogeneous cellular networks. In [13], the authors investigated the ASE of the hierarchical cell structure (HCS) networks consisting of macrocell and local area cell with partial cochannel sharing. Besides, more researches were carried out on conventional cellular networks overlaid with shorter range femtocell hotspots. Chandrasekhar et. al. proposed and analyzed an optimum decentralized spectrum allocation policy of such network with respect to ASE [14]. Moreover, they presented a comprehensive dynamic system level simulation based on 3GPP Long Term Evolution (LTE) standard for heterogeneous cellular networks and showed that the two access schemes, namely, open access picocells and closed access femtocells, have different impacts on the system ASE [15]. In [16], the authors proposed several distributed opportunistic medium access control policies for femtocell-overlaid cellular networks and analyzed their performance in terms of ASE. Furthermore, ASE was jointly analyzed with area power consumption (APC) from a green communication perspective. In [17], the authors developed a deployment and operation algorithm for hierarchical cell structure to minimize the total energy consumption while satisfying the requirement of ASE. In [18], the authors carried out a comprehensive analysis for APC and ASE of green communication system. Through simulation, Arshad et. al. investigated the optimum deployment strategy in terms of APC given a target ASE [19]. In [20], the authors analyzed the tradeoff between ASE and APC in heterogeneous networks which offload the high QoS users through femtocells. In these papers, ASE was calculated by using either the cell area covered by the macro BS or using the intensity of the femtocells in a unit area according to a certain distribution, Therefore, the actual small "spatial footprint" of relay transmissions had not been analytically quantified.

Motivated by these observations, we first derive the analytical expression of ASE for the downlink transmission of a single-cell wireless system with infrastructure RSs. Then we analyze the downlink ASE performance of relay enhanced cellular systems in presence of the co-channel interference over Rayleigh fading environment.

1.2 Wireless Transmissions

In Chapter 4, we generalize the ASE metric and develop a new performance metric to evaluate the spatial spectral efficiency of arbitrary wireless transmissions. It is well known that wireless transmissions generate electromagnetic pollution to the surrounding environment over its operating spectrum. The size of the polluted area

depends on the transmitting power, the radiation pattern of transmit antenna, propagation environment, and etc. In general, if a particular frequency band is heavily "polluted", i.e., a significant level of transmitted signal power is observed, over a certain area, simultaneous transmission over the same frequency band in the area may suffer from high interference level. Neighboring transceiver can function properly only when enjoying high signal to interference ratio (SIR) or equipped with effective interference mitigation capability. As such, an alternative design goal for future green wireless systems is to *achieve high-data-rate transmissions with minimum electromagnetic pollution in both spectral and spatial dimensions*. To compare the effectiveness of different wireless transmission schemes in approaching such goals, we need a performance metric that can take into account this spatial effect of radio transmissions in the evaluation of transmission efficiency.

Most conventional performance metrics for wireless transmissions focus on the quantification of either spectrum utilization efficiency or link reliability. In particular, ergodic capacity and average spectrum efficiency evaluate the spectral efficiency of wireless links, where the former serves as the upper bound of achievable average spectrum efficiency [11]. The link reliability is usually quantified in terms of outage probability, average error rate, and average packet loss rate [21,22]. On another front, various energy efficiency metrics have been developed and investigated, mainly at the component and equipment level [23]. In the system/network level, ETSI defined energy efficiency metric as the ratio of coverage area over the power consumption at the base station. Recently, area power consumption (W/Km^2) is introduced and used to optimize base station deployment strategies for cellular network in [24]. Note that most energy efficiency metrics can not be readily related to the link spectral efficiency or reliability, as they often conflict with each other. For example, a general tradeoff framework between energy efficiency and spectral efficiency for OFDMA systems was built to characterize their relationship in [25]. Bit per Joule (bit/J), defined as the ratio of achievable rate over the power consumption, is a widely used performance metric to quantify the energy utilization efficiency of emerging wireless systems [26]. Recently, this performance metric is applied to the analysis of CoMP cellular systems as well as heterogeneous networks [27, 28]. Still, Bit per Joule metric does not take into account the spatial effect of wireless transmissions and is mainly applicable to cellular networks.

In Chapter 2 and Chapter 3, we analyzed the spatial spectral efficiency of cellular networks with relays using the ASE performance metric. Note that the area used in

ASE definition is either the individual cell radius in a single cell scenario or the reuse distance in cellular networks, not related to the properties of target radio transmissions. The effect of actual "footprint" of wireless transmission was not considered. Therefore, the application of ASE metric was still limited to infrastructure based cellular systems. In this chapter, we develop a new performance metric, termed as generalized area spectral efficiency (GASE), to evaluate the actual "footprint" of arbitrary wireless transmission. GASE is defined as the ratio of overall effective ergodic capacity of the transmission link under consideration over the affected area of the transmission. The *affected area* is defined as the area where a significant amount of transmission power is observed and parallel transmissions over the same frequency will suffer high interference level. The affected area characterizes the negative effect of radio transmission in terms of electromagnetic pollution while transmitting information to target receivers. Note that any wireless transmission will generate interference to neighboring transceivers if they operate over the same frequency band. We use affected area to quantify such spatial effect of wireless transmissions. The affected area is directly related to the properties of target transmission and makes the GASE metric applicable to arbitrary transmissions. Note that the size of the affected area depends on various factors, including transmission power, propagation environment, as well as antenna radiation patterns. In particular, the average radius of the affected area will be proportional to the transmission power. Therefore, GASE also characterizes the transmission power utilization efficiency in achieving per unit bandwidth throughput and, as such, serves as a suitable quantitative metric for measuring the greenness of wireless communication systems.

1.3 Randomly Distributed Wireless Network

In Chapter 5, we study the spatial spectral efficiency of wireless networks with Poisson distributed nodes using the GASE performance metric. With the development of wireless communication technology, a variety of wireless network models are emerging, such as ad hoc network, wireless sensor network, cognitive network, and etc. Those networks are usually confined in a specific geometrical area with dense node distribution. Nodes in the network typically share the same spectrum bandwidth without centralized coordination, and thus generate interference to each other. Therefore, spatial property and node intensity are essential to the system performance. In chapter 4, we use GASE to evaluate the spectral efficiency as well as spatial utilization

efficiency of arbitrary wireless transmissions. We then extend the analysis to the network scenario. In particular, we take into account the mutual co-channel interference among the nodes that randomly distributed in the network. We also consider the impact of node intensity as well as node coordination schemes on the system GASE performance.

In wireless networks, a collection of nodes share the same spectrum bandwidth to increase the system spectrum utilization efficiency. From conventional point of view, the side effect of this approach is severe co-channel interference, which may deteriorate the system performance. Therefore, knowledge of interference statistics is essential to the performance analysis of wireless networks. In particular, the statistics of co-channel interference in wireless networks are affected by the following essential physical parameters, namely: (1) spatial distribution of interferers; (2) propagation characteristics of the medium, including path loss, shadowing and fading; (3) spatial region over which the interferers are distributed. Specifically, if no knowledge regarding to node locations is available a priori, a typical assumption is that the nodes are distributed according to a homogeneous Poisson point process [29, 30]. Intensive research has been carried out on the application of Poisson point process to wireless networks, including network connectivity and coverage [31–34], packet throughput [35], error probability and link capacity [36, 37]. If we further assume individual interference power follows a distance-dependent decaying power law, then the aggregate interference at the receiver can be modeled as shot noise [38] associated with a particular Poisson point process. In [36], it showed that the shot noise interference from a homogeneous Poisson field of interferers distributed over the entire space can be modeled using the symmetric α-stable distribution. Following this work, α-stable distribution has been extensively applied to characterizing the interference in wireless networks [39–43]. The interference statistics are given by their moment generating function (MGF). However, due to the complexities of these MGF expressions, no closed-form PDF and cumulative distribution function (CDF) were given except for several special cases, limiting the usage of the interference statistics in the derivation. In this dissertation, we further develop these results and apply them into the GASE analysis.

We also consider the impact of node coordination on system GASE performance. First, we consider a more practical wireless network in which carrier sense multiple access with collision avoidance (CSMA/CA) mechanism is employed. In CSMA/CA network, two close nodes are prohibited to transmit simultaneously, and thus ensures

a minimum distance between each active transmitter. In this scenario, we introduce Matèrn point process [44] to model the spatial distribution of transmitter-receiver pairs in CSMA/CA networks. Matèrn point process is established from its underlying Poisson point process by dependent thinning operations, which retains certain points of a Poisson point process in such a way that the distance of any pairs of points are always greater than a threshold. The statistics we derived in Poisson field is still valid by imposing a guard zone around the transmitter. However, special treatment should be exercised on the calculation of the affected area. Through mathematical analysis and numerical examples, we compare the performance, in terms of ergodic capacity, affected area, and GASE of wireless ad hoc networks with and without implementing CSMA/CA mechanism.

Finally, we analyze the GASE of a two-tier cognitive network. Cognitive radio is used as a promising technology to improve the spectrum utilization by allowing the unlicensed (secondary) user share a frequency bandwidth with the licensed (primary) owner under the condition that no harmful interference is caused to the licensee [45]. Typically, there are three main cognitive radio schemes [46]: interweave, overlay and underlay. With interweave scheme, cognitive users opportunistically exploit the primary radio spectrum only when primary users are detected to be idle. In overlay scheme, cognitive users help maintain and/or improve primary users' communication while utilizing some spectrum resources for their own communication needs [47]. The underlay scheme allows cognitive users share the frequency bandwidth of primary users only if the resultant interference power level at the primary receiver is below a given threshold [48, 49]. These schemes either explore the time-spectrum hole or use sophisticated techniques to protect the primary network. In this dissertation, we propose a new scheme from the spatial spectrum hole perspective. In particular, primary network first establishes its primary affected area. Secondary nodes can transmit only if they are outside the primary affected area. This scheme allows the secondary network fully explore the spatial spectrum resource in the primary network, but it also increases the interference level of the entire network. Through numerical examples, we show the effect of secondary cognitive users on the total ergodic capacity and affected area, the tradeoff of which is best characterized by the GASE metric.

1.4 Propagation Channel Model

In this dissertation, we assume all the transmitters are equipped with omni-directional antennas and share the same frequency bandwidth. Each transmitter communicates with one and only one receiver. The transmitted signal will experience path loss and multipath fading effect. For the sake of clarity, we ignore the shadowing effect. Specifically, the received signal power P_r at distance d from a transmitter is given by $P_r = \frac{P_t \cdot Z}{(d/d_{\text{ref}})^a}$, where P_t is the common transmission power, a is the path loss exponent, Z is an independent random variable (RV) that models the multipath fading effect, and d_{ref} is the reference distance. Without loss of generality, we set $d_{\text{ref}} = 1\text{m}$. The term $1/d^a$ indicates the path loss model follows a decaying power law of the distance between transmitter and receiver. For the Rayleigh fading channel model under consideration, Z is an exponential RV with unit mean, i.e. $Z \sim \mathcal{E}(1)$.

Chapter 2

Spatial Spectral Efficiency Analysis for Single-Cell Wireless Relay System

In this chapter, we first introduce the notion of ASE into a single-cell wireless relay system and provide its accurate quantifications. Through accurate mathematical analysis, we derive the analytical expression of ASE for the downlink transmission of a single-cell wireless system with infrastructure RSs. Our analysis takes into account the random distribution of mobile users and the path loss/fading effects of the wireless channel. We consider the ideal frequency reuse case, where the channel can be arbitrarily used outside the affected area of each transmission steps. Through selected numerical examples, we show that relay-enhanced cellular systems, while not always leading to a higher spectral efficiency than conventional systems, can achieve much higher overall ASE. We also apply the ASE performance metric to the design and optimization of relay-enhanced cellular system. Followed by the ASE analysis in single cell scenario, we further study the ASE performance in multi-cell relay system in presence of the co-channel interference from the dominant co-channel cells. We accurately quantify the effect of co-channel interference on the ASE of infrastructure-relay enhanced wireless networks. In particular, we first determine the interference power at a particular target mobile station (MS) from an arbitrary co-channel BS and/or RSs, which is then applied to obtain the exact analytical expression of ASE. Two transmission strategies for infrastructure-relay assisted systems are considered, depending on whether the BS will transmit simultaneously during the relay trans-

mission stage (a simple in-cell frequency reuse strategy) or not. Through selected numerical examples, we show that the relay-assisted systems can achieve higher ASE when the reuse distance is relative small, even without simple in-cell frequency reuse. We also show that for a given target coverage area for BS/RS and reuse distance, there is an optimal choice of transmitting power for RSs which maximizes the ASE.

2.1 System Model

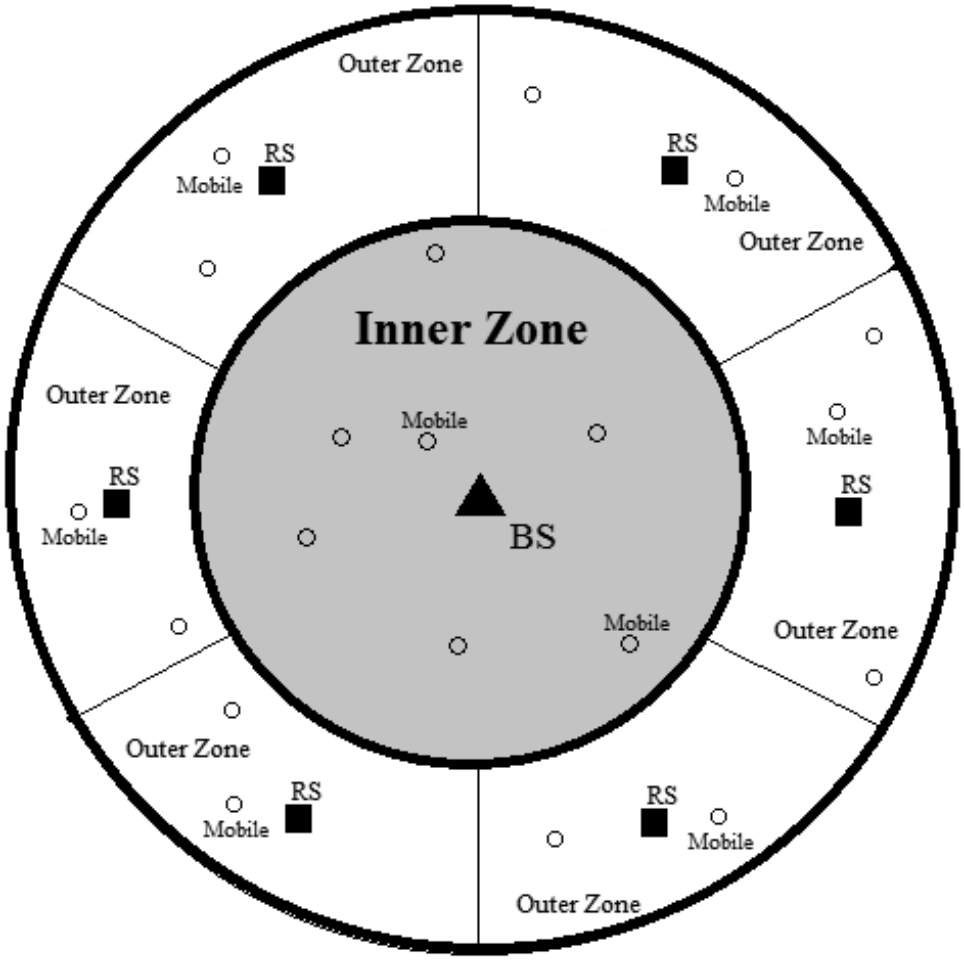

Figure 2.1: Network architecture of single-cell relay system.

The infrastructure-relay enhanced single-cell wireless systems under consideration is shown in Fig. 2.1. In particular, we consider a circular area served by a central

BS and six RSs. The RSs are located on a circle of distance $D_{\rm br}$ from the BS. In this scenario, two transmission modes can be applied to serve an user: the direct transmission mode and the relay transmission mode. We assume the mode selection is based on user locations. Specifically, the service area is divided into two different coverage zones: the inner zone and the outer zone [5]. The inner zone is approximated by a circle with radius $R_{\rm bs}$ while the outer zone by an annulus with radius $R_{\rm rs} = R - R_{\rm bs}$, where R is the radius of the relay-enhanced cell. In the inner zone, mobile users are directly served by the central BS, while in the outer zone, they are connected with the central BS through one of the RSs. All the mobiles are assumed to be independently and uniformly distributed in the cell. We will consider the optimal design of R_{bs} and D_{br} based on the following analytical results.

We consider a TDMA system where the users are served in different time slots of equal duration. In each time slot, one user in the coverage area is randomly selected for service. Specifically, BS directly transmits to the target mobiles in the assigned time slot if the user is in the inner zone. For outer zone users, we assume the half-duplex decode and forward relaying operation. Specifically, each RS transmission operates in two phases: in the first time slot, BS sends data to the RS to which the target mobile connects. Then in the following time slot, RS relays the received data to the target mobile while BS remains idle.

2.2 ASE Analysis

In the following, we derive the analytical expression of ASE for the infrastructure-relay enhanced single-cell system. By definition, ASE can be calculated as the ratio of average achieved data rate per unit bandwidth, or the equivalent ergodic channel capacity, denoted by $\overline{C}$, over the size of the affected area, denoted by $A_{\rm aff}$, i.e. [10]

$$\text{ASE} = \frac{\overline{C}}{A_{\rm aff}}. \tag{2.1}$$

The affected area $A_{\rm aff}$ refers to the area where considerable amount of transmission power can be received, i.e., greater than a power threshold level, which severely interferes other transmission over the same channel. We assume the channel can be arbitrarily reused outside of the affected area with, for example, the dynamic spectrum access or cognitive radio technologies. As intuitively expected, the affected area is always larger than the target service area. With the adopted path loss and fading

model, the affected area depends on the transmission power and the received signal power threshold. Note that the transmission power also affects the coverage of the target area. Therefore, the transmission power and cell radius need to be properly selected such that the transmissions outside the affected area can both satisfy the coverage requirement and create negligible interference to other cells. For clarity, we consider the maximum achievable ASE of relay enhanced system for a given transmission power and target service area.

Direct Transmission Mode

When the target user locates in the inner zone, the user is served in direct transmission mode. In this mode, the downlink capacity at distance r over Rayleigh fading channel can be determined as

$$C(r) = \int_0^\infty \log_2(1 + \frac{p}{N}) \frac{1}{\bar{p}(r)} e^{-\frac{p}{\bar{p}(r)}} \mathrm{d}p, \tag{2.2}$$

where N is the total noise power. With some manipulations, it can be simplified as

$$C(r) = \frac{1}{\ln 2} E_1 \left(\frac{N}{P_{\mathrm{bs}}} r^a \right) e^{\frac{N}{P_{\mathrm{bs}}} r^a}, \tag{2.3}$$

where P_{bs} is the transmission power of BS, r is the distance from BS to the user, $E_1(\cdot)$ is the *exponential integral* function, which is given by

$$E_1(x) = \int_x^\infty \frac{e^{-t}}{t} \mathrm{d}t.$$

Therefore, the average capacity over the entire area of the inner zone is given by

$$\overline{\mathrm{C}}_{\mathrm{inner}} = \int_0^{R_{bs}} C(r) f_{\mathrm{r}}(r) \mathrm{d}r, \tag{2.4}$$

where $f_{\mathrm{r}}(r)$ is the PDF of the distance from BS to a inner zone user. As we assume that the users are uniformly distributed in the service area, the distribution function $f_{\mathrm{r}}(r)$ is given by

$$f_{\mathrm{r}}(r) = \frac{2r}{R_{\mathrm{bs}}^2}, \qquad 0 \le r \le R_{\mathrm{bs}}. \tag{2.5}$$

Finally, the average capacity is obtained after substituting (2.3) and (2.5) into (2.4) as

$$\overline{\mathrm{C}}_{\mathrm{inner}} = \int_0^{R_{\mathrm{bs}}} \frac{1}{\ln 2} E_1\left(\frac{N}{P_{\mathrm{bs}}} r^a\right) e^{\frac{N}{P_{\mathrm{bs}}} r^a} \frac{2r}{R^2} \mathrm{d}r. \tag{2.6}$$

For a particular received signal power threshold $p_{\min}$, we define the affected probability P_{aff} at distance r as

$$P_{\mathrm{aff}} = \Pr\left\{p(r) > p_{\min}\right\}.$$

Over Rayleigh fading channels, this probability is given by

$$P_{\mathrm{aff}}(p_{\min}, r) = e^{-\frac{p_{\min}}{\bar{p}(r)}}. \tag{2.7}$$

where $\bar{p}(r)$ is the average received signal power determined by path loss. The affected area of BS transmission can be calculated as

$$\mathrm{A}_{\mathrm{aff}}^{\mathrm{BS}} = 2\pi \int_0^{\infty} P_{\mathrm{aff}}(p_{\min}, r) r \mathrm{d}r. \tag{2.8}$$

Substituting (2.7) into (2.9), we can arrive at

$$\mathrm{A}_{\mathrm{aff}}^{\mathrm{BS}} = \frac{2\pi\Gamma\left(\frac{2}{a}\right)}{a \cdot \left(p_{\min}/P_{\mathrm{bs}}\right)^{2/a}}. \tag{2.9}$$

According to (2.1), ASE of the inner zone can be calculated as

$$\mathrm{ASE}_{\mathrm{inner}} = \frac{\overline{\mathrm{C}}_{\mathrm{inner}}}{\mathrm{A}_{\mathrm{aff}}^{\mathrm{BS}}}, \tag{2.10}$$

where $\overline{\mathrm{C}}_{\mathrm{inner}}$ is given in (2.6).

Relay Transmission Mode

With relay transmission, the information to a mobile user needs to be transmitted over the same bandwidth in two time slots. Therefore, the achieved data rate to an user with relay transmission is the half of the minimum of the capacities of BS to RS link and RS to mobile link. For the sake of clarity, we assume that the bottleneck is always the link from RS to mobile, which will be justified in the numerical result section with Monte Carlo simulation. Also note that the infrastructure RS can usually

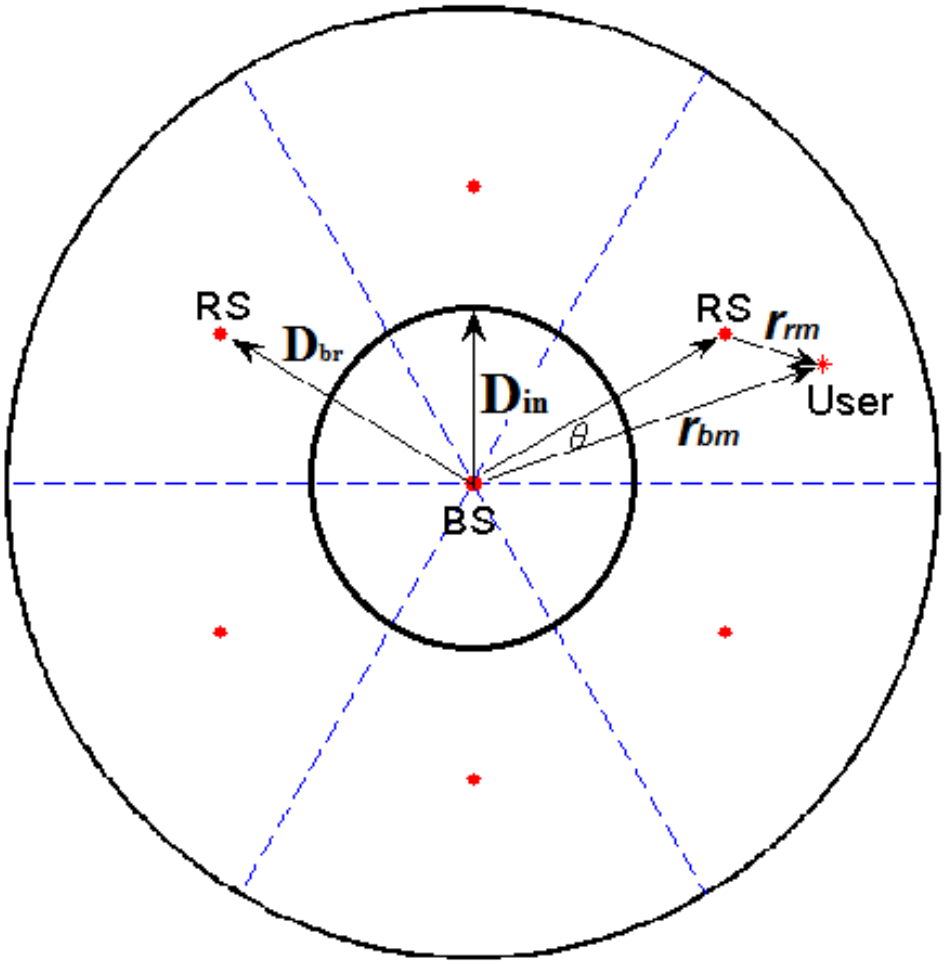

Figure 2.2: Geometry of relay transmission mode.

be installed to have good, likely line of sight (LoS), connections with the BS. As a result, the achieved data rate with relay transmission is simplified to the half of the capacity of the RS to mobile link in the following analysis.

As shown in Fig. 2.2, we use d denote the distance from RS to the target user at distance r from the BS. Given the angle θ between BS-RS and BS-user directions, d can be calculated as

$$d = \sqrt{r^2 + D_{\text{br}}^2 - 2rD_{\text{br}}\cos\theta}. \tag{2.11}$$

Following a similar procedure as in previous section, the capacity of relay transmission

to a user that is distance r away from BS as

$$C(d) = \int_0^\infty \log_2(1 + \frac{p}{N}) \frac{1}{\bar{p}(d)} e^{-\frac{p}{\bar{p}(d)}} \mathrm{d}p. \tag{2.12}$$

Over Rayleigh fading channels, it can be written as

$$C(d) = \frac{1}{\ln 2} E_1 \left(\frac{N}{P_{\mathrm{rs}}} d^a \right) e^{\frac{N}{P_{\mathrm{rs}}} d^a}, \tag{2.13}$$

where P_{rs} is the transmission power of RS. After averaging over the coverage area of RS, the average capacity of a user in a RS service area is given by

$$\overline{\mathrm{C}}_{\mathrm{outer}} = \int_0^{\frac{\pi}{6}} \int_{R_{\mathrm{bs}}}^{R} \frac{1}{\ln 2} E_1 \left(\frac{N}{P_{\mathrm{rs}}} d^a \right) e^{\frac{N}{P_{\mathrm{rs}}} d^a} f_{\mathrm{r}}(r) f_{\Theta}(\theta) \mathrm{d}r \mathrm{d}\theta. \tag{2.14}$$

With uniform user distribution assumption, the PDF of location for users in the outer zone are given by

$$\begin{cases} f_{\mathrm{r}}(r) = \frac{2r}{(R - R_{\mathrm{bs}})^2}, & R_{\mathrm{bs}} \leq r \leq R \\ f_{\Theta}(\theta) = \frac{6}{\pi}, & 0 \leq \theta \leq \frac{\pi}{6}. \end{cases} \tag{2.15}$$

Similar to the previous section, the affected area of RS transmission is given by

$$\mathrm{A}_{\mathrm{aff}}^{\mathrm{RS}} = \frac{\Gamma\left(\frac{2}{a}\right)}{a \cdot \left(p_{\min}/P_{\mathrm{rs}}\right)^{2/a}}. \tag{2.16}$$

Note that the two transmission steps in relay transmission mode affect different areas. Relay transmission enjoys the smaller "footprint" in the second transmission time slot. Given (2.14) and (2.16), ASE of the relay transmission mode is given by

$$\mathrm{ASE}_{\mathrm{outer}} = \frac{1}{2} \left(\frac{\frac{1}{2}\overline{\mathrm{C}}_{\mathrm{outer}}}{\mathrm{A}_{\mathrm{aff}}^{\mathrm{BS}}} + \frac{\frac{1}{2}\overline{\mathrm{C}}_{\mathrm{outer}}}{\mathrm{A}_{\mathrm{aff}}^{\mathrm{RS}}} \right). \tag{2.17}$$

Combine the result of direct and relay transmission mode, we can arrived at the ASE of the system as

$$\mathrm{ASE}_{\mathrm{relay}} = \frac{\hat{A}_{\mathrm{BS}}}{\hat{A}_{\mathrm{total}}} \cdot \mathrm{ASE}_{\mathrm{inner}} + \frac{\hat{A}_{\mathrm{RS}}}{\hat{A}_{\mathrm{total}}} \cdot \mathrm{ASE}_{\mathrm{outer}} \tag{2.18}$$

where $\hat{A}_{\mathrm{BS}}$ and $\hat{A}_{\mathrm{RS}}$ denote the service area of the BS and RS, given by $\hat{A}_{\mathrm{BS}} = \pi R_{bs}^2$ and $\hat{A}_{\mathrm{RS}} = \pi R^2 - \pi R_{bs}^2$ respectively, and $\hat{A}_{\mathrm{total}} = \hat{A}_{\mathrm{BS}} + \hat{A}_{\mathrm{RS}}$.

2.3 Numerical Example

In this section, we compare the ASE of infrastructure-relay enhanced single-cell system with conventional system. Note that ASE of conventional system can be easily shown, by following the same process as we derive ASE of the inner zone, as

$$\mathrm{ASE}_{\mathrm{conv}} = \frac{\overline{C}_{\mathrm{conv}}}{A_{\mathrm{aff}}^{\mathrm{conv}}} \tag{2.19}$$

where $A_{\mathrm{aff}}^{\mathrm{conv}}$ denotes the affected area given in (2.9). The ergodic capacity of conventional cell is

$$\overline{C}_{\mathrm{conv}} = \int_0^R C(r) p_{\mathrm{r}}'(r) \mathrm{d}r = \frac{2}{R^2} \int_0^R r C(r) \mathrm{d}r. \tag{2.20}$$

The system parameters are listed in Table 2.1.

Table 2.1: System parameters of single-cell wireless relay system

Item	Nominal Value
BS transmission power P_{bs}	36 dBm
RS transmission power P_{rs}	29 dBm
Minimum received power p_{min}	-40 dBm
Path-loss exponential a	4
Noise power N	-100 dBm

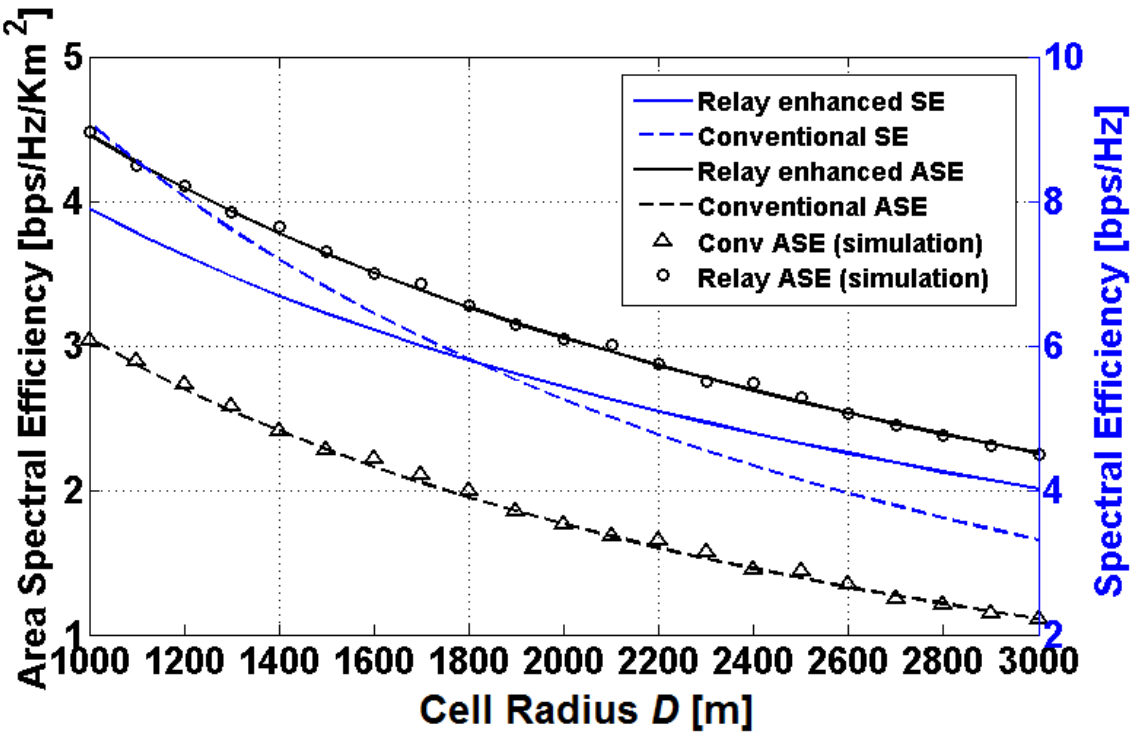

Figure 2.3: ASE/spectral efficiency as function of cell radius R for conventional and relay enhanced system.

In Fig. 2.3, we compare the ASE of relay enhanced system with conventional system. In particular, we set $R_{bs} = \frac{1}{2}R$, $D_{br} = \frac{3}{4}R$. The simulation results are shown as discrete dots, which match well with the analytical results. Note that the simulation results are obtained assuming that both hops of relay transmission can be the bottleneck. Therefore, the assumption that the bottleneck is always the link from RS to mobile in the analysis leads to negligible inaccuracy. We can see that, while the ASE of both systems decrease as the cell radius R increases, the relay enhanced cell shows much better performance than that of the conventional one for all values of cell radius R. Another commonly used performance metric for wireless system is overall spectral efficiency. For conventional system, spectral efficiency is equal to $\overline{C}_{\text{conv}}$, whereas for relay enhanced system, spectral efficiency is given by

$$\text{SE}_{\text{relay}} = \frac{\hat{A}_{\text{BS}}}{\hat{A}_{\text{total}}} \cdot \overline{C}_{\text{inner}} + \frac{\hat{A}_{\text{RS}}}{\hat{A}_{\text{total}}} \cdot \frac{\overline{C}_{\text{outer}}}{2} \tag{2.21}$$

We also compare the spectral efficiency performance of these two systems in Fig. 2.3. We can figure that when the cell radius R is small, the conventional cell enjoys better spectral efficiency than that of the relay enhanced one, partly due to the half duplexing constraint of relay transmission. We can also see that only when R is large enough, the relay enhanced system shows better spectral efficiency performance.

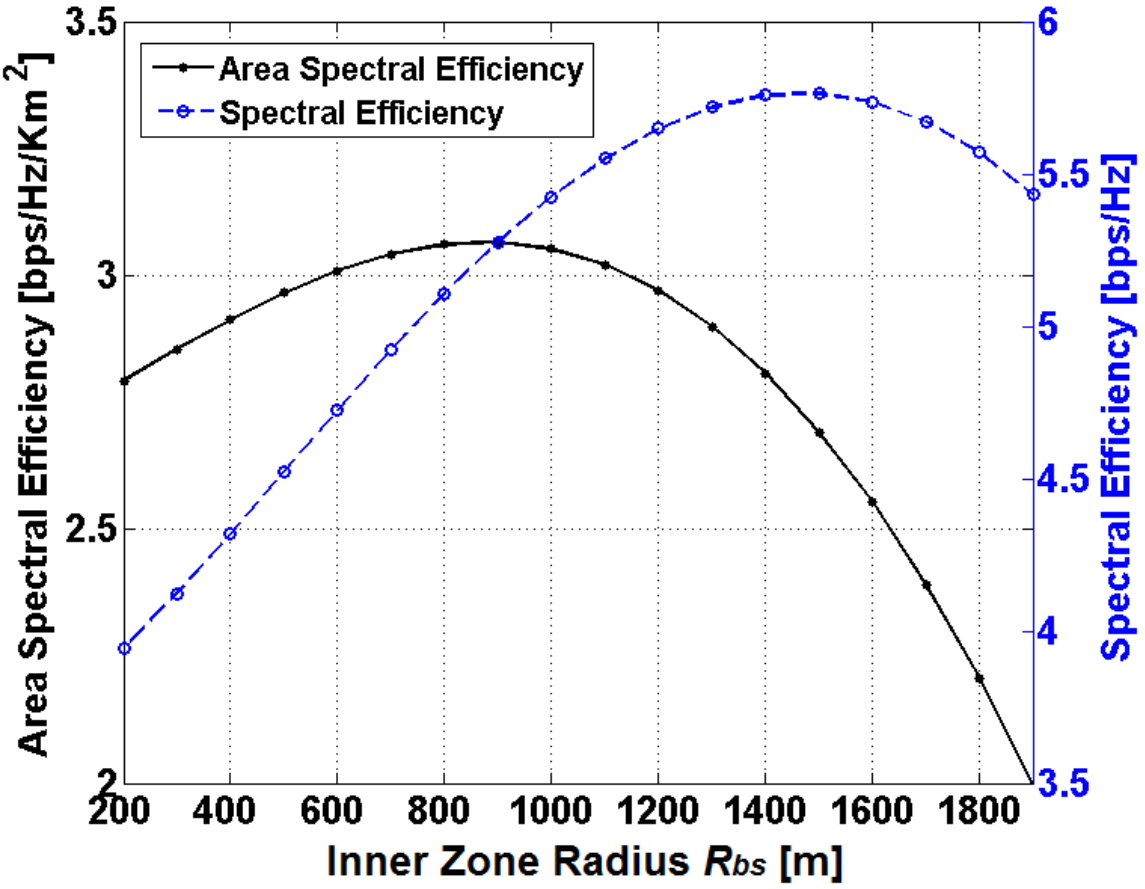

Figure 2.4: ASE/spectral efficiency of relay enhanced system as function of inner zone radius R_{bs}.

In Fig. 2.4, we plot ASE and spectral efficiency of relay enhanced system as the function of inner zone radius R_{bs} with cell radius R fixed to 2000m and $D_{br} = \frac{3}{4}R$. It clearly shows that for both performance metrics, there is an optimal choice of R_{bs} value. On the other hand, the optimal R_{bs} value to maximize ASE is much smaller than that maximizes spectral efficiency. Intuitively, this can be explained that ASE metric takes into account the smaller footprints of relay transmission and therefore encourage more relay transmission in the cell coverage area.

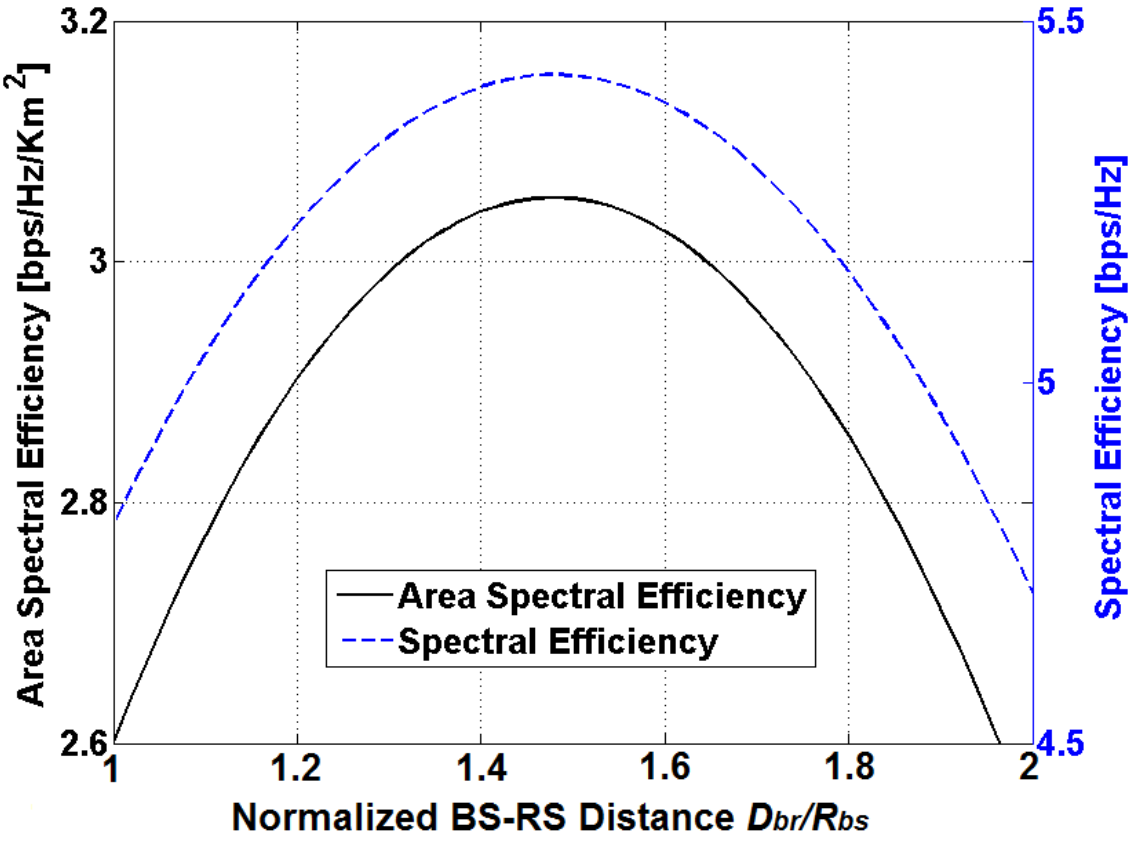

Figure 2.5: ASE/spectral efficiency of relay enhanced system as function of normalized BS-RS distance D_{br}/R_{bs}.

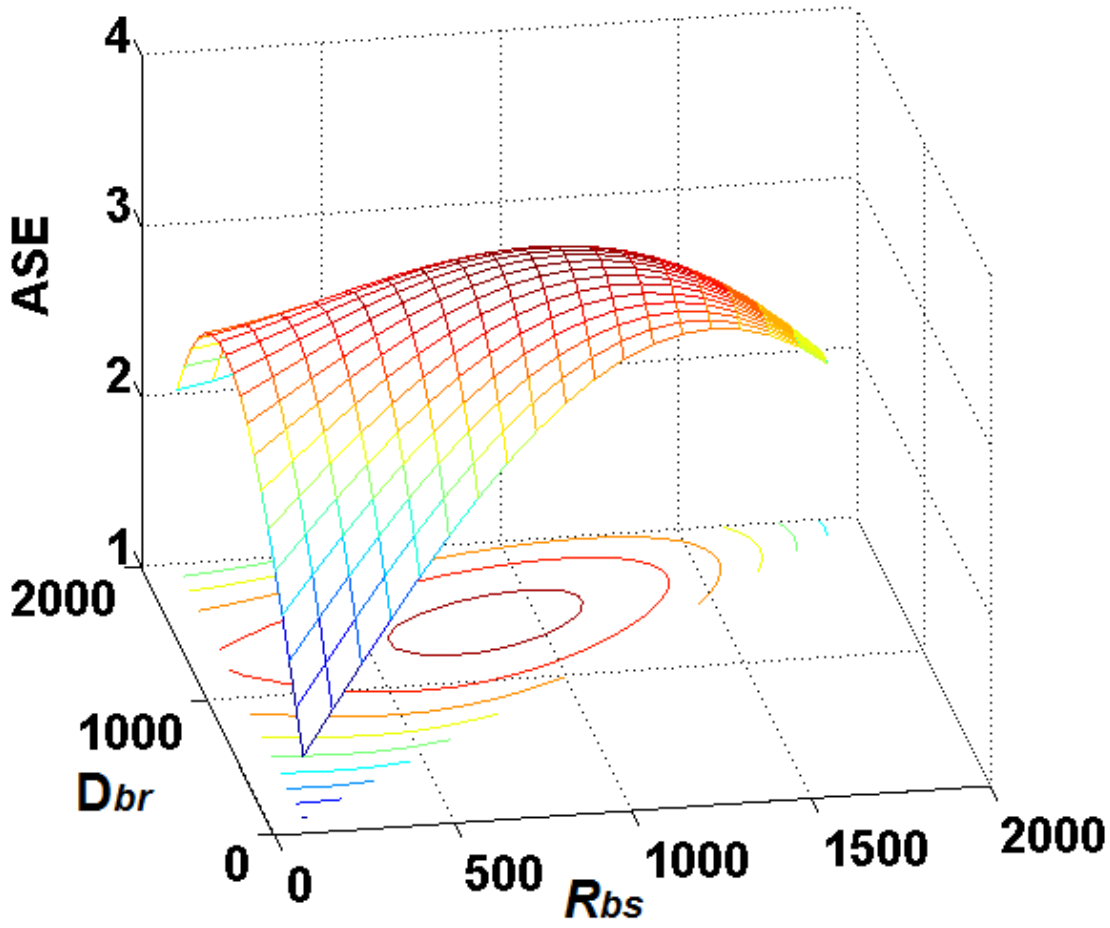

Figure 2.6: ASE of relay enhanced system as function of inner zone radius R_{bs} and BS-RS distance D_{br}.

In Fig. 2.5, we plot ASE and spectral efficiency of relay enhanced cell as the function of the normalized BS-RS distance D_{br}/R_{bs} with cell radius R fixed to 2000m and $R_{bs} = \frac{1}{2}R$. It shows that the optimal value of D_{br} in terms of maximizing spectral efficiency also maximizes ASE. This is due to the fact that D_{br} affects only the capacity of relay transmission given in (2.14). Finally, as an additional numerical example, Fig. 2.6 plots ASE as function of both the inner zone radius R_{bs} and the BS-RS distance D_{br}, which helps jointly select the optimal values of R_{bs} and D_{br} for relay enhanced system.

2.4 Conclusion

In this chapter, we applied the concepts of ASE to study the performance of single-cell wireless relay system. ASE can capture the small spacial footprint of relay transmission. We derive the closed-form expression of ASE of the relay-enhanced single-cell system and the conventional system. In the next step of research, we will develop more effective frequency reuse strategy to explore the benefit of relay transmission.

Chapter 3

Spatial Spectral Efficiency Analysis for Multi-Cell Wireless Relay System

In this chapter, we investigate the spatial spectral efficiency of multi-cell wireless relay network while taking into account its smaller spatial footprints. Specifically, we derive the exact statistics of the co-channel interference from dominant co-channel cells, which may operate in either direct transmission mode or relay transmission mode. Our analysis takes into account the random distribution of the mobile users and the path loss/fading effects. In addition, we also consider two transmission strategies for relay enhanced cellular systems, depending on whether the BS will transmit simultaneously during the relay transmission stage (a "simple in-cell frequency reuse" strategy) or not. For both strategies, the accurate analytical expression of the overall ASE of relay enhanced cellular systems are obtained. Through selected numerical examples, we show that the relay enhanced cellular systems can achieve higher ASE than conventional systems with properly chosen system parameters. We also show that the quality of BS-RS link can significantly affect the overall system ASE performance.

3.1 System Model

We consider the downlink transmission of a multi-cell wireless relay system. As illustrated in Fig. 3.1, there are six dominant co-channel cells, affecting the trans-

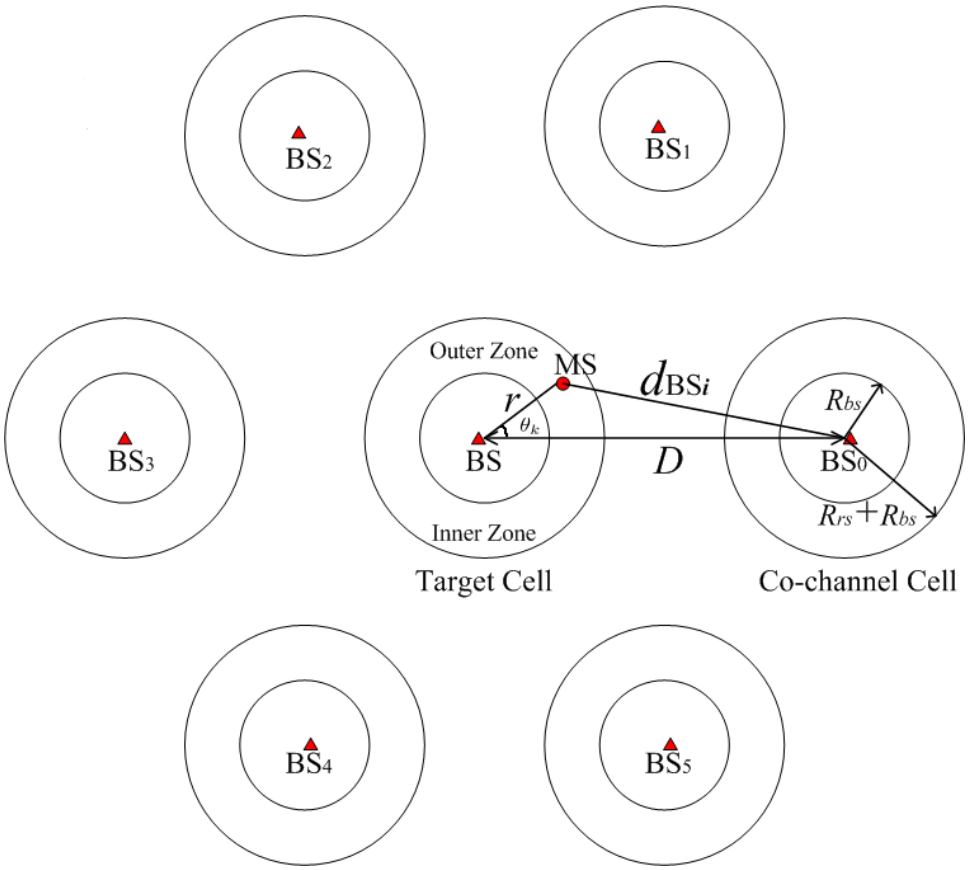

Figure 3.1: Network architecture of multi-cell relay system.

mission of the center target cell. The BSs of the co-channel cells are labeled as BS_i, $i \in \{0, 1, \ldots, 5\}$. The distance between target cell and the dominant co-channel cells is denoted by D, usually known as *reuse distance*. For each cell, infrastructure relays have been implemented to enhance the cell edge coverage. The individual cell architecture is identical to the one we considered in chapter 2, as shown in Fig. 2.1. We assume that MSs are independently and uniformly distributed in their respective cells and scheduled in a round-robin fashion to ensure fairness. The PDFs of MSs' location coordinates (r, θ) are given by

$$\begin{cases} p_r(r) = \frac{2r}{(R_{bs}+R_{rs})^2}, & 0 \le r \le R_{bs} + R_{rs}, \\ p_\theta(\theta) = \frac{1}{2\pi}, & 0 \le \theta \le 2\pi. \end{cases} \tag{3.1}$$

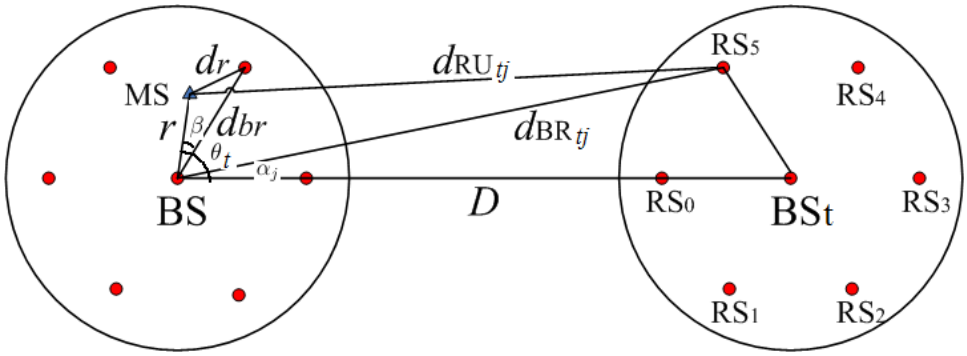

Figure 3.2: Interference from co-channel cells in relay mode.

It follows that the probability that the scheduled user is in the inner zone and served directly by BS is given by $\mathcal{P}_{\mathrm{d}} = \frac{\pi R_{bs}^2}{\pi(R_{bs}+R_{rs})^2}$. The probability that the scheduled user is in the outer zone is then equal to $\mathcal{P}_{\mathrm{r}} = 1 - \mathcal{P}_{\mathrm{d}}$.

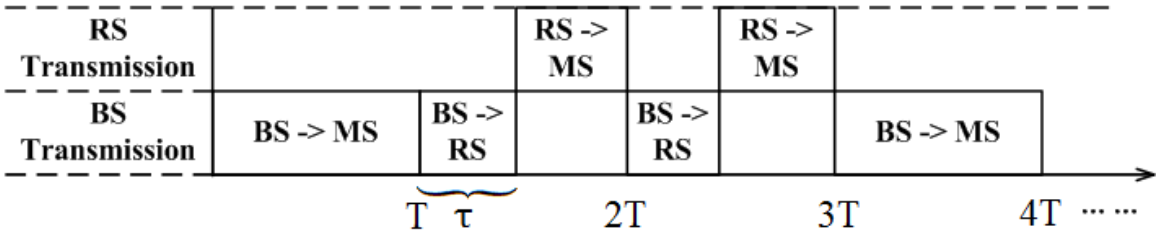

(a) Without in-cell frequency reuse

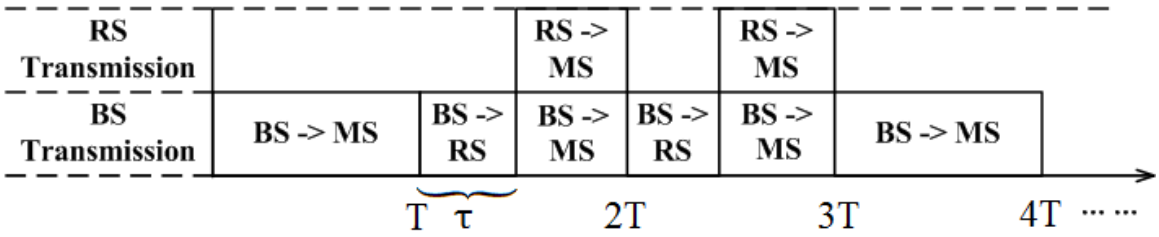

(b) With in-cell frequency reuse

Figure 3.3: Transmission strategies.

We consider a generic TDMA system, where transmissions to scheduled MSs occur in time slots of equal duration T. In addition, RSs perform half-duplex *decode-and-forward* (DF) relaying operation, as they cannot transmit and receive at the same time. For that purpose, the transmission time slots for MSs in the outer zone are further divided into two subslots. In the first subslot, assumed to be of duration τ, BS transmits to the corresponding RS, which then forwards its decoded information

to the target receiver in the second subslot of duration $T-\tau$. Since the infrastructure RSs are usually installed with line-of-sight (LoS) connection to the BS, we assume that the BS to RS hop always enjoys higher capacity than the RS to MS hop, which typically does not enjoy a LoS connection. Therefore, the duration of the first subslot is less than or equal to that of the second subslot, i.e. $\tau \leq T/2$. Fig. 3.3 illustrates the sample transmission slots.

3.2 ASE Analysis

ASE characterizes the average spectrum utilization efficiency per unit area of the cellular systems. Mathematically speaking, ASE can be defined as the ratio of the average ergodic capacity of a cell over the utilization area of the frequency bandwidth of interest. Since the frequency reuse distance is D, the utilization area is given by $\pi(D/2)^2$. Then ASE of the cellular system, denoted by η, can be calculated as

$$\eta = \frac{\overline{\mathrm{C}}}{\pi(D/2)^2}, \tag{3.2}$$

where $\overline{\mathrm{C}}$ denotes the average ergodic capacity of the target cell and can be evaluated by averaging the ergodic capacity of an MS at certain location (r, θ) over the cell coverage area Ω, i.e.

$$\overline{\mathrm{C}} = \iint_{\Omega} \mathrm{C}(r,\theta) \cdot p_r(r) \cdot p_\theta(\theta)\, \mathrm{d}r\, \mathrm{d}\theta, \tag{3.3}$$

where $\mathrm{C}(r,\theta)$ is the ergodic capacity of an MS at coordinates (r,θ). Let Γ denotes the instantaneous received SINR at coordinates (r,θ). Considering co-channel interference, Γ can be written as

$$\Gamma = \frac{\mathrm{P_{rx}}}{\mathcal{I}_{\mathrm{total}} + N}, \tag{3.4}$$

where $\mathcal{I}_{\mathrm{total}}$ denotes the total interference power from co-channel cells and N is the noise power. It follows that $\mathrm{C}(r,\theta)$ can be calculated using the probability density function (PDF) of Γ, $f_\Gamma(\gamma)$, as

$$\mathrm{C}(r,\theta) = \int_0^\infty \log_2(1+\gamma) \cdot f_\Gamma(\gamma)\, \mathrm{d}\gamma. \tag{3.5}$$

Therefore, to calculate ASE of cellular systems, we need to obtain the statistics of the received SINR of the MS at certain location in the cell coverage area. Note that $\mathcal{I}_{\text{total}}$ for conventional systems is simply the total received signal power from the six dominant co-channel BSs. For relay enhanced systems, $\mathcal{I}_{\text{total}}$ consists of received signal power from transmitting BSs and/or RSs of the co-channel cells. In the following, we first determine the statistics of total interference power $\mathcal{I}_{\text{total}}$, which is then applied to the evaluation of $\mathrm{C}(r, \theta)$.

Interference analysis

Based on the system model presented in previous section, every co-channel cell will be operating in either direct transmission mode or relay transmission mode with probability $\mathcal{P}_{\text{d}}$ and $\mathcal{P}_{\text{r}}$, respectively. Let $n \in \{0, 1, \cdots, 6\}$ denotes the number of co-channel cells performing direct transmission while other $6 - n$ co-channel cells are performing relay transmission. Let $\mathbf{u}_n$ denotes the index set of cells in direct mode and $\overline{\mathbf{u}}_n = \mathbb{S} - \mathbf{u}_n$, where $\mathbb{S} = \{0, 1, \cdots, 5\}$, is the complementary set of $\mathbf{u}_n$. Therefore, for a particular set $\mathbf{u}_n$, the total interference $\mathcal{I}_{\text{total}|\mathbf{u}_n}$ can be written as the summation of the interference from the co-channel cells in direct mode and that from the co-channel cells in relay mode, i.e.

$$\mathcal{I}_{\text{total}|\mathbf{u}_n} = \sum_{k \in \mathbf{u}_n} \mathcal{I}_{\text{BS}_k} + \sum_{t \in \overline{\mathbf{u}}_n} \mathcal{I}_{\text{RS}_t}. \tag{3.6}$$

where $\mathcal{I}_{\text{BS}_k}$ and $\mathcal{I}_{\text{BS}_t}$ denote the interference from the k^{th} co-channel cell that performs direct transmission and t^{th} co-channel cell that performs relay transmission, respectively.

When the k^{th} co-channel cell is operating in direct mode, the amount of interference power $\mathcal{I}_{\text{BS}_k}$ that it generates to the MS in the target cell is an exponential random variable with average given by

$$\overline{\mathcal{I}}_{\text{BS}_k} = \mathrm{P}_{\text{BS}} / d_{\text{BS}_k}^{a}, \tag{3.7}$$

where d_{BS_k} is the distance from the BS of the k^{th} co-channel cell to the MS, which can be calculated, with reference to Fig. 3.1, as

$$d_{\text{BS}_k} = \sqrt{r^2 + D^2 - 2rD\cos\theta_k}, \tag{3.8}$$

where D is the reuse distance and θ_k is the angle between serving BS to co-channel BS_k and serving BS to MS directions. Note that the distance d_{BS_k} to different co-channel BSs varies as the value of θ_k changes.

We now consider $\mathcal{I}_{\mathrm{RS}_t}$, the interference power generated by co-channel cells operating in relay transmission mode. The interference power from a RS transmission is also an exponential random variable with mean related to the distance from the RS to the target MS. Specifically, the average interference power from the j^{th} $(j = 0, 1, \cdots, 5)$ RS of t^{th} co-channel cell, denoted as RS_{tj}, is given by $\overline{\mathcal{I}}_{\mathrm{RS}_{tj}} = \mathrm{P}_{\mathrm{RS}}/d^a_{\mathrm{RU}_{tj}}$, where P_{RS} is the transmission power of RS and $d_{\mathrm{RU}_{tj}}$ is the distance from RS_{tj} to the target MS. According to the geometry shown in Fig. 3.2, we have

$$d_{\mathrm{RU}_{tj}} = \sqrt{r^2 + d^2_{\mathrm{BR}_{tj}} - 2r d_{\mathrm{BR}_{tj}} \cos(\theta_t - \alpha_j)}, \tag{3.9}$$

where $d_{\mathrm{BR}_{tj}} = \sqrt{d^2_{br} + D^2 - 2d_{br}D\cos(\frac{\pi}{3}j)}$ is the distance from RS_{tj} to the central BS, and $\alpha_j = \arcsin\left\{\frac{d_{br}}{d_{\mathrm{BR}_{tj}}}\sin(\frac{\pi}{3}j)\right\}$ is the angle between BS-BS and BS-RS_{tj} directions.

We assume that the RSs have equal probability to transmit. Based on the relaying mode of operation, the interference power of the co-channel cell are from the co-channel BS for τ/T percent of the time and from one of the six RSs for $(T-\tau)/T$ percent of the time, as illustrated in Fig. 3.3a. Therefore, the interference from t^{th} co-channel cell that performs relay transmission is given by

$$\mathcal{I}_{\mathrm{RS}_t} = \frac{\tau}{T} \times \mathcal{I}_{\mathrm{BS}_t} + \frac{T-\tau}{T} \times \frac{1}{6}\sum_{j=0}^{5} \mathcal{I}_{\mathrm{RS}_{tj}}. \tag{3.10}$$

Note that we allow the operation of different co-channel cells to be unsynchronized here.

Finally, the total interference conditioning on $\mathbf{u}_n$, $\mathcal{I}_{\mathrm{total}|\mathbf{u}_n}$, is the summation of received signal power from transmitting BS and/or RS of the co-channel cells. Substituting (3.10) into (3.6) and after some simplifications, $\mathcal{I}_{\mathrm{total}|\mathbf{u}_n}$ can be written as

$$\mathcal{I}_{\mathrm{total}|\mathbf{u}_n} = \sum_{k\in\mathbf{u}_n} \mathcal{I}_{\mathrm{BS}_k} + \frac{\tau}{T}\sum_{t\in\overline{\mathbf{u}}_n} \mathcal{I}_{\mathrm{BS}_t} + \frac{T-\tau}{6T}\sum_{t\in\overline{\mathbf{u}}_n}\sum_{j=0}^{5} \mathcal{I}_{\mathrm{RS}_{tj}}. \tag{3.11}$$

Ergodic capacity analysis

In this section, we derive the ergodic capacity $\mathrm{C}(r,\theta)$ for an arbitrary MS at location (r,θ) in the target cell under Rayleigh fading. We first show that under Rayleigh fading model, the statistics of Γ can be expressed in terms of the MGF of total co-channel interference $\mathcal{I}_{\text{total}}$.

Statistics of SINR over Rayleigh fading channel

The cumulative distribution function (CDF) of Γ given in (3.4), $F_{\Gamma}(\gamma)$, can be written as

$$F_{\Gamma}(\gamma) = \int_0^{\infty} \Pr\left\{ \mathrm{P}_{\text{rx}} < (y+N)\cdot\gamma \mid \mathcal{I}_{\text{total}} = y \right\} f_{\mathcal{I}_{\text{total}}}(y)\,\mathrm{d}y. \tag{3.12}$$

Note that for Rayleigh fading environment,

$$\Pr\left\{ \mathrm{P}_{\text{rx}} < (y+N)\cdot\gamma \mid \mathcal{I}_{\text{total}} = y \right\} = 1 - e^{-(y+N)\gamma/\overline{\mathrm{P}}_{\text{rx}}}, \tag{3.13}$$

then $F_{\Gamma}(\gamma)$ can be obtained, after applying the definition of MGF, as

$$F_{\Gamma}(\gamma) = 1 - e^{-N\gamma/\overline{\mathrm{P}}_{\text{rx}}} \mathcal{M}_{\mathcal{I}_{\text{total}}}(-\gamma/\overline{\mathrm{P}}_{\text{rx}}), \tag{3.14}$$

where $\mathcal{M}_{\mathcal{I}_{\text{total}}}(s)$ denotes the MGF of total co-channel interference $\mathcal{I}_{\text{total}}$. Under Rayleigh fading assumption, $\mathcal{I}_{\text{BS}_m}$ and $\mathcal{I}_{\text{RS}_{tj}}$ are exponential random variables with mean $\overline{\mathcal{I}}_{\text{BS}_k}$ and $\overline{\mathcal{I}}_{\text{RS}_{tj}}$, respectively. It follows that the MGF of total interference $\mathcal{I}_{\text{total}|\mathbf{u}_n}$, given in (3.11), is given by

$$\mathcal{M}_{\mathcal{I}_{\text{total}|\mathbf{u}_n}}(s) = \left(\prod_{k\in\mathbf{u}_n} \mathcal{M}_{\mathcal{I}_{\text{BS}_k}}(s) \right) \cdot \left(\prod_{t\in\overline{\mathbf{u}}_n} \mathcal{M}_{\mathcal{I}_{\text{BS}_t}}\left(\frac{\tau}{T}s\right) \right) \cdot \left(\prod_{t\in\overline{\mathbf{u}}_n} \prod_{j=0}^{5} \mathcal{M}_{\mathcal{I}_{\text{RS}_{tj}}}\left(\frac{T-\tau}{6T}s\right) \right), \tag{3.15}$$

where the MGFs of $\mathcal{I}_{\text{BS}_k}$ and $\mathcal{I}_{\text{RS}_{tj}}$ are given by

$$\mathcal{M}_{\mathcal{I}_{\text{BS}_k}}(s) = (1 - \overline{\mathcal{I}}_{\text{BS}_k}\cdot s)^{-1}, \tag{3.16}$$

and

$$\mathcal{M}_{\mathcal{I}_{\text{RS}_{tj}}}(s) = (1 - \overline{\mathcal{I}}_{\text{RS}_{tj}}\cdot s)^{-1}, \tag{3.17}$$

respectively. Let $\mathbb{U}_n$ denotes the set of all possible $\mathbf{u}_n$'s, i.e. elements of power set $\wp(\mathbb{S})$ with n entries. Noting that the probability of each $\mathbf{u}_n$ is $\mathcal{P}_{\rm d}^n\mathcal{P}_{\rm r}^{6-n}$, the MGF of total interference $\mathcal{I}_{\rm total}$ can be finally obtained as

$$\begin{aligned}\mathcal{M}_{\mathcal{I}_{\rm total}}(s) =& \sum_{n=0}^{6}\sum_{\mathbf{u}_n\in\mathbb{U}_n}\mathcal{P}_{\rm d}^n\mathcal{P}_{\rm r}^{6-n}\Bigg\{\prod_{k\in\mathbf{u}_n}\left(1-\overline{\mathcal{I}}_{{\rm BS}_k}\cdot s\right)^{-1}\\ &\times\prod_{t\in\overline{\mathbf{u}}_n}\prod_{j=0}^{5}\left(1-\overline{\mathcal{I}}_{{\rm BS}_t}\cdot\frac{\tau}{T}s\right)^{-1}\cdot\left(1-\overline{\mathcal{I}}_{{\rm RS}_{tj}}\cdot\frac{T-\tau}{6T}s\right)^{-1}\Bigg\}.\end{aligned}\tag{3.18}$$

Finally, the CDF of the received SINR Γ is obtained in closed-form as

$$\begin{aligned}F_\Gamma(\gamma) =& 1-e^{-\frac{N\gamma}{\overline{\rm P}_{\rm rx}}}\sum_{n=0}^{6}\sum_{\mathbf{u}_n\in\mathbb{U}_n}\mathcal{P}_{\rm d}^n\mathcal{P}_{\rm r}^{6-n}\Bigg\{\prod_{k\in\mathbf{u}_n}\left(1+\frac{\overline{\mathcal{I}}_{{\rm BS}_k}}{\overline{\rm P}_{\rm rx}}\gamma\right)^{-1}\\ &\times\prod_{t\in\overline{\mathbf{u}}_n}\prod_{j=0}^{5}\left(1+\frac{\overline{\mathcal{I}}_{{\rm BS}_t}}{\overline{\rm P}_{\rm rx}}\cdot\frac{\tau}{T}\gamma\right)^{-1}\cdot\left(1+\frac{\overline{\mathcal{I}}_{{\rm RS}_{tj}}}{\overline{\rm P}_{\rm rx}}\cdot\frac{T-\tau}{6T}\gamma\right)^{-1}\Bigg\}.\end{aligned}\tag{3.19}$$

Average ergodic capacity

The ergodic capacity $\mathrm{C}(r,\theta)$ for an arbitrary MS at location (r,θ) in the target cell can be calculated using the CDF of the received SINR $F_\Gamma(\gamma)$ given in (3.5). For users in the inner zone, i.e. $0\le r\le R_{bs}$ and $0\le\theta\le 2\pi$, $\mathrm{C_i}(r,\theta)$ can be calculated, after integration by part and some manipulations, as

$$\mathrm{C_i}(r,\theta)=\frac{1}{\ln 2}\int_0^\infty\frac{e^{-N\cdot\gamma}}{\gamma+1/\overline{\rm P}_{\rm i}}\mathcal{M}_{\mathcal{I}_{\rm total}}(-\gamma)\,\mathrm{d}\gamma,\tag{3.20}$$

where $\overline{\rm P}_{\rm i}$ is the average received signal power from the serving BS given by ${\rm P}_{\rm BS}/r^a$. The users in the outer zone, i.e. with $R_{bs}\le r\le R_{bs}+R_{rs}$ and $0\le\theta\le 2\pi$, will be served in the relay mode. As noted earlier, we assume that the RS to MS hop transmission is always the bottle neck, due to the smaller transmission power and size of RSs. Since RS transmits for $T-\tau$ time period in each time interval T, $\mathrm{C}(r,\theta)$ for user in the outer zone can be calculated as

$$\mathrm{C_o}(r,\theta)=\frac{T-\tau}{T\ln 2}\int_0^\infty\frac{e^{-N\cdot\gamma}}{\gamma+1/\overline{\rm P}_{\rm o}}\mathcal{M}_{\mathcal{I}_{\rm total}}(-\gamma)\,\mathrm{d}\gamma,\tag{3.21}$$

where $\overline{\mathrm{P}}_{\mathrm{o}}$ is the average received signal power from the serving RS given by $\mathrm{P}_{\mathrm{RS}}/d_r^a$ where, as illustrated in Fig. 3.2, $d_r = \sqrt{r^2 + d_{br}^2 - 2rd_{br}\cos\beta}$ and β is the angle between BS-RS and BS-MS directions, given by $\beta = \mod(\theta, \frac{\pi}{6})$.

Finally, the average ergodic capacity of a relay enhanced cell can be obtained by averaging over the whole cell coverage area as

$$\begin{aligned}\overline{\mathrm{C}} = \mathcal{P}_{\mathrm{d}} \int_0^{2\pi} \int_{R_0}^{R_{bs}} \mathrm{C}_{\mathrm{i}}(r,\theta) \cdot p_r(r) \cdot p_\theta(\theta)\,\mathrm{d}r\,\mathrm{d}\theta \\ + \mathcal{P}_{\mathrm{r}} \int_0^{2\pi} \int_{R_{bs}}^{R_{bs}+R_{rs}} \mathrm{C}_{\mathrm{o}}(r,\theta) \cdot p_r(r) \cdot p_\theta(\theta)\,\mathrm{d}r\,\mathrm{d}\theta. \end{aligned} \tag{3.22}$$

3.3 In-cell Frequency Reuse

In this section, we apply a simple in-cell frequency reuse scheme to make full use of the time slots in relay mode and hence increase the spectral utilization efficiency. As illustrated in Fig. 3.3b, we allow BS to transmit to another MS in the inner zone during the time slot that RS communicates with MS in the outer zone. Due to the simultaneous transmission in relay mode, the total interference will be increased while an extra multiplexing capacity, denoted as $\mathrm{C}_{\mathrm{mul}}$, will be included into the calculation of the total capacity. We will analyze the effect of this simple in-cell reuse scheme by evaluating the ASE of the resulting cellular system.

Analysis for inner zone user

As we apply the in-cell frequency reuse scheme to every co-channel cell, BS will transmit for the entire time slot T rather than τ when performing relay transmission. Therefore, the total interference for inner zone user conditioning on $\mathbf{u}_n$, $\widetilde{\mathcal{I}}^{\mathrm{i}}_{\mathrm{total}|\mathbf{u}_n}$, can be written as

$$\widetilde{\mathcal{I}}^{\mathrm{i}}_{\mathrm{total}|\mathbf{u}_n} = \sum_{k=0}^{5} \mathcal{I}_{\mathrm{BS}_k} + \frac{T-\tau}{6T} \sum_{t\in\overline{\mathbf{u}}_n} \sum_{j=0}^{5} \mathcal{I}_{\mathrm{RS}_{tj}}, \tag{3.23}$$

where $\mathcal{I}_{\mathrm{BS}_k}$ and $\mathcal{I}_{\mathrm{RS}_{tj}}$ are exponential random variables. Thus for users in the inner zone, the ergodic capacity $\mathrm{C}_{\mathrm{i}}(r,\theta)$ can be calculated using (3.20) with the MGF of

$\widetilde{\mathcal{I}}^{\mathrm{i}}_{\mathrm{total}}$, given by

$$\mathcal{M}_{\widetilde{\mathcal{I}}^{\mathrm{i}}_{\mathrm{total}}}(s) = \sum_{n=0}^{6} \sum_{\mathbf{u}_n \in \mathbb{U}_n} \mathcal{P}_{\mathrm{d}}^{n} \mathcal{P}_{\mathrm{r}}^{6-n} \left\{ \prod_{k=0}^{5} \mathcal{M}_{\mathcal{I}_{\mathrm{BS}_k}}(s) \times \prod_{t \in \overline{\mathbf{u}}_n} \prod_{j=0}^{5} \mathcal{M}_{\mathcal{I}_{\mathrm{RS}_{tj}}} \left(\frac{T-\tau}{6T} s \right) \right\}. \tag{3.24}$$

Analysis for outer zone user

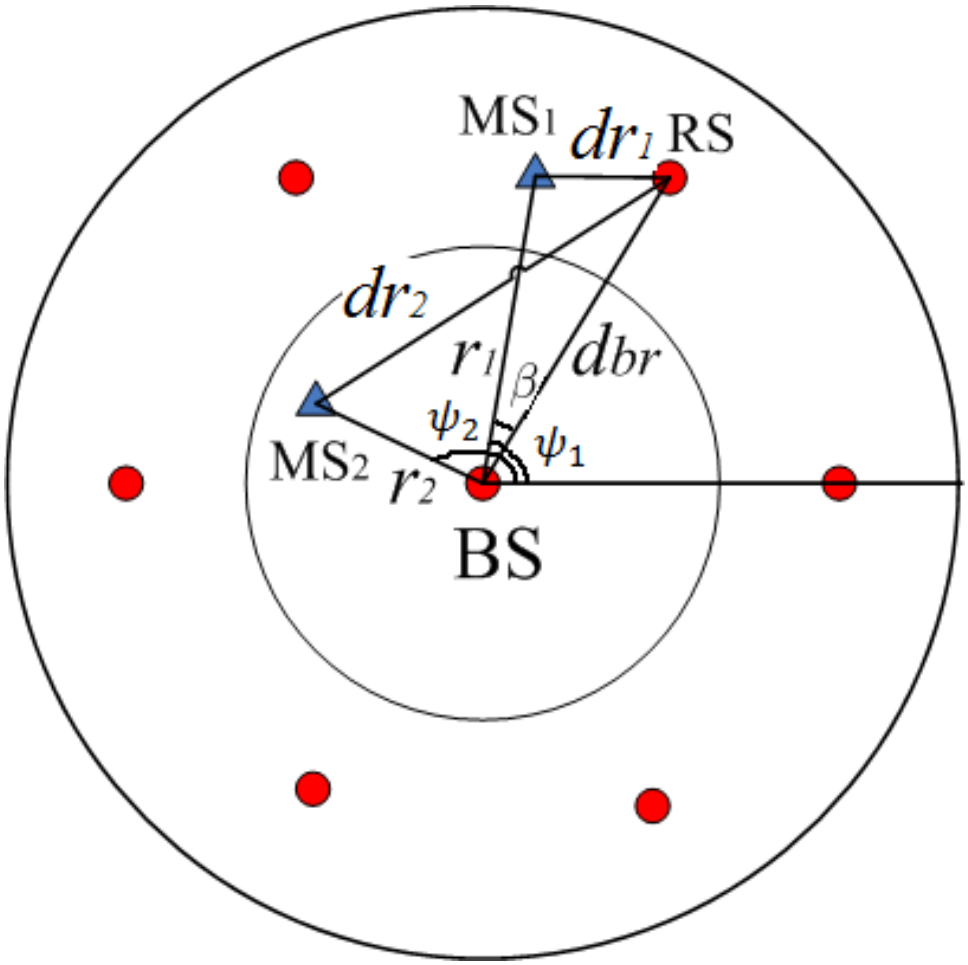

Figure 3.4: Geometry for in-cell frequency reuse case.

As illustrated in Fig. 3.4, the BS generates an extra interference $\mathcal{I}^{\mathrm{o}}_{\mathrm{BS}}$ to MS_1 at (r_1, ψ_1) in the outer zone of target cell, which can be modeled as an exponential random variable with mean $\overline{\mathcal{I}}^{\mathrm{o}}_{\mathrm{BS}} = \mathrm{P}_{\mathrm{BS}}/r_1^a$. The total interference for MS_1, denoted as $\widetilde{\mathcal{I}}^{\mathrm{o}}_{\mathrm{total}}$, is given by $\widetilde{\mathcal{I}}^{\mathrm{o}}_{\mathrm{total}} = \widetilde{\mathcal{I}}^{\mathrm{i}}_{\mathrm{total}} + \mathcal{I}^{\mathrm{o}}_{\mathrm{BS}}$. Thus for users in the outer zone, the ergodic

capacity $\mathrm{C_o}(r,\theta)$ can be calculated using (3.21) with the average received signal power of $\overline{\mathrm{P}}_{\mathrm{o}} = \mathrm{P_{RS}}/d_{r_1}^a$ and the MGF of $\mathcal{I}_{\mathrm{total}}^{\mathrm{o}}$, given by

$$\mathcal{M}_{\widetilde{\mathcal{I}}_{\mathrm{total}}^{\mathrm{o}}}(s) = \sum_{n=0}^{6} \sum_{\mathbf{u}_n \in \mathbb{U}_n} \mathcal{P}_{\mathrm{d}}^n \mathcal{P}_{\mathrm{r}}^{6-n} \left\{ \prod_{k=0}^{5} \mathcal{M}_{\mathcal{I}_{\mathrm{BS}_k}}(s) \times \prod_{t \in \overline{\mathbf{u}}_n} \prod_{j=0}^{5} \mathcal{M}_{\mathcal{I}_{\mathrm{RS}_{tj}}}\left(\frac{T-\tau}{6T}s\right) \right\} \times \mathcal{M}_{\mathcal{I}_{\mathrm{BS}}^{\mathrm{o}}}(s), \tag{3.25}$$

where $\mathcal{M}_{\mathcal{I}_{\mathrm{BS}}^{\mathrm{o}}}(s) = \left(1 - \overline{\mathcal{I}}_{\mathrm{BS}}^{\mathrm{o}} \cdot s\right)^{-1}$ is the MGF of $\mathcal{I}_{\mathrm{BS}}^{\mathrm{o}}$. Meanwhile, for MS_2 at (r_2, ψ_2) in the inner zone served in parallel by BS, the interference generated by transmitting RS, $\mathcal{I}_{\mathrm{RS}}^{\mathrm{mul}}$, is an exponential random variable with mean $\mathrm{P_{RS}}/d_{r_2}^a$, where $d_{r_2} = \sqrt{r_2^2 + d_{br}^2 - 2r_2 d_{br}\cos(\psi_2 - (\psi_1 - \beta))}$. Therefore, the total interference for MS_2, denoted as $\widetilde{\mathcal{I}}_{\mathrm{total}}^{\mathrm{mul}}$, is given by $\widetilde{\mathcal{I}}_{\mathrm{total}}^{\mathrm{mul}} = \widetilde{\mathcal{I}}_{\mathrm{total}}^{\mathrm{i}} + \mathcal{I}_{\mathrm{RS}}^{\mathrm{mul}}$. The ergodic capacity $\mathrm{C_{mul}}(r,\theta)$ can be calculated using (3.21) with the average received signal power of $\overline{\mathrm{P}}_{\mathrm{mul}} = \mathrm{P_{BS}}/r_2^a$ and the MGF of $\widetilde{\mathcal{I}}_{\mathrm{total}}^{\mathrm{mul}}$, given by

$$\mathcal{M}_{\widetilde{\mathcal{I}}_{\mathrm{total}}^{\mathrm{mul}}}(s) = \sum_{n=0}^{6} \sum_{\mathbf{u}_n \in \mathbb{U}_n} \mathcal{P}_{\mathrm{d}}^n \mathcal{P}_{\mathrm{r}}^{6-n} \left\{ \prod_{k=0}^{5} \mathcal{M}_{\mathcal{I}_{\mathrm{BS}_k}}(s) \times \prod_{t \in \overline{\mathbf{u}}_n} \prod_{j=0}^{5} \mathcal{M}_{\mathcal{I}_{\mathrm{RS}_{tj}}}\left(\frac{T-\tau}{6T}s\right) \right\} \times \mathcal{M}_{\mathcal{I}_{\mathrm{RS}}^{\mathrm{mul}}}(s), \tag{3.26}$$

where $\mathcal{M}_{\mathcal{I}_{\mathrm{RS}}^{\mathrm{mul}}}(s) = \left(1 - \overline{\mathcal{I}}_{\mathrm{RS}}^{\mathrm{mul}} \cdot s\right)^{-1}$ is the MGF of $\mathcal{I}_{\mathrm{RS}}^{\mathrm{mul}}$.

Finally, the average ergodic capacity of a relay enhanced cell with the simple in-cell frequency reuse scheme can be obtained by properly averaging over the whole cell coverage area as

$$\begin{aligned} \overline{\mathrm{C}} = {} & \mathcal{P}_{\mathrm{d}} \int_0^{2\pi} \int_{R_0}^{R_{bs}} \mathrm{C_i}(r,\theta) \cdot p_r(r) \cdot p_\theta(\theta)\, \mathrm{d}r\, \mathrm{d}\theta \\ & + \mathcal{P}_{\mathrm{r}} \int_0^{2\pi} \int_{R_{bs}}^{R_{bs}+R_{rs}} \mathrm{C_o}(r,\theta) \cdot p_r(r) \cdot p_\theta(\theta)\, \mathrm{d}r\, \mathrm{d}\theta \\ & + \mathcal{P}_{\mathrm{r}} \int_0^{2\pi} \int_{R_0}^{R_{bs}} \mathrm{C_{mul}}(r,\theta) \cdot p_r(r) \cdot p_\theta(\theta)\, \mathrm{d}r\, \mathrm{d}\theta, \end{aligned} \tag{3.27}$$

which can then be applied in (3.2) to calculate ASE of the resulting relay enhanced cellular system with in-cell reuse.

3.4 Numerical Examples

In this chapter, we present several numerical examples to study the ASE performance of infrastructure relay enhanced cellular systems. Specifically, we first focus on the

effect of relay position as well as the time duration allocation for relay transmission. Then we illustrate the effect of cellular system parameters, including the number of channel subsets, inner zone radius, and BS transmission power. In all the figures, the simulation results (in dots) and the analysis results (in lines) show good match with each other. The system parameters are listed in Table 3.1.

Table 3.1: System parameters of multi-cell wireless relay system

Item	Nominal Value
BS transmission power P_{BS}	36 dBm
RS transmission power P_{RS}	29 dBm
Minimum received power $p_{\min}$	-40 dBm
Path-loss exponential a	4
Time division τ	0.4
Noise power N	-100 dBm
Inner zone radius R_{bs}	1000 m
Outer zone radius R_{rs}	400 m
Relay position d_{br}	1200 m
Reuse distance D	4200 m

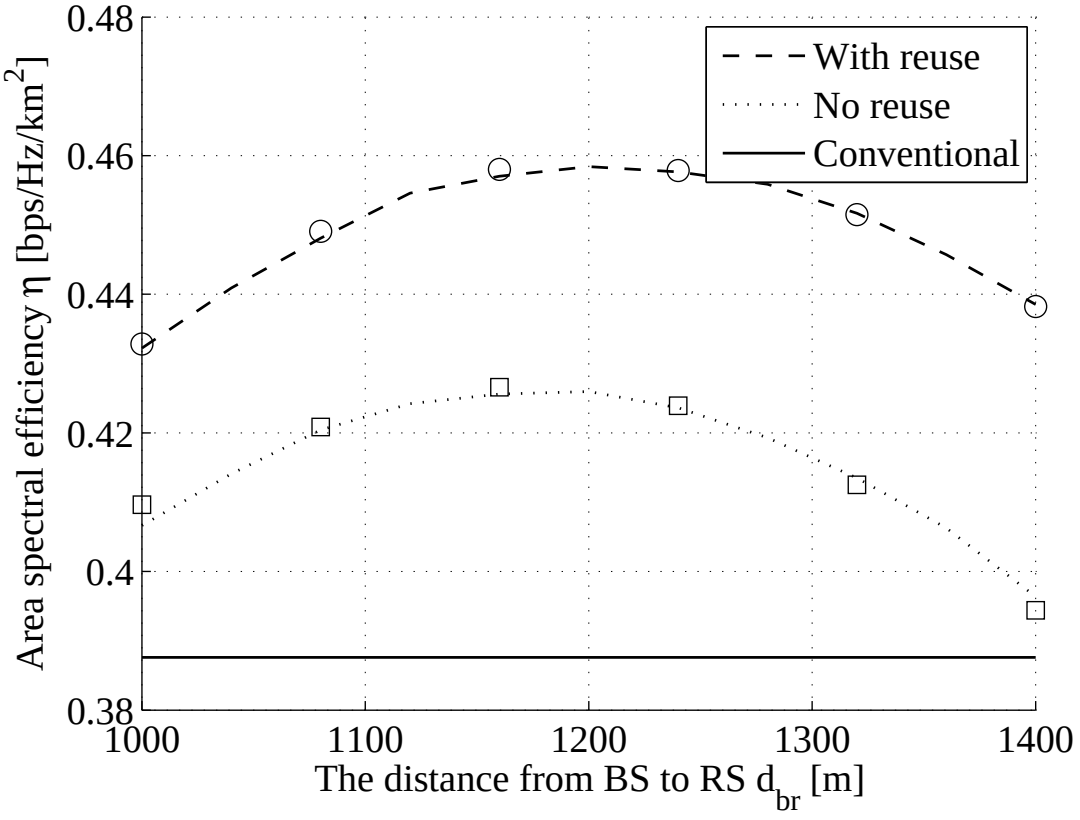

Figure 3.5: The effect of relay position d_{br} on the system overall ASE performance.

In Fig. 3.5, we examine the effect of relay position on the overall ASE performance. We plot ASE as function of the distance between BS and RSs, d_{br}, while keeping R_{bs} and R_{rs} unchanged. We can clearly see that the in-cell frequency reuse scheme offers better ASE performance than without in-cell reuse case. We also notice that there is an optimal relay position in terms of maximizing ASE for relay enhanced systems with or without in-cell frequency reuse. With the optimal relay locations, the relay enhanced cellular systems have much better ASE performance than conventional system. On the other hand, such performance advantage decreases or even diminishes for without in-cell reuse case if the relay location is not properly chosen. Therefore, proper selection of RS positions is essential to relay enhanced cellular systems. Another interesting observation is that the optimal relay location for in-cell reuse case is closer to cell boundary than without in-cell reuse case, to alleviate the effect of mutual interference due to parallel transmission in the cell.

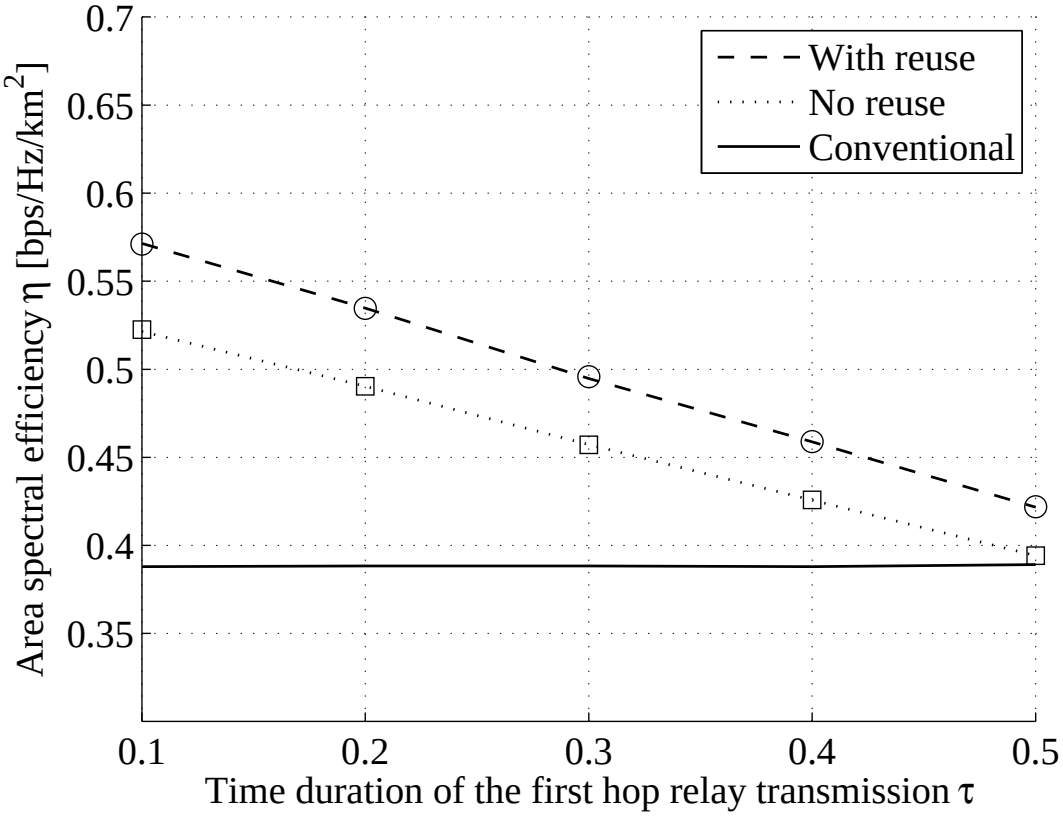

Figure 3.6: The effect of time slot τ on the system overall ASE performance.

In Fig. 3.6, we plot the system ASE performance as function of subslot duration for BS-RS transmission, τ, while fixing relay location at the center of the outer zone. Fig. 3.6 shows that ASE for both with and without in-cell reuse cases are monotonically decreasing as τ increases from $0.1T$ to $0.5T$. When τ is $0.5T$, i.e. the subslots for BS and RS transmission are of equal duration, the ASE performance of relay enhanced systems is slightly better than that of the conventional system without relaying. Recall that better BS to RS link quality permits smaller τ. Therefore, for cellular systems to benefit from infrastructure relay, especially in terms of overall ASE, the BS-RS link should be designed with good quality.

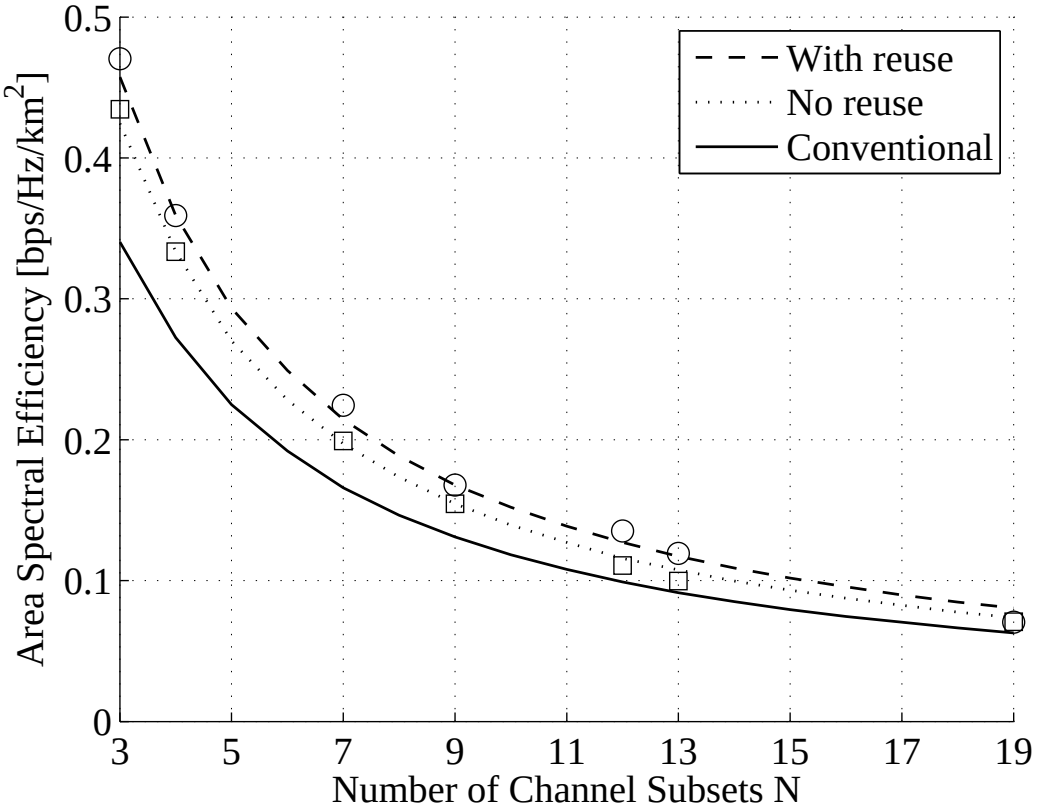

Figure 3.7: The effect of number of channel subsets $\mathcal{N}$ on the system overall ASE performance.

In cellular systems with hexagon cell structure, the reuse distance D and cell radius $R = R_{bs} + R_{rs}$ are related as $D = \sqrt{3\mathcal{N}}R$, where $\mathcal{N}$ is the number of channel subsets, satisfying $\mathcal{N} = p^2 + q^2 + pq$ $(p, q \in \mathbb{Z})$. In Fig. 3.7, we plot the ASE of relay enhanced cellular system as function of the number of channel subsets $\mathcal{N}$. The simulation result for the first seven possible values of $\mathcal{N}$, i.e. $\mathcal{N} = \{3, 4, 7, 9, 12, 13, 19\}$ are also plotted. It clearly shows that ASE is a decreasing function of the number of channel subsets $\mathcal{N}$. As the number of channel subsets increases, the reuse distance between two co-channel cells increases correspondingly. On one hand, large reuse distance leads to a decrease in co-channel interference and thus an improvement in capacity; on the other hand, it also increases the area that a particular frequency bandwidth occupied. The decreasing curve shows that the improvement in capacity cannot catch up with the increase in area. For comparison, we also include the ASE performance of conventional system without relays. The result shows that for all values of $\mathcal{N}$, no matter with or without in-cell frequency reuse scheme, the relay enhanced systems enjoy better ASE performance than that of the conventional systems; and the in-cell frequency reuse scheme is better than the without reuse case.

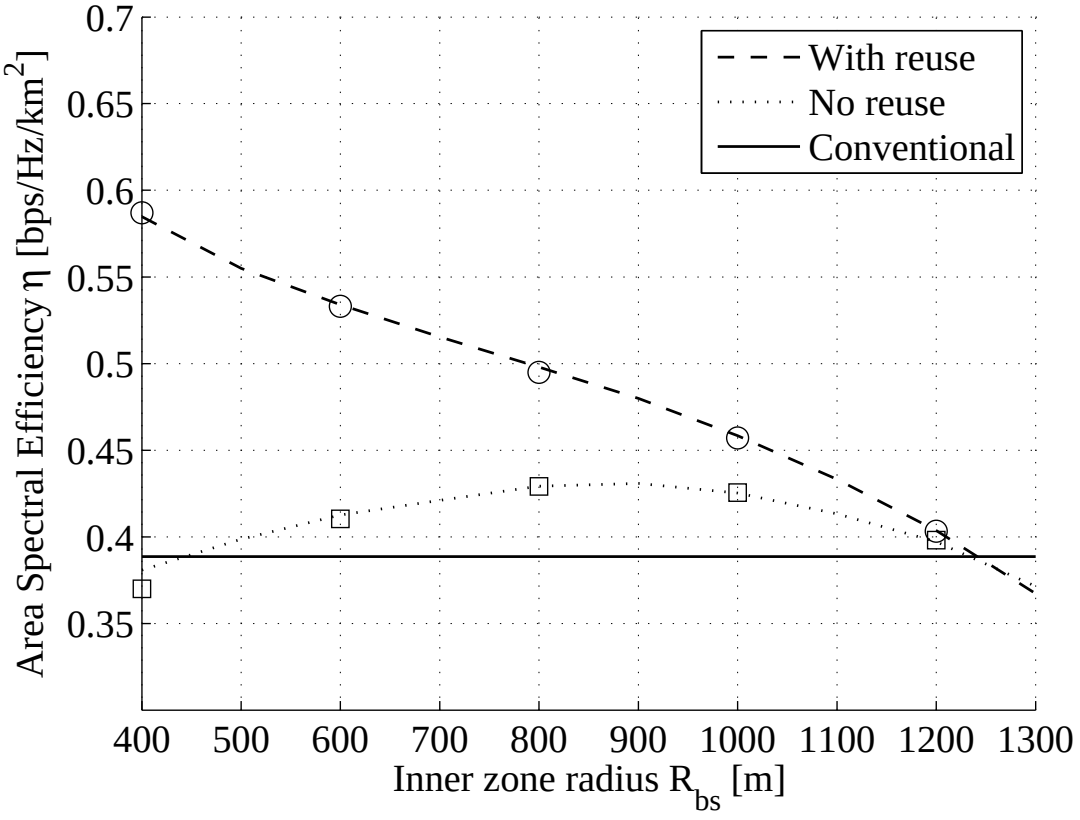

Figure 3.8: The effect of inner zone radius R_{bs} on the system overall ASE performance.

In Fig. 3.8, we plot ASE as function of the inner zone radius R_{bs}. The result shows that R_{bs} has different effect on the ASE performance for with and without in-cell frequency reuse case. With in-cell frequency reuse, ASE is a monotonically decreasing function of R_{bs}. This is due to smaller R_{bs} leads to larger outer zone, which increases the in-cell frequency reuse opportunity. Under this circumstance, the system benefits more from the reuse scheme. Without in-cell frequency reuse, there is an optimal value of the inner zone radius in terms of ASE. Recall that relay transmission is performed in half-duplex mode, which causes a penalty on the capacity. On the other hand, the system benefits from the smaller interference of the relay transmission step. Therefore, for too small R_{bs}, the system relies on relay transmission most of the time, and the penalty on capacity dominates; while for too large R_{bs}, the system fail to explore the benefit of smaller interference. As a result, there is an optimal value of the inner zone radius. We also note that, if the inner zone is too large, the ASE performance of relay enhanced cellular network is even worse than that of the conventional network without relays.

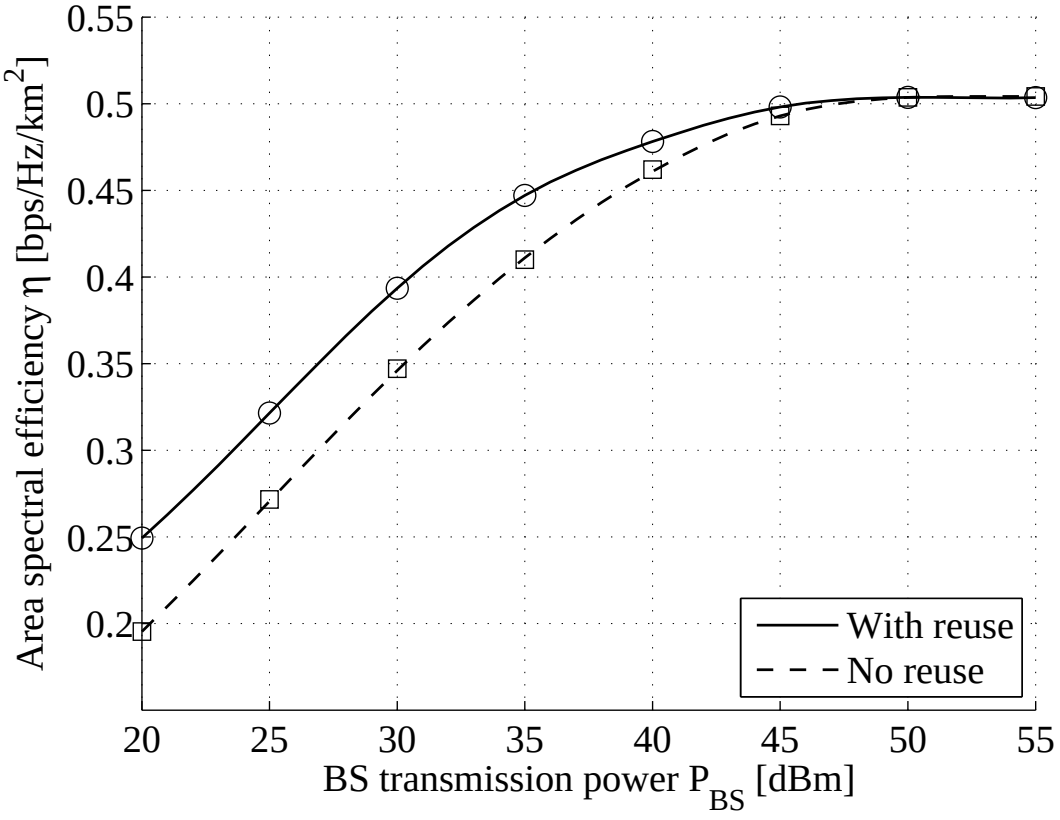

Figure 3.9: The effect of the BS transmission power P_{BS} on the system overall ASE performance.

In Fig. 3.9, we plot ASE as function of BS transmission power P_{BS}. As we increase the BS transmission power, the system overall ASE performance increases as well. This is because for small P_{BS}, the system coverage is poor and thus the capacity is small. As P_{BS} increasing, the system capacity is limited by inter cell interference. Another interesting observation is that, for small values of P_{BS}, the system benefits from the in-cell frequency reuse scheme. However, this benefit shrinks as P_{BS} increasing. It can be explained that the capacity generated by the in-cell frequency reuse cannot compensate the negative effect of the additional interference. Therefore, in order to implement the in-cell frequency reuse, the BS transmission power should be carefully chosen. Similar observations have observed for the effect of RS transmission power P_{RS}. The analytical result in this work can be used to optimally choose the system transmission power.

3.5 Conclusion

In this chapter, we investigated the ASE performance of multi-cell wireless relay system. We analyzed the total interference from the dominant co-channel cells operating either in direct or relay modes over Rayleigh fading channels, based on which we obtained the statistics of the SINR of an arbitrary MS in the target cell. We then derived the exact analytical expressions of ergodic capacity and ASE of the relay enhanced cellular systems with and without in-cell frequency reuse. Through selected numerical examples, we showed that for relay enhanced system, both the RSs position and BS-RS links should be properly selected in order to obtain better ASE performance than the conventional systems without relays.

Chapter 4

Spatial Spectral Efficiency Analysis for Arbitrary Wireless Transmissions

In this chapter, we present a comprehensive study on the GASE metric for various transmission scenarios of practical interest. We first formally introduce the definition of GASE by illustrating its evaluation for conventional point-to-point transmission. Then we extend the analysis to four transmission scenarios, namely dual-hop relay transmission [50–53], three-node cooperative relay transmission [40, 54–59], two-user X channels [60–62], and underlay cognitive radio transmission [45, 46, 48, 49, 63–66]. Cognitive radio has received significant attention lately as it can help to greatly improve the spectrum utilization of licensed frequency bandwidth [45]. Typically, there are three main cognitive radio paradigms [46]: interweave, overlay and underlay. With the underlay paradigm, the secondary cognitive users can access the frequency bandwidth of the primary radio only if the resultant interference power level at the primary receiver is below a given threshold [48, 49]. Recently, intensive research has been carried out to quantify the capacity gains of underlay cognitive radio transmission [63–66]. These research focused on the benefit of spectrum sharing by imposing a interference constraint on the primary receiver. However, the spatial property of parallel radio transmissions are overlooked in these analysis. In particular, the area affected by simultaneous transmission should also be considered when evaluating overall system spectrum utilization efficiency, especially in dense frequency reuse scenario. For each communication scenario, the generic formula of GASE are presented with

specific closed-form expressions for Rayleigh fading environment derived whenever feasible. Selected numerical examples are presented and discussed to illustrate the mathematical formulation and demonstrate the new insights that GASE metric brings into wireless system design.

4.1 Generalized Area Spectral Efficiency

In this section, we formally introduce the definition of GASE metric and illustrate its evaluation for conventional point-to-point transmission. Consider a point-to-point wireless link between generic source S and destination D. The source S is transmitting with power P_t using an omni-directional antenna. For analytical tractability and presentation clarity, we assume that the transmitted signal experiences both path loss and multipath fading effects, ignoring the shadowing effect. We also assume that the fading channel is slowly varying and, as such, the transmitter can adapt its transmission rate with the channel condition for reliable transmission.

GASE is defined as the ratio of the ergodic capacity of the link, denoted by $\overline{\mathrm{C}}$, over the size of the affected area of the transmission, denoted by A. Mathematically, if we denote GASE by η, we have $\eta = \overline{\mathrm{C}}/\mathrm{A}$. The affected area refers to the area where a significant amount of transmission power is observed, i.e., the received signal power P_r is greater than a certain threshold value $P_{\min}$, which will lead to significant amount of interference to neighboring transceivers. The value of $P_{\min}$ should be selected based on the interference sensitivity of neighboring wireless transmissions. In particular, if the neighbouring transmission is insensitive to interference, e.g., spread spectrum or ultra wideband (UWB) systems, $P_{\min}$ may be set to a large value. Otherwise, it should be set to the same order of magnitude to background noise. The same $P_{\min}$ value should be used to compare different design for the target transmission. For point-to-point link, the probability that an incremental area of distance r from the transmitter is affected is equal to the probability that the received signal power, $P_r(r)$, is greater than $P_{\min}$, i.e., $\mathbb{P}\{P_t \cdot Z/r^a \geq P_{\min}\}$. It follows that the affected area of point-to-point transmission can be determined as

$$\begin{aligned} \mathrm{A} &= \int_0^{2\pi} \int_0^{\infty} \int_{P_{\min} \cdot r^a / P_t}^{\infty} f_Z(z)\, \mathrm{d}z\, r \mathrm{d}r \mathrm{d}\theta \\ &= 2\pi \int_0^{\infty} \big(1 - F_Z\big(P_{\min} \cdot r^a / P_t\big)\big)\, r \mathrm{d}r. \end{aligned} \tag{4.1}$$

Meanwhile, the instantaneous link capacity between source S and destination D is given by $\mathrm{C} = \log_2\left(1 + \frac{P_t}{Nd^a} \cdot z\right)$, where z denotes a particular realization of fading power gain Z and N is the noise power. As such, the ergodic capacity can be calculated by averaging the instantaneous link capacity over the distribution of Z. Mathematically speaking, we have

$$\overline{\mathrm{C}} = \int_0^\infty \log_2\left(1 + \frac{P_t}{Nd^a} \cdot z\right) \mathrm{d}F_Z(z), \tag{4.2}$$

where $F_Z(\cdot)$ is the cdf of Z. Note that we ignore the effect of external interference from neighbouring transmission in non affected area in the capacity calculation. We assume that if $P_{\min}$ is chosen properly, due to the channel reciprocity property, the neighbouring transmission from non affected area will not generate significant interference to the target transmission. The effect of such external interference on the ergodic capacity as well as GASE will be addressed in our future work.

Therefore, the GASE for point-to-point link can be calculated as

$$\eta = \frac{\int_0^\infty \log_2\left(1 + \frac{P_t}{Nd^a} \cdot z\right) \mathrm{d}F_Z(z)}{2\pi \int_0^\infty \left(1 - F_Z\left(P_{\min} \cdot r^a / P_t\right)\right) r \mathrm{d}r}. \tag{4.3}$$

Under Rayleigh fading environment, Z is an exponential RV with unit mean, i.e., $Z \sim \mathcal{E}(1)$. The affected area of point-to-point transmission specializes, with the help of [67, Eq. 3.326.2], to

$$\mathrm{A} = \frac{2\pi}{a}\Gamma\left(\frac{2}{a}\right)\left(\frac{P_t}{P_{\min}}\right)^{2/a}, \tag{4.4}$$

where $\Gamma(\cdot)$ denotes the Gamma function. As we can see from (4.4), the affected area for the point-to-point link over Rayleigh fading is proportional to $P_t^{2/a}$, where a is the path loss exponent. Meanwhile, the ergodic capacity of the point-to-point link is given by

$$\overline{\mathrm{C}} = \frac{1}{\ln 2}\,\mathrm{E}_1\left(\frac{d^a N}{P_t}\right)\exp\left(\frac{d^a N}{P_t}\right), \tag{4.5}$$

where $\mathrm{E}_1(x) = \int_x^\infty \frac{e^{-t}}{t}\mathrm{d}t$ is the exponential integral function [67]. Finally, we can obtain the closed-form expression of GASE for point-to-point transmission over Rayleigh fading as

$$\eta = \frac{\frac{1}{\ln 2}\,\mathrm{E}_1\left(\frac{d^a N}{P_t}\right)\exp\left(\frac{d^a N}{P_t}\right)}{\frac{2\pi}{a}\Gamma\left(\frac{2}{a}\right)\left(\frac{P_t}{P_{\min}}\right)^{2/a}}. \tag{4.6}$$

It worths noting that, by including the factor $P_t^{2/a}$ in the denominator, the GASE performance metric also quantifies the energy utilization efficiency of wireless transmissions in achieving certain ergodic capacity while taking into account radio propagation effects. The conventional bit per Joule metric, specialized to C/P_t for point-to-point transmission, is roughly equivalent to the special case of GASE metric with $a = 2$.

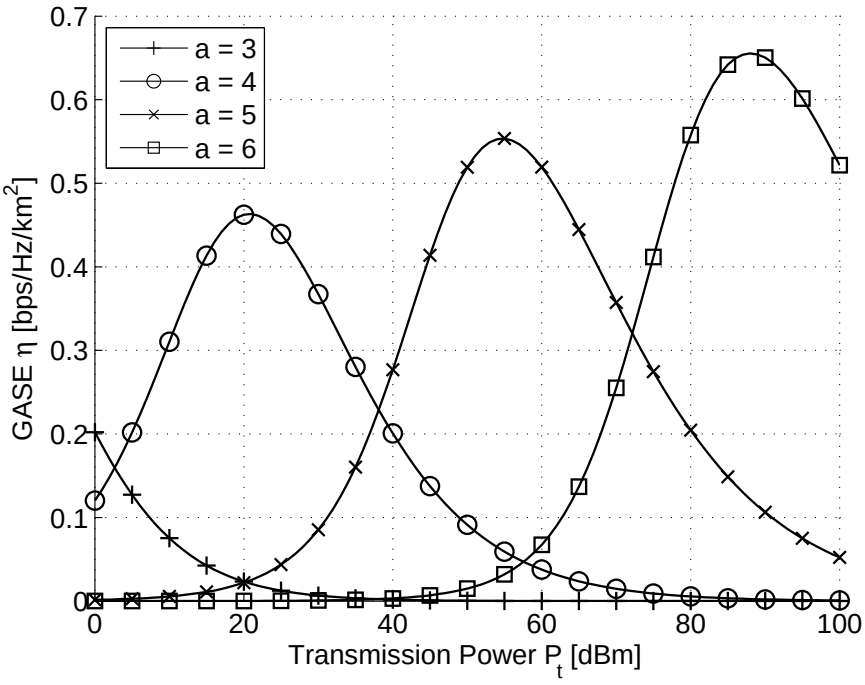

Figure 4.1: The effect of transmission power P_t on η.

In Fig. 4.1, we plot the GASE of point-to-point link under Rayleigh fading environment as function of the transmission power P_t for different path loss exponent a. The threshold $P_{\min} = -80$ dBm, the distance between transmitter and receiver $d = 1000$ m, and the noise power $N = -100$ dBm. It is interesting to see that, unlike conventional spectral efficiency metric, the GASE η is not a monotonic function of P_t in general. Only when a is very small will GASE η be a monotonically decreasing function of the transmission power P_t. For medium to large a, GASE is proportional to P_t when P_t is relatively small, which implies that the ergodic capacity increases faster than the affected area in this region. When P_t becomes large, the affected area increases faster, which leads to a decreasing GASE. As such, an optimal P_t value exists in terms of maximizing the GASE of point-to-point transmission. These be-

haviors of η can be mathematically verified with the following limiting results based on (4.6),

$$\lim_{P_t \to 0^+} \eta = \begin{cases} \infty, & a < 2; \\ \log_2 e \cdot \frac{P_{\min}}{\pi N d^2}, & a = 2; \\ 0, & a > 2, \end{cases} \tag{4.7}$$

and

$$\lim_{P_t \to \infty} \eta = 0. \tag{4.8}$$

It is straightforward although tedious to verify that η is a concave function of P_t. As such, there exist optimal values for P_t that maximize the GASE for point-to-point link for $a > 2$ cases, which can be analytically obtained by solving $\frac{d}{dP_t}\eta = 0$ for P_t. After substituting (4.6) into it and some manipulations, we arrive at the following equation that the optimal P_t^* satisfies

$$\left(\frac{d^a N}{P_t^*} + \frac{2}{a}\right) \mathrm{E}_1\left(\frac{d^a N}{P_t^*}\right) \exp\left(\frac{d^a N}{P_t^*}\right) = 1. \tag{4.9}$$

Various numerical methods can be used to solve this integral equation for P_t^*. Note that the optimal transmitting power value is proportional to the product $d^a N$, but independent of the minimum power threshold $P_{\min}$. Essentially, for a certain propagation environment and source-destination distance, P_t^* leads to the largest ergodic capacity per unit affected area. The transmission power is therefore optimally utilized with consideration of the spatial effect of radio transmission.

Fig. 4.1 also shows that the larger the path loss exponent a, the larger the maximum achievable GASE. Meanwhile, we need to use higher transmission power to achieve this maximum GASE. This observation indicates that when the path loss effect is significant, it is beneficial to use high transmission power as the affected area is not growing quickly. On the other hand, when there is severe shadowing effect between the S-D link, the GASE performance will suffer from the excessive increase of the transmission power P_t. In such scenario, relay transmission is the ideal solution to increase link throughput without significantly increasing the spatial footprint. In the next section, we examine the GASE performance of relay transmission.

4.2 GASE Analysis for Dual-Hop Relay Transmission

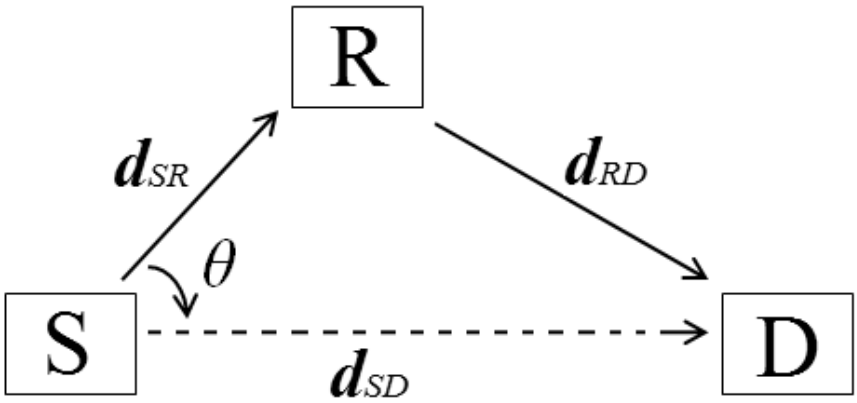

Figure 4.2: Dual hop relay transmission.

In this section, we consider the scenario where S transmits data to D with the help of the intermediate relay node R, as illustrated in Fig. 4.2. Specifically, relay R carries out either decode-and-forward (DF) or amplify-and-forward (AF) operation in a half-duplex mode. We assume the relay transmission occurs in two successive time slots of equal duration T. The distance from source to relay and relay to destination are denoted by d_{SR} and d_{RD}, respectively. We assume that direct S-D transmission is not possible, due to for example deep shadowing. The GASE performance of cooperative three-node network will be considered in the next section.

The transmission power of the source and relay node are denoted by P_S and P_R, respectively. The ergodic capacity of the relay transmission can be calculated, noting the half-duplex constraint, as

$$\overline{\mathrm{C}}_R = \frac{1}{2}\int_0^\infty \log_2(1+\gamma)\cdot f_{\Gamma_{\mathrm{eq}}}(\gamma)\,\mathrm{d}\gamma, \tag{4.10}$$

where $f_{\Gamma_{\mathrm{eq}}}(\cdot)$ denotes the PDF of the equivalent end-to-end SNR Γ_{eq}. For DF relaying protocol, $\Gamma_{\mathrm{eq}}^{DF}$ is equal to $\min\{\Gamma_{SR}, \Gamma_{RD}\}$, whereas for AF protocol, $\Gamma_{\mathrm{eq}}^{AF}$ is given by $\Gamma_{\mathrm{eq}}^{AF} = \frac{\Gamma_{SR}\cdot\Gamma_{RD}}{\Gamma_{SR}+\Gamma_{RD}+1}$ [53], where Γ_{SR} and Γ_{RD} are the instantaneous received SNR

of S-R hop and R-D hop, respectively. The affected area for the first and second relay transmission step, denoted as A_{SR} and A_{RD}, can be calculated using (4.4) with correspondent transmission power P_S and P_R, respectively. Note that A_{SR} and A_{RD} will not be affected at the same time as S and R transmit alternatively. Therefore, the overall GASE for dual-hop relay transmission is calculated by averaging GASE of source and relay transmission steps, while noting that each step finishes half of data transmission, as

$$\eta_R = \frac{1}{2}\left\{ \frac{\overline{\mathrm{C}}_R}{\mathrm{A}_{SR}} + \frac{\overline{\mathrm{C}}_R}{\mathrm{A}_{RD}} \right\}. \tag{4.11}$$

Under Rayleigh fading environment, the received SNR Γ_{ij} ($i \in \{S, R\}, j \in \{R, D\}$ and i $\neq j$) can be expressed as $\Gamma_{ij} = \bar{\gamma}_{ij} \cdot Z$, where $\bar{\gamma}_{ij} = \frac{P_i}{d_{ij}^a \cdot N}$ is the average received SNR related to the distance from the transmitter i to receiver j, d_{ij}. Z is an exponential RV with unit mean. It follows that the PDF of $\Gamma_{\mathrm{eq}}^{DF}$ can be obtained, noting that $\Gamma_{\mathrm{eq}}^{DF}$ is the minimum of two exponential RVs, as

$$f_{\Gamma_{\mathrm{eq}}^{DF}}(\gamma) = \alpha_1 \cdot e^{-\alpha_1 \gamma}, \tag{4.12}$$

where $\alpha_1 = \frac{1}{\bar{\gamma}_{SR}} + \frac{1}{\bar{\gamma}_{RD}}$. Then the ergodic capacity for DF case can be derived as

$$\overline{\mathrm{C}}_{DF} = \frac{1}{2\ln 2}\, \mathrm{E}_1(\alpha_1) \exp(\alpha_1). \tag{4.13}$$

Finally, GASE of DF relay transmission for Rayleigh fading scenario is given, after applying (4.4) and (4.13) into (4.11), by

$$\eta_R^{DF} = \frac{1}{4\ln 2} \left\{ \frac{\mathrm{E}_1(\alpha_1)\exp(\alpha_1)}{\frac{2\pi}{a}\Gamma\left(\frac{2}{a}\right)\left(\frac{P_S}{P_{\min}}\right)^{2/a}} + \frac{\mathrm{E}_1(\alpha_1)\exp(\alpha_1)}{\frac{2\pi}{a}\Gamma\left(\frac{2}{a}\right)\left(\frac{P_R}{P_{\min}}\right)^{2/a}} \right\}. \tag{4.14}$$

For AF relaying, the PDF of the equivalent SNR $\Gamma_{\mathrm{eq}}^{AF}$ is approximately obtained as [68, eq. (18)]

$$f_{\Gamma_{\mathrm{eq}}^{AF}}(\gamma) = 2\beta_1 \gamma e^{-\alpha_1 \gamma} \left\{ \alpha_1\, \mathrm{K}_1(2\beta_1\gamma) + 2\beta_1\, \mathrm{K}_0(2\beta_1\gamma) \right\}, \tag{4.15}$$

where $\beta_1 = \frac{1}{\sqrt{\bar{\gamma}_{SR} \cdot \bar{\gamma}_{RD}}}$, $\mathrm{K}_0(\cdot)$ and $\mathrm{K}_1(\cdot)$ is the second kind modified Bessel function of the zero-order and first-order, respectively [67]. Substituting (4.15) into (4.10), we

can calculate ergodic capacity of relay transmission with AF protocol as

$$\overline{\mathrm{C}}_{AF} = \int_0^\infty \log_2(1+\gamma)\beta_1\gamma e^{-\alpha_1\gamma} \times \Big\{\alpha_1 \,\mathrm{K}_1(2\beta_1\gamma) + 2\beta_1 \,\mathrm{K}_0(2\beta_1\gamma)\Big\}\mathrm{d}\gamma. \tag{4.16}$$

The GASE performance of AF-based relay transmissions can be similarly calculated by applying (4.16) in (4.11).

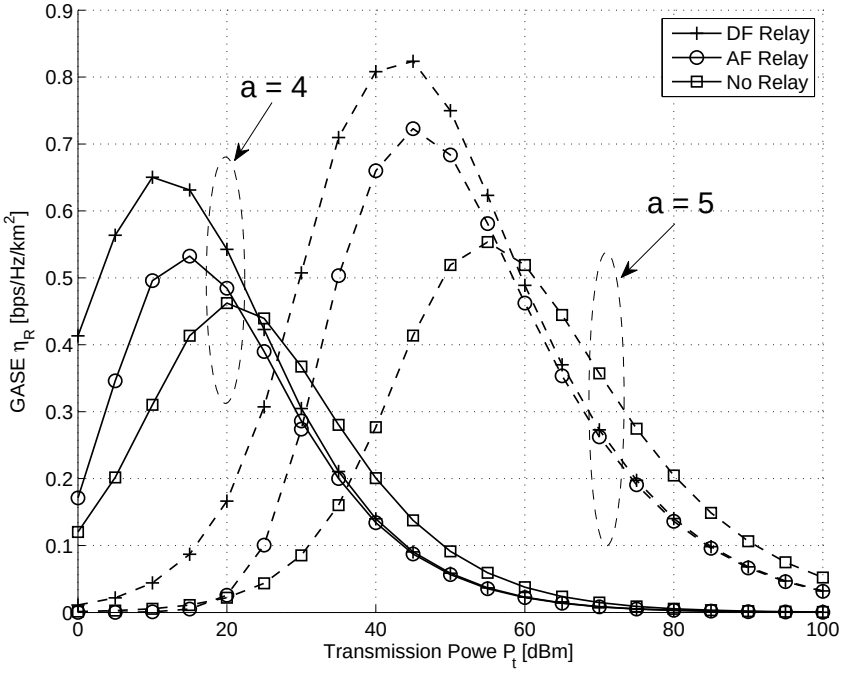

Figure 4.3: Comparison of the dual-hop relay transmission and point-to-point transmission.

In Fig. 4.3, we compare the GASE of dual-hop relay transmission with point-to-point transmission. The distance between source to destination $d_{SD} = 1000$ m, between source to relay $d_{SR} = d_{RD} = 500$ m, and the angle $\theta = 0$. Specifically, the GASE of both DF and AF cases are plotted as function of common transmission power $P_S = P_R = P_t$ for different values of path loss exponent a. The relay node R is assumed to be at the center point along the line between S and D. As we can see, similar to the point-to-point transmission case, there exist optimal values for transmitting power P_t in terms of maximizing GASE of dual-hop relay transmission. Based on the analytical results on GASE, the optimal transmitting power for relay

transmissions can be obtained by solving the following optimization problem

$$\max_{P_S, P_R \in \mathbb{R}^+} \eta_R \quad s.t. \quad P_S < P_{\max}, P_R < P_{\max}, \tag{4.17}$$

where $P_{\max}$ is the maximum transmission power of the nodes. For DF relaying under Rayleigh fading environment, after applying (4.13) and (4.4), the objective function specializes to

$$\eta_R^{DF} = \frac{a}{8\pi \ln 2 \cdot \Gamma\left(\frac{2}{a}\right)} \mathrm{E}_1(\alpha_1) \exp(\alpha_1) \times \left(\left(\frac{P_S}{P_{\min}} \right)^{-2/a} + \left(\frac{P_R}{P_{\min}} \right)^{-2/a} \right). \tag{4.18}$$

The resulting optimization problem can be easily solved numerically. We also note from Fig. 4.3 that the maximum GASE of relay transmission are much higher and can be achieved with much smaller transmission power than point-to-point transmission. From this perspective, introducing a relay node can greatly improve the greenness of wireless transmissions. On the other hand, if the transmission power are set too large, the GASE of point-to-point transmission becomes slightly larger than that of relay transmission, partly due to the half duplex constraint on relay transmission. Therefore, dual-hop relay transmission is more energy efficient than point-to-point transmission only when the transmission power is adjusted to proper values.

4.3 GASE Analysis for Cooperative Relay Transmission

Previous section investigates the GASE performance of relay transmission and ignores the direct source to destination link. In this section, we utilize GASE metric to quantify the spectrum as well as power utilization efficiency of cooperative transmissions while taking into account the spatial effects of each transmission stage. We focus on a three-node cooperative relay transmission where relaying is activated only if it will lead to higher instantaneous capacity. In particular, the source node decides to perform either direct or relay transmission to communicate with the destination node based on the instantaneous link capacity. Therefore, the instantaneous capacity

of such three-node cooperative transmission is given by

$$\mathrm{C}_{\text{inst}} = \max\left\{\mathrm{C}_{\mathrm{d}}, \mathrm{C}_{\mathrm{r}}\right\}, \tag{4.19}$$

where C_{d} and C_{r} are the instantaneous capacity of direct transmission and relay transmission, respectively. C_{d} is related to the instantaneous received SNR of S-D link, Γ_{SD}, as

$$\mathrm{C}_{\mathrm{d}} = \log_2(1+\Gamma_{SD}), \tag{4.20}$$

The instantaneous capacity of relay transmission C_{r} is given by

$$\mathrm{C}_{\mathrm{r}} = \frac{1}{2}\log_2(1+\Gamma_{\mathrm{eq}}), \tag{4.21}$$

where Γ_{eq} is the equivalent received SNR of the relay channel, and the factor $\frac{1}{2}$ is due to the half-duplex constraint. Substituting (4.20) and (4.21) into (4.19), the instantaneous capacity specializes to

$$\begin{aligned}\mathrm{C}_{\text{inst}} &= \frac{1}{2}\max\left\{\log_2(1+\Gamma_{SD})^2, \log_2(1+\Gamma_{eq})\right\} \\ &= \frac{1}{2}\log_2\left\{1+\underbrace{\max\left\{\Gamma_{SD}^2+2\Gamma_{SD}, \Gamma_{\mathrm{eq}}\right\}}_{\Gamma_{\mathrm{C}}}\right\},\end{aligned} \tag{4.22}$$

where Γ_{C} is the overall equivalent received SNR of the three-node cooperative transmission. The ergodic capacity can be derived by averaging the instantaneous capacity over the distribution of Γ_{C}, i.e.,

$$\overline{\mathrm{C}} = \int_0^\infty \frac{1}{2}\log_2\left(1+\gamma\right)\cdot f_{\Gamma_{\mathrm{C}}}(\gamma)\,\mathrm{d}\gamma, \tag{4.23}$$

where $f_{\Gamma_{\mathrm{C}}}(\gamma)$ is the PDF of Γ_{C}. Meanwhile, the probability that the system performs direct transmission is equal to the probability that $\mathrm{C}_{\mathrm{d}} > \mathrm{C}_{\mathrm{r}}$, i.e.,

$$\mathcal{P}_{\mathrm{d}} = \mathbb{P}\left\{\Gamma_{SD}^2+2\Gamma_{SD} > \Gamma_{\mathrm{eq}}\right\}. \tag{4.24}$$

Accordingly, the probability that the system performs relay transmission is given by $\mathcal{P}_{\mathrm{r}} = 1-\mathcal{P}_{\mathrm{d}}$.

The GASE of three-node cooperative transmission, denoted by η_C, can be cal-

culated, while noting that the affected areas of source and relay transmissions are different, as

$$\eta_C = \mathcal{P}_{\rm d} \cdot \frac{\overline{\rm C}_{\rm d}}{{\rm A}_{SR}} + \mathcal{P}_{\rm r} \cdot \frac{1}{2}\left(\frac{\overline{\rm C}_{\rm r}}{{\rm A}_{SR}} + \frac{\overline{\rm C}_{\rm r}}{{\rm A}_{RD}}\right), \tag{4.25}$$

where ${\rm A}_{SR}$ and ${\rm A}_{RD}$ are the affected areas for the source and relay transmission steps, which can be calculated using (4.4) with correspondent transmission power; $\overline{\rm C}_{\rm d}$ and $\overline{\rm C}_{\rm r}$ are the average ergodic capacity under direct and relay transmission. In what follows, we will calculate $\overline{\rm C}_{\rm d}$ and $\overline{\rm C}_{\rm r}$ for DF and AF relaying protocols under Rayleigh fading environment.

4.3.1 DF Relaying Protocol

Under Rayleigh fading environment, $\Gamma_{SD} = \overline{\gamma}_{SD} \cdot Z$ and $Z \sim \mathcal{E}(1)$, $\mathcal{P}_{\rm d}$ can be specialized to

$$\mathcal{P}_{\rm d} = \frac{1}{\overline{\gamma}_{SD}} \int_0^\infty F_{\Gamma_{\rm eq}}(x^2 + 2x) \exp(-x/\overline{\gamma}_{SD})\, {\rm d}x. \tag{4.26}$$

With DF relaying, the PDF of equivalent received SNR over relay link, $\Gamma_{\rm eq}^{DF}$, is given by (4.12). Substituting (4.12) into (4.26) and carrying out integration, we can obtain the probability that the system performs direct transmission with DF relaying protocol, as

$$\mathcal{P}_{\rm d}^{DF} = 1 - \frac{1}{\overline{\gamma}_{SD}} \mathfrak{D}(\alpha_1, \alpha_2), \tag{4.27}$$

where $\alpha_1 = \frac{1}{\overline{\gamma}_{SR}} + \frac{1}{\overline{\gamma}_{RD}}$, $\alpha_2 = \frac{2}{\overline{\gamma}_{SR}} + \frac{2}{\overline{\gamma}_{RD}} + \frac{1}{\overline{\gamma}_{SD}}$, and $\mathfrak{D}(\alpha_1, \alpha_2)$ is defined as

$$\mathfrak{D}(\alpha_1, \alpha_2) \triangleq \int_0^\infty e^{-\alpha_1 t^2 - \alpha_2 t} {\rm d}t = \frac{1}{2}\sqrt{\frac{\pi}{\alpha_1}} e^{\frac{\alpha_2^2}{4\alpha_1}} \, {\rm erfc}\left(\frac{\alpha_2}{2\sqrt{\alpha_1}}\right), \tag{4.28}$$

where ${\rm erfc}(x) = \frac{2}{\sqrt{\pi}} \int_x^\infty e^{-t^2} {\rm d}t$ is the complementary error function [67].

The equivalent SNR of the three-node cooperative network with DF protocol is given by

$$\Gamma_{\rm C}^{DF} = \max\left\{\Gamma_{SD}^2 + 2\Gamma_{SD}, \Gamma_{\rm eq}^{DF}\right\}. \tag{4.29}$$

It can be shown that the PDF of $\Gamma_{\rm C}^{DF}$ under the condition $\Gamma_{SD}^2 + 2\Gamma_{SD} > \Gamma_{\rm eq}^{DF}$ is given by

$$f_{\Gamma_{\rm C}^{DF}}(\gamma \mid \Gamma_{SD}^2 + 2\Gamma_{SD} > \Gamma_{\rm eq}^{DF}) = \frac{\overline{\gamma}_{SD} \cdot f_{\Gamma_{SD}}(\xi) \cdot F_{\Gamma_{\rm eq}^{DF}}(\gamma)}{2(\xi + 1) \cdot (\overline{\gamma}_{SD} - \mathfrak{D}(\alpha_1, \alpha_2))}, \tag{4.30}$$

where $\xi = \sqrt{\gamma + 1} - 1$. Substituting (4.30) into (4.23) and making some manipula-

tions, we can obtain the average ergodic capacity of direct transmission as

$$\overline{\mathrm{C}}_{\mathrm{d}}^{DF} = \frac{1}{\ln 2\,(\overline{\gamma}_{SD} - \mathfrak{D}(\alpha_1,\alpha_2))}\left\{\overline{\gamma}_{SD}\cdot e^{\frac{1}{\overline{\gamma}_{SD}}}\,\mathrm{E}_1(\frac{1}{\overline{\gamma}_{SD}}) - \int_0^{\infty}\ln(1+t)e^{-\alpha_1 t^2-\alpha_2 t}\,\mathrm{d}t\right\}. \quad (4.31)$$

Following the same procedure, we can arrive at the PDF of Γ_{C}^{DF} under the condition $\Gamma_{SD}^2 + 2\Gamma_{SD} < \Gamma_{\mathrm{eq}}^{DF}$ as

$$f_{\Gamma_{\mathrm{C}}^{DF}}(\gamma \mid \Gamma_{SD}^2 + 2\Gamma_{SD} < \Gamma_{\mathrm{eq}}^{DF}) = \frac{\overline{\gamma}_{SD}\cdot f_{\Gamma_{\mathrm{eq}}^{DF}}(\gamma)\cdot F_{\Gamma_{SD}}(\xi)}{\mathfrak{D}(\alpha_1,\alpha_2)}. \quad (4.32)$$

It follows that the average ergodic capacity of relay transmission is given by

$$\overline{\mathrm{C}}_{\mathrm{r}}^{DF} = \frac{1}{\ln 2\cdot\mathfrak{D}(\alpha_1,\alpha_2)}\left\{\overline{\gamma}_{SD}\cdot e^{\alpha_1}\,\mathrm{E}_1(\alpha_1) - \int_0^{\infty}\ln(1+t)\cdot e^{-\alpha_1 t-\frac{1}{\overline{\gamma}_{SD}}(\sqrt{1+t}-1)}\mathrm{d}t\right\}. \quad (4.33)$$

4.3.2 AF Relaying Protocol

With AF relaying protocol, the PDF of the equivalent received SNR over relay link, $\Gamma_{\mathrm{eq}}^{AF}$, is given by (4.15). Substituting (4.15) into (4.26), we can obtain the probability that the source node performs direct transmission, denoted by $\mathcal{P}_{\mathrm{d}}^{AF}$, i.e.,

$$\mathcal{P}_{\mathrm{d}}^{AF} = 1 - \frac{1}{\overline{\gamma}_{SD}}\mathfrak{A}(\beta_1,\beta_2), \quad (4.34)$$

where $\mathfrak{A}(\beta_1,\beta_2)$ is defined to be

$$\mathfrak{A}(\beta_1,\beta_2) \triangleq \int_0^{\infty} 2\beta_1(t^2+2t)e^{-\beta_2(t^2+2t)}\,\mathrm{K}_1(2\beta_1(t^2+2t))\,\mathrm{d}t, \quad (4.35)$$

where $\beta_1 = \frac{1}{\sqrt{\overline{\gamma}_{SR}\cdot\overline{\gamma}_{RD}}}$, $\beta_2 = \frac{1}{\overline{\gamma}_{SD}} + \frac{1}{\overline{\gamma}_{SR}} + \frac{1}{\overline{\gamma}_{RD}}$.

The equivalent SNR of the three-node cooperative transmission with AF protocol is given by

$$\Gamma_{\mathrm{C}}^{AF} = \max\left\{\Gamma_{SD}^2 + 2\Gamma_{SD}, \Gamma_{\mathrm{eq}}^{AF}\right\}. \quad (4.36)$$

The PDF of Γ_{C}^{AF} under the condition $\Gamma_{SD}^2 + 2\Gamma_{SD} > \Gamma_{\mathrm{eq}}^{AF}$ can be obtained as

$$f_{\Gamma_{\mathrm{C}}^{AF}}(\gamma \mid \Gamma_{SD}^2 + 2\Gamma_{SD} > \Gamma_{\mathrm{eq}}^{AF}) = \frac{\overline{\gamma}_{SD}\cdot f_{\Gamma_{SD}}(\xi)\cdot F_{\Gamma_{\mathrm{eq}}^{AF}}(\gamma)}{2(\xi+1)\cdot(\overline{\gamma}_{SD} - \mathfrak{A}(\beta_1,\beta_2))}. \quad (4.37)$$

Correspondingly, we can calculate the average ergodic capacity of direct transmission

$\overline{\mathrm{C}}_{\mathrm{d}}^{AF}$ by averaging the instantaneous capacity over the PDF of Γ_{C}^{AF} under the condition $\Gamma_{SD}^2 + 2\Gamma_{SD} > \Gamma_{\mathrm{eq}}^{AF}$ given in (4.37), as

$$\overline{\mathrm{C}}_{\mathrm{d}}^{AF} = \int_0^\infty \frac{1}{2}\log_2\left(1+\gamma\right) \cdot \frac{\overline{\gamma}_{SD} \cdot f_{\Gamma_{SD}}(\xi) \cdot F_{\Gamma_{\mathrm{eq}}^{AF}}(\gamma)}{2(\xi+1)\cdot(\overline{\gamma}_{SD} - \mathfrak{A}(\beta_1,\beta_2))}\,\mathrm{d}\gamma. \tag{4.38}$$

Similarly, the PDF of Γ_{C}^{AF} under the condition $\Gamma_{SD}^2 + 2\Gamma_{SD} < \Gamma_{\mathrm{eq}}^{AF}$ is given by

$$f_{\Gamma_{\mathrm{C}}^{AF}}(\gamma \mid \Gamma_{SD}^2 + 2\Gamma_{SD} < \Gamma_{\mathrm{eq}}^{AF}) = \frac{\overline{\gamma}_{SD} \cdot f_{\Gamma_{\mathrm{eq}}^{AF}}(\gamma) \cdot F_{\Gamma_{SD}}(\xi)}{\mathfrak{A}(\beta_1,\beta_2)}, \tag{4.39}$$

which can be applied to the calculation of $\overline{\mathrm{C}}_{\mathrm{r}}^{AF}$. The resulting expression is omitted for conciseness.

4.3.3 Numerical Examples

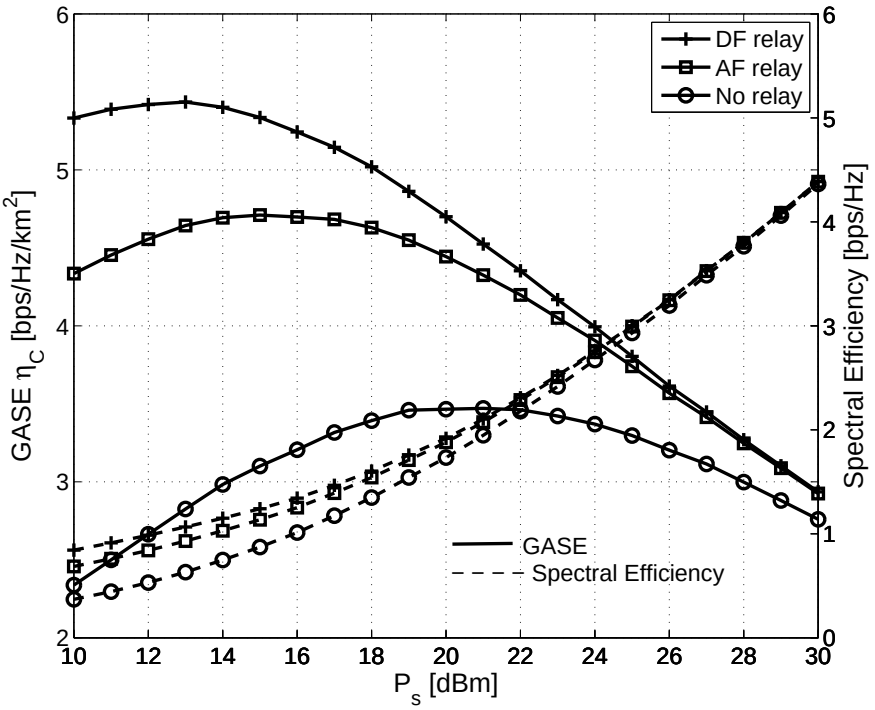

Figure 4.4: The effect of the source node transmission power P_S on GASE with DF and AF relaying protocol.

In Fig. 4.4 we plot the GASE and spectral efficiency as function of the source node transmission power P_S for DF and AF relaying protocol. The relay transmission power $P_R = 10$ dBm, the distances between source, relay and destination are $d_{SD} = 1000$ m, $d_{SR} = d_{RD} = 500$ m, respectively. For comparison, we include the GASE curve of conventional point-to-point transmission without relays. It shows that the cooperative transmission always enjoy better GASE performance than its conventional counterpart. Meanwhile, the DF relaying protocol has slightly better overall performance than AF relaying protocol. However, this performance gain shrinks as the transmission power P_S increases. Unlike spectral efficiency, whose performance curves are monotonically increasing function with respect to P_S, the GASE curves show a peak as transmission powers increase. This observation indicates that increasing the transmission power can lead to a higher spectral efficiency but can not necessarily increase GASE. Therefore, GASE provide a new perspective on transmission power selection for wireless transmitters. Another interesting observation is that the optimal transmission power, in terms of maximizing the GASE, for point-to-point transmission is much larger than that for cooperative relay transmission. In summary, cooperative relay transmission can enjoy much higher energy efficiency than point-to-point transmission when the relay is properly located.

4.4 GASE Analysis for Two-User X Channels

In this section, we generalize the GASE analysis to parallel interference channels, as illustrated in Fig. 4.5. Specifically, two transmitters, S_1 and S_2, send information to two receivers, D_1 and D_2, respectively, over the same frequency band. Such interference channels, also known as X channels, occur due to insufficient spatial separation between transmitters/receivers and as a result, there are mutual interference between transmissions. There has been growing interest on the capacity analysis and precoder design for X channels where both transmitters and receivers have multiple antennas, which can be explored for interference mitigation [60–62]. In this dissertation, we investigate the area spectral efficiency of the benchmark scenario where all transmitters and receivers have a single antenna, while leaving the MIMO X channel as a topic for future research.

The distance and channel power gain from S_i to D_j, $i, j \in \{1, 2\}$ are denoted by d_{ij} and $|h_{ij}|^2$, respectively. Assuming that the same transmitting power P_t is used at

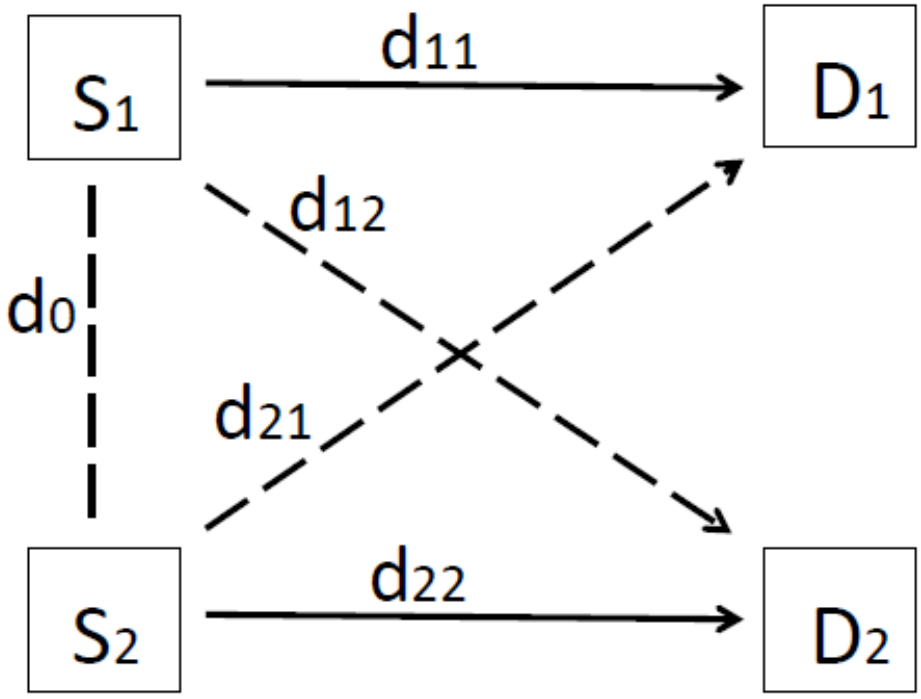

Figure 4.5: Two-user X channels

S_1 and S_2, the instantaneous sum capacity of the X channel is given by

$$\mathrm{C}^X = \log_2(1+\Gamma_1) + \log_2(1+\Gamma_2), \tag{4.40}$$

where Γ_i, $i = 1, 2$, denote the received signal to interference plus noise ratio (SINR) at receiver D_i, given by

$$\Gamma_1 = \frac{P_t|h_{11}|^2}{P_t|h_{21}|^2 + N}, \quad \Gamma_2 = \frac{P_t|h_{22}|^2}{P_t|h_{12}|^2 + N}. \tag{4.41}$$

It follows that the ergodic capacity of the X channel can be calculated as

$$\overline{\mathrm{C}}^X = \sum_{i=1}^{2} \int_0^\infty \log_2(1+\gamma) \cdot f_{\Gamma_i}(\gamma) \mathrm{d}\gamma, \tag{4.42}$$

where $f_{\Gamma_i}(\cdot)$ is the PDF of SINR Γ_i. Based on definition for affected area adopted in this work, a particular area is affected if the total received signal power from both transmitter is greater than $P_{\min}$. Specifically, the probability that an area of distance

r_1 to transmitter S_1 and distance r_2 to transmitter S_2 is affected can be calculated as the probability that the total received signal power $P_r(r_1) + P_r(r_2)$ is greater than $P_{\min}$, i.e. $\Pr[P_r(r_1) + P_r(r_2) \geq P_{\min}]$. It follows that the affected area of parallel transmission can be calculated as

$$\mathrm{A}_{\mathrm{aff}}^{X} = \frac{1}{2\pi} \int_0^{2\pi} \int_0^{\infty} \Pr[P_r(r_1) + P_r(r_2) \geq P_{\min}] r_1 \mathrm{d}r_1 \mathrm{d}\theta, \tag{4.43}$$

where $r_2 = \sqrt{r_1^2 + d_0^2 - 2r_1 d_0 \cos\theta}$ and d_0 is the distance between S_1 and S_2. Note that we use the location of S_1 as the origin in the about integration. The GASE of two-user X channels can finally be calculated as $\eta_g^X = \overline{\mathrm{C}}^X / \mathrm{A}_{\mathrm{aff}}^X$.

For Rayleigh fading environment, $|h_{ij}|^2$ are modeled as independent exponential random variables with mean $1/d_{ij}^a$. Then CDF of Γ_i can be derived as

$$F_{\Gamma_i}(\gamma) \;\; = \;\; 1 - \frac{\rho_i}{\gamma + \rho_i} \exp(-\gamma/\bar{\gamma}_{ii}), \;\; i = 1, 2, \tag{4.44}$$

where $\bar{\gamma}_{ii} = P_t/(N d_{ii}^a)$, $\rho_1 = (d_{21}/d_{11})^a$ and $\rho_2 = (d_{12}/d_{22})^a$. It follows that the ergodic capacity of X channel over Rayleigh fading can be calculated, after substituting (4.44) into (4.50) with applying integration by part, as

$$\overline{\mathrm{C}}^X = \sum_{i=1}^{2} \begin{cases} \frac{1}{\ln 2} \frac{\rho_i}{1-\rho_i} \left\{ \mathrm{E}_1(\frac{\rho_i}{\bar{\gamma}_{ii}}) \exp(\frac{\rho_i}{\bar{\gamma}_{ii}}) - \mathrm{E}_1(\frac{1}{\bar{\gamma}_{ii}}) \exp(\frac{1}{\bar{\gamma}_{ii}}) \right\} & \rho_i \neq 1 \\ \frac{1}{\ln 2} \left\{ 1 - \frac{1}{\bar{\gamma}_{ii}} \mathrm{E}_1(\frac{1}{\bar{\gamma}_{ii}}) \exp(\frac{1}{\bar{\gamma}_{ii}}) \right\} & \rho_i = 1. \end{cases} \tag{4.45}$$

Specifically, the ergodic capacity is a function of ρ_i and $\bar{\gamma}_{ii}$, which are determined by transmission power P_t, path loss exponent a and the distance between the transmitter S_i and receiver D_j. It is easy to verify that when $\rho_i \to \infty$, which means the interfering transmitters are far from the desired receiver, the sum capacity of X channels becomes the sum of the ergodic capacity of two point-to-point channels.

For Rayleigh fading environment, the PDF of the total received signal power at a location of distance r_1 to transmitter S_1 and distance r_2 to transmitter S_2, $Z = \mathcal{P}_r(r_1) + \mathcal{P}_r(r_2)$, can be obtained as

$$f_Z(z) = \begin{cases} \frac{1}{P_t/r_1^a - P_t/r_2^a} \left(e^{-\frac{r_1^a}{P_t} z} - e^{-\frac{r_2^a}{P_t} z} \right), & r_1 \neq r_2 \\ \frac{z r_1^{2a}}{P_t^2} e^{-\frac{r_1^a}{P_t} z}, & r_1 = r_2. \end{cases} \tag{4.46}$$

Accordingly, the probability that this location is affected is determined as

$$\Pr[P_r(r_1)+P_r(r_2)\geq P_{\min}]=\begin{cases}\frac{1}{1-(r_1/r_2)^a}e^{-\frac{P_{\min}r_1^a}{P_t}}+\frac{1}{1-(r_2/r_1)^a}e^{-\frac{P_{\min}r_2^a}{P_t}}, & r_1\neq r_2\\ (P_{\min}r_1^a/P_t+1)e^{-\frac{P_{\min}r_1^a}{P_t}}, & r_1=r_2.\end{cases} \tag{4.47}$$

Substituting (4.57) into (4.55), we can numerically calculate the affected area, which can then be applied, together with (4.45), to evaluate the GASE of two-user X channels over Rayleigh fading environment.

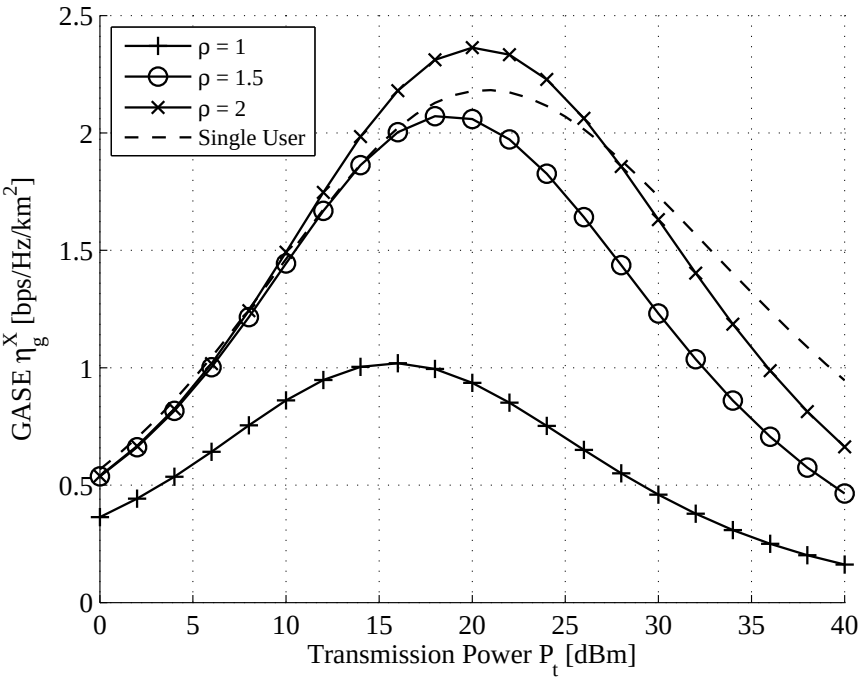

Figure 4.6: The effect of transmission power P_t on η_g^X.

Fig. 4.6 plots the GASE of X channels over Rayleigh fading as the function of the common transmitting power of both transmitters P_t for different value of $\rho_1 = \rho_2 = \rho$. The distance $d = d_0 = 1000$ m, $d_{11} = d_{22} = 1000$ m, respectively. Note that ρ is the ratio of the distance to interfering transmitter to desired transmitter, which characterizes the severeness of mutual interference between transmissions. For reference, we also plot the GASE of single user point-to-point channel η_g^S with the same system configuration. As we can see, two-user parallel transmission can achieve higher GASE than single user transmission only when ρ is much greater than 1, i.e.

interfering transmitter is much farther away than desired transmitter. The reason is that when ρ is small, the capacity benefit due to parallel transmission is limited because of mutual interference while the parallel transmission will affect a larger area than single user transmission. Similar to the single user transmission case, there is an optimal choice of the transmitting power level for each value of ρ. Finally, when comparing the curves for X channel with $\rho = 2$ and single user cases, we notice that although the X channel achieves higher maximum GASE, its GASE performance deteriorates faster than single users cases as P_t increases, mainly due to the increasing level of interference.

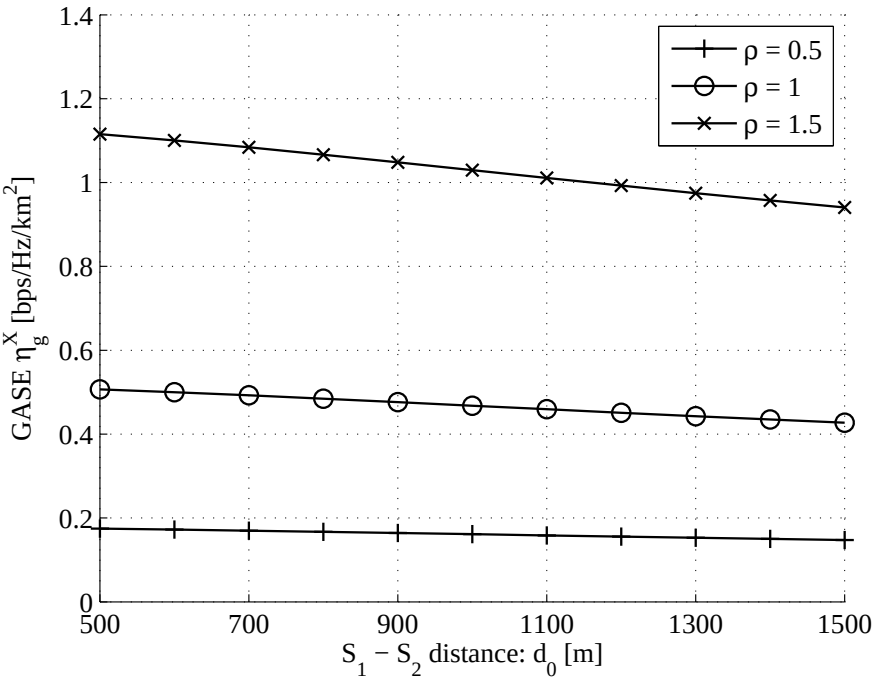

Figure 4.7: The effect of distance d_0 on η_g^X.

In Fig. 4.7, we examine the effect of the distance between two transmitters d_0 on the GASE performance for X channel. Note that the distance between the receiver and the interference transmitter d_{21} should satisfy $|d_0 - d_{11}| < d_{21} < |d_0 + d_{11}|$, Therefore, $\rho_1 = d_{21}/d_{11}$ should be bounded as $|d_0/d_{11} - 1| < \rho_1 < |d_0/d_{11} + 1|$. Similar bound applies to ρ_2. We can see that the GASE slightly decreases as d_0 increases when ρ is small and the decrease becomes more noticeable as ρ becomes larger. We also observe that the effect of the distance ratio ρ on the area spectral

efficiency of X channels is much more significant than d_0.

4.5 GASE Analysis for Underlay Cognitive Radio Transmission

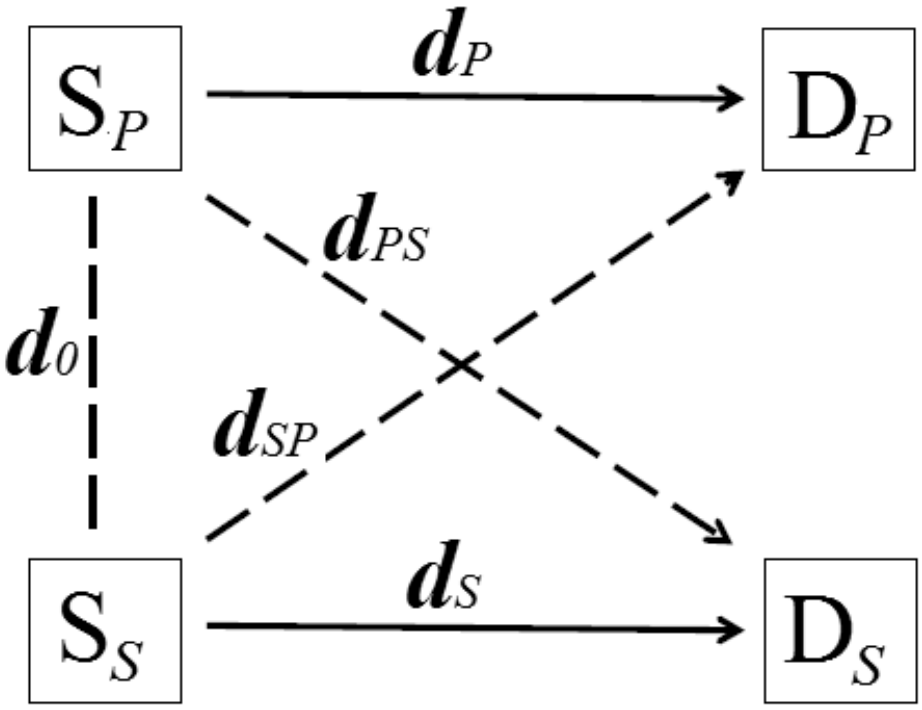

Figure 4.8: System model of underlay cognitive radio transmission.

So far, we have studied the scenarios where only a single transmitter is operating at any time. In this section, we generalize the analysis to consider the case where parallel transmission occurs. Specifically, we extend the GASE analysis to underlay cognitive radio transmission and examine the effect of interference on overall spectral utilization efficiency while taking into account the larger spatial footprint of parallel transmission. We consider the transmission scenario as illustrated in Fig. 4.8. The primary user S_P transmits to the primary receiver D_P with transmission power P_1. Meanwhile, the secondary user S_S opportunistically communicates with the secondary receiver D_S using the same frequency bandwidth with transmission power P_2. Both transmitters use omni-directional antennas. As such, the primary user (secondary

user) will generate interference on the secondary receiver (primary receiver). The distance of the transmission link between S_P (S_S) and D_P (D_S) is denoted as d_P (d_S); whereas the distance of the interference link between S_P (S_S) and D_S (D_P) is denoted as d_{PS} (d_{SP}). The distance between P_T and S_T is denoted as d_0. In the underlay paradigm, the secondary user is allowed to utilize the primary user's spectrum as long as the interference it generates on the primary receiver is below a pre-determined threshold I_{th}. Otherwise, the secondary user should remain silent. We assume that, by exploring the channel reciprocity, the secondary transmitter can predict the amount of interference that its transmission will generate to the primary receiver.

We first focus on the scenario where parallel secondary transmission occurs, i.e., the received interference power from secondary transmitter at the primary receiver is less than I_{th}. Based on the path loss and fading model adopted in this work, this interference power is given by $P_2 \cdot Z/d_{SP}^a$. As such, the probability that the parallel transmission occurs is then given by $\mathcal{P} = \mathbb{P}\left\{P_2 \cdot Z/d_{SP}^a < I_{th}\right\}$. Under Rayleigh fading environment, this probability specializes to

$$\mathcal{P} = 1 - \exp\left(-\frac{I_{th} \cdot d_{SP}^a}{P_2}\right). \tag{4.48}$$

Ergodic capacity analysis

In the underlay cognitive transmission scenario, the total instantaneous capacity of both primary and secondary transmissions is given by $\mathrm{C}_{CR} = \log_2\left(1+\Gamma_p\right) + \log_2\left(1+\Gamma_s\right)$, where Γ_p and Γ_s denote the received signal-to-interference-plus-noise ratio (SINR) at primary receiver D_P and secondary receiver D_S, respectively. Based on the adopted path loss and fading models, Γ_p and Γ_s can be shown to be given by

$$\Gamma_p = \frac{P_1 \cdot Z_P/d_P^a}{P_2 \cdot Z_{SP}/d_{SP}^a + N}, \quad \Gamma_s = \frac{P_2 \cdot Z_S/d_S^a}{P_1 \cdot Z_{PS}/d_{PS}^a + N}, \tag{4.49}$$

respectively. It follows that the ergodic capacity of the parallel transmission channel can be calculated as

$$\overline{\mathrm{C}}_{CR} = \underbrace{\int_0^\infty \log_2(1+\gamma) \cdot \mathrm{d}F_{\Gamma_p}(\gamma)}_{\overline{\mathrm{C}}_{CR}^p} + \underbrace{\int_0^\infty \log_2(1+\gamma) \cdot \mathrm{d}F_{\Gamma_s}(\gamma)}_{\overline{\mathrm{C}}_{CR}^s}, \tag{4.50}$$

where $F_{\Gamma}(\cdot)$ denotes the cdf of SINR Γ.

Under Rayleigh fading environment, the cdf of Γ_p, $F_{\Gamma_p}(\cdot)$, can be derived, while considering the interference constraint on D_P, as

$$F_{\Gamma_p}(\gamma) = 1 - \exp\left(-\frac{d_{SP}^a \cdot I_{th}}{P_2}\right) - \frac{\rho_p}{\gamma+\rho_p}\exp\left(-\frac{d_P^a \cdot N}{P_1}\gamma\right) \times \left\{1 - \exp\left(-\frac{d_{SP}^a \cdot I_{th}}{P_2}\right)\exp\left(-\frac{d_P^a \cdot I_{th}}{P_1}\gamma\right)\right\}, \tag{4.51}$$

where $\rho_p = \frac{P_1}{P_2}\left(\frac{d_{SP}}{d_P}\right)^a$. It follows that the ergodic capacity of the primary user in the parallel channel over Rayleigh fading can be calculated, after substituting (4.51) into the first part of (4.50) and applying integration by part, as

$$\overline{\mathrm{C}}_{CR}^{p} = \begin{cases} \frac{1}{\ln 2}\frac{\rho_p}{1-\rho_p}\left\{\mathfrak{F}\left(\frac{d_P^a N}{P_1}\rho_p\right) - \mathfrak{F}\left(\frac{d_P^a N}{P_1}\right) - \exp\left(-\frac{d_{SP}^a I_{th}}{P_2}\rho_p\right) \times \left\{\mathfrak{F}\left(\frac{d_P^a (N+I_{th})}{P_1}\rho_p\right) - \mathfrak{F}\left(\frac{d_P^a N}{P_1}\right)\right\}, & \rho_p \neq 1, \\ \frac{1}{\ln 2}\left\{1 - \frac{d_P^a N}{P_1}\mathfrak{F}\left(\frac{d_P^a N}{P_1}\right) - \exp\left(-\frac{d_{SP}^a I_{th}}{P_2}\right) \times \left\{1 - \frac{d_P^a (N+I_{th})}{P_1}\mathfrak{F}\left(\frac{d_P^a (N+I_{th})}{P_1}\right)\right\}\right\}, & \rho_p = 1, \end{cases} \tag{4.52}$$

where $\mathfrak{F}(x) \triangleq \exp(x)\cdot \mathrm{E}_1(x)$.

The cdf of Γ_s can be similarly obtained, but without the interference power constraint, as

$$F_{\Gamma_s}(\gamma) = 1 - \frac{\rho_s}{\gamma+\rho_s}\exp\left(-\frac{d_S^a N}{P_2}\gamma\right), \tag{4.53}$$

where $\rho_s = \frac{P_2}{P_1}\left(\frac{d_{PS}}{d_S}\right)^a$. Finally, the ergodic capacity of the secondary user with the presence of primary user interference is given by

$$\overline{\mathrm{C}}_{CR}^{s} = \begin{cases} \frac{1}{\ln 2}\frac{\rho_s}{1-\rho_s}\left\{\mathfrak{F}\left(\frac{d_S^a N}{P_2}\rho_s\right) - \mathfrak{F}\left(\frac{d_S^a N}{P_2}\right)\right\}, & \rho_s \neq 1, \\ \frac{1}{\ln 2}\left\{1 - \frac{d_S^a N}{P_2}\mathfrak{F}\left(\frac{d_S^a N}{P_2}\right)\right\}, & \rho_s = 1. \end{cases} \tag{4.54}$$

Affected area analysis

Based on the definition of affected area adopted in this work, a particular area is affected if the total received signal power from both transmitters is greater than $P_{\min}$. Specifically, the probability that an incremental area of distance r_p to the

primary transmitter S_P and distance r_s to secondary transmitter S_S is affected can be calculated as the probability that the total received signal power $P_r(r_p)+P_r(r_s)$ is greater than $P_{\min}$, i.e., $\mathbb{P}\Big\{P_r(r_p)+P_r(r_s)\geq P_{\min}\Big\}$. It follows that the affected area of parallel transmission can be calculated as

$$\mathrm{A}_{CR}^{pt}=\int_0^{2\pi}\int_0^{\infty}\mathbb{P}\Big\{P_r(r_p)+P_r(r_s)\geq P_{\min}\Big\}r_p\mathrm{d}r_p\mathrm{d}\theta, \tag{4.55}$$

where $r_s=\sqrt{r_p^2+d_0^2-2r_pd_0\cos\theta}$. Note that we use the location of S_P as the origin in the about integration.

Under Rayleigh fading environment, the PDF of the total received signal power at a location of distance r_p to transmitter S_P and distance r_s to transmitter S_S, $X=P_r(r_p)+P_r(r_s)$, can be obtained as

$$f_X(x)=\begin{cases}\frac{1}{\lambda_p-\lambda_s}\Big(e^{-\lambda_p x}-e^{-\lambda_s x}\Big), & \lambda_p\neq\lambda_s,\\ \frac{x}{\lambda_p^2}e^{-\lambda_p x}, & \lambda_p=\lambda_s,\end{cases} \tag{4.56}$$

where $\lambda_i=P_i/r_i^a$, $i\in\{p,s\}$. Accordingly, the probability that this location is affected is determined as

$$\mathbb{P}\Big\{P_r(r_p)+P_r(r_s)\geq P_{\min}\Big\}=\begin{cases}\frac{1}{1-\lambda_p/\lambda_s}e^{-P_{\min}/\lambda_p}+\frac{1}{1-\lambda_s/\lambda_p}e^{-P_{\min}/\lambda_s}, & \lambda_p\neq\lambda_s\\ (1+P_{\min}/\lambda_p)e^{-P_{\min}/\lambda_p}, & \lambda_p=\lambda_s.\end{cases} \tag{4.57}$$

Substituting (4.57) into (4.55), we can numerically calculate the affected area of underlay cognitive radio transmission with parallel transmission, A_{CR}^{pt}. The GASE of parallel transmission over Rayleigh fading channel can be calculated as

$$\eta_{CR}^{pt}=\frac{\overline{\mathrm{C}}_{CR}^{p}+\overline{\mathrm{C}}_{CR}^{s}}{\mathrm{A}_{CR}^{pt}}. \tag{4.58}$$

When the parallel secondary transmission is prohibited, i.e., the interference power constraint $P_2\cdot Z/d_{SP}^a<I_{th}$ on D_P is not satisfied, the secondary user is not allowed to utilize the primary user's spectrum. Therefore, the parallel transmission channel simplifies to the point-to-point link, whose GASE η_{CR}^{st} is given by (4.6) with the transmission power P_t and distance d substituted by P_1 and d_P, respectively. Finally,

GASE for underlay cognitive radio transmission can be written as

$$\eta_{CR} = \mathcal{P} \cdot \eta_{CR}^{pt} + (1 - \mathcal{P}) \cdot \eta_{CR}^{st}. \tag{4.59}$$

Note that the GASE expression derived above for underlay cognitive radio transmission will reduce to that for the X channels, resulted from insufficient spatial separation between receivers [60–62], when the interference threshold approaches infinity. In particular, when $I_{th} \to \infty$, $\mathcal{P}$ approaches to 1, which means two transmitters, S_P and S_S, always transmit simultaneously over the same frequency band. The GASE of X channels is then given by [69, eq. 17]

$$\eta_X = \frac{\overline{\mathrm{C}}_{CR}^{p'} + \overline{\mathrm{C}}_{CR}^{s}}{\mathrm{A}_{CR}^{pt}}, \tag{4.60}$$

where

$$\overline{\mathrm{C}}_{CR}^{p'} = \lim_{I_{th}\to\infty} \overline{\mathrm{C}}_{CR}^{p} = \begin{cases} \frac{1}{\ln 2}\frac{\rho_p}{1-\rho_p}\left\{\mathfrak{F}\left(\frac{d_P^a N}{P_1}\rho_p\right) - \mathfrak{F}\left(\frac{d_P^a N}{P_1}\right)\right\}, & \rho_p \neq 1, \\ \frac{1}{\ln 2}\left\{1 - \frac{d_P^a N}{P_1}\mathfrak{F}\left(\frac{d_P^a N}{P_1}\right)\right\}, & \rho_p = 1. \end{cases} \tag{4.61}$$

and $\overline{\mathrm{C}}_{CR}^{s}$ and A_{CR}^{pt} are given in (4.54) and (4.55), respectively.

Numerical examples

In Fig. 4.9, we investigate the effect of the maximum tolerable interference power I_{th} on GASE performance of underlay cognitive radio systems. To simplify the notation and discussion, we denote the ratio of the interfering link distance to transmission link distance for primary receiver by $\kappa_p = d_{SP}/d_P$ and that for the secondary receiver by $\kappa_s = d_{PS}/d_S$. Note that the distance of the interfering link between S_S and D_P, d_{SP}, should satisfy $|d_0 - d_P| < d_{SP} < |d_0 + d_P|$. Therefore, $\kappa_p = d_{SP}/d_P$ should be bounded as $|d_0/d_P - 1| < \kappa_p < |d_0/d_P + 1|$. Similar bound applies to κ_s. In Fig. 4.9, we plot GASE of underlay cognitive radio transmission as function of I_{th} while fixing $\kappa_p = \kappa_s = \kappa = 1.5$. The transmission power $P_1 = P_2 = 20$ dBm, the threshold $P_{\min} = -100$ dBm, and the distance $d_0 = d_P = d_S = 100$ m. We can see that as I_{th} decreasing, the GASE performance of underlay cognitive radio transmission converges to that of the point-to-point transmission case. This behavior can be explained that when $I_{th} \to 0$, the probability of parallel transmission $\mathcal{P}$ given in (4.48) approaches to

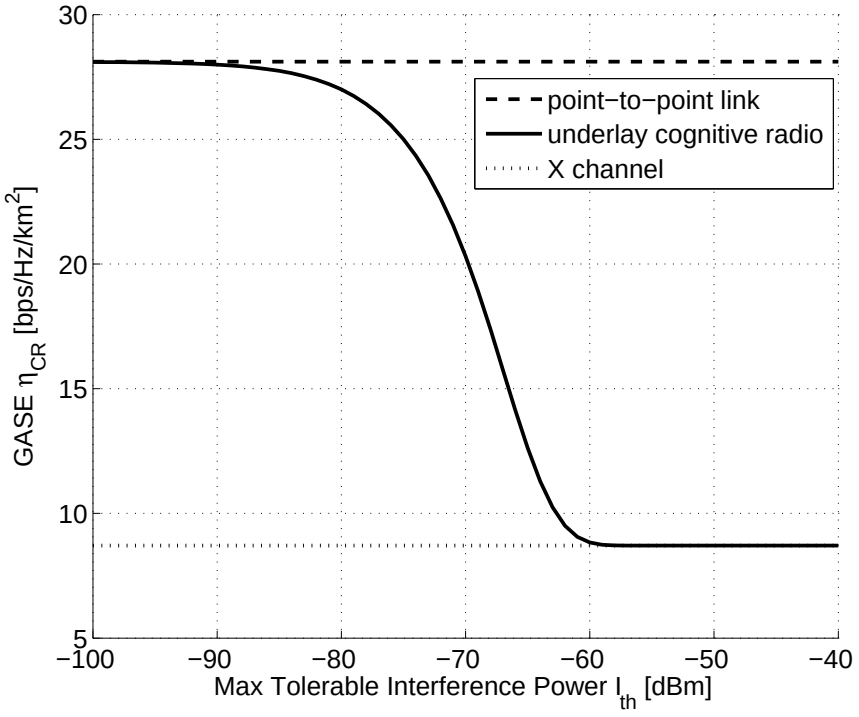

Figure 4.9: The effect of the max tolerable interference power I_{th} on GASE.

0. On the other hand, when $I_{th} \to \infty$, the GASE performance of underlay cognitive radio transmission converges to that of X channels, as expected by intuition. We also notice that the GASE performance of underlay cognitive radio transmission is always worse than that of point-to-point transmission case but better than X channel transmission for the chosen system parameters. In the next numerical example, we explore under what scenario underlay cognitive transmission will lead to better GASE performance.

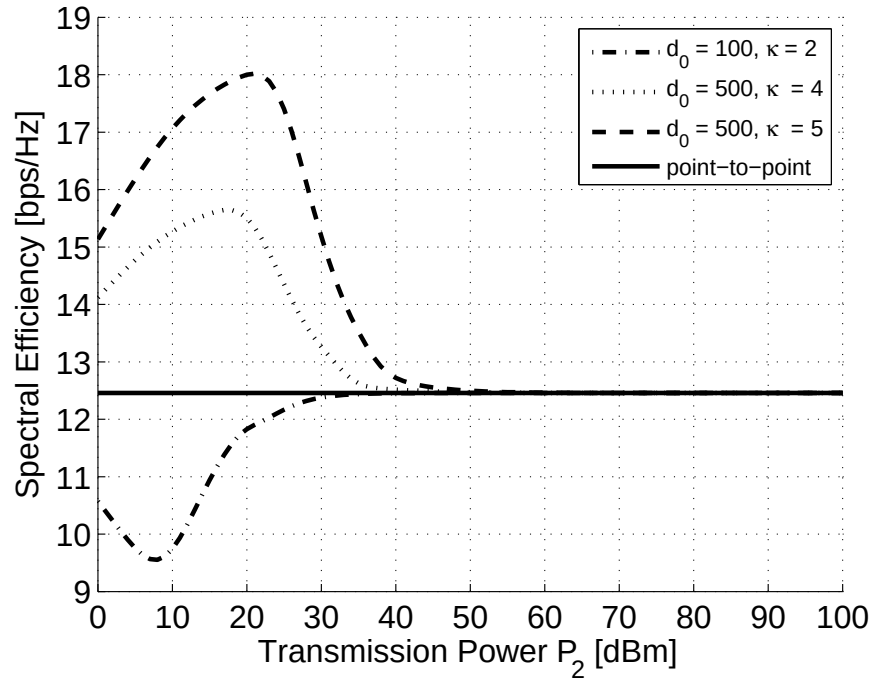

(a) Spectral Efficiency

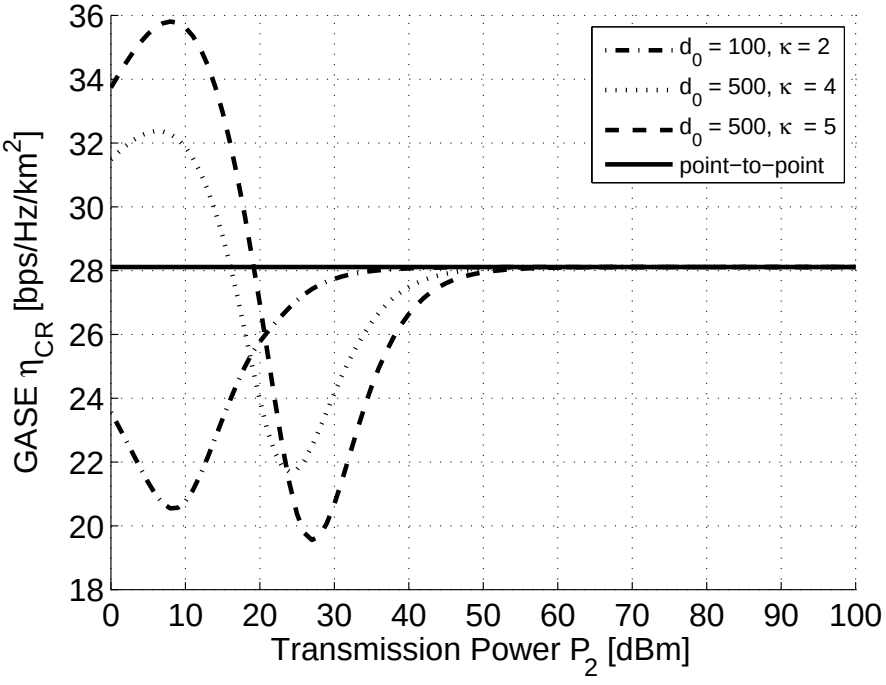

(b) GASE

Figure 4.10: The effect of the transmission power of secondary user P_2 on the system overall spectral efficiency and GASE.

In Fig. 4.10, we compare GASE metric with conventional spectral efficiency of underlay cognitive radio systems. The primary transmission power $P_1 = 20$ dBm, the threshold $P_{\min} = -100$ dBm and interference threshold $I_{th} = -80$ dBm, and the distance $d_P = d_S = 100$ m. Specifically, we plot overall spectral efficiency in Fig. 4.10a and GASE in Fig. 4.10b as function of the transmission power of secondary user P_2 for different system parameters. As we can see, when the interfering transmitter is close to the target receiver, i.e., κ is small, introducing underlay cognitive transmission always deteriorates the overall system spectral efficiency as well as the GASE performance. Basically, capacity gain incurred by the spectrum sharing through parallel transmission cannot compensate the capacity loss caused by the mutual interference, even with underlaying interference threshold requirement. The interference requirement at the primary user may protect the primary user transmission but the secondary transmission will suffer severe interference from primary user transmission. This observation also justifies the practical understanding that the radio spectrum should not be simultaneously used by other transmissions very close to the transmitter and/or the receiver. On the other hand, when κ is large, the underlay cognitive radio transmission results in different behaviors in terms of spectral efficiency and GASE. First, the underlay cognitive radio transmission always benefits from the secondary user transmission in terms of spectral efficiency when the transmission power is not very large, as shown in Fig. 4.10a. However, with respect to the GASE performance metric, the underlay cognitive radio transmission may benefit from the secondary user only if its transmission power is carefully selected. Otherwise, the overall GASE performance may be greatly deteriorated by the secondary cognitive transmission, as shown in Fig. 4.10b. Therefore, subject to GASE performance metric, the power allocation for spectrum sharing transmission should be carefully designed. Finally, both of the spectral efficiency and GASE curve show the same asymptotic approach to point-to-point link as increasing P_2. This is because when $P_2 \to \infty$, the probability of parallel transmission $\mathcal{P}$ given in (4.48) approaches to 0. Under this circumstance, the performance of the cognitive radio transmission approaches to that of the point-to-point link, as shown in the large P_2 region in Fig. 4.10.

4.6 Conclusion

In this chapter, we generalized the conventional ASE performance metric to study the performance of arbitrary wireless transmissions while considering the spatial effect of wireless transmissions. We carried out a comprehensive study on the resulting GASE performance metric by considering point-to-point transmission, dual-hop relay transmission, cooperative relay transmission, two-user X channel as well as cognitive radio transmission. Through analytical results and selected numerical examples, we showed that our research provided a new perspective on the design, evaluation and optimization of arbitrary wireless transmissions, especially with respect to the transmission power selection. Meanwhile, we show that relay transmission is power efficient and can greatly improve the greenness of wireless transmissions. Finally, the study on underlay cognitive radio transmission implied that, if the power of secondary transmitter is not properly chosen, the secondary user may degrade the GASE performance of overall system, even worse than that of the point-to-point primary transmission only case. While the analysis focuses on single antenna per node scenario, the generalization of the analysis to multiple antenna cases is straightforward. The GASE metric can also apply to the spectral utilization efficiency of wireless ad hoc network and femtocell enhanced cellular systems after proper adaptation.

Chapter 5

Spatial Spectral Efficiency Analysis for Randomly Distributed Wireless System

In this chapter, we study the spatial spectral efficiency for randomly distributed wireless networks. We first develop the aggregate interference statistics in Poisson field over Rayleigh fading channels. Specifically, we derived the generic closed-form MGF expression of aggregate interference. This result is generic and can be applied both in finite and infinite region. Then we apply the closed-from MGF expression of aggregate interference in the calculation of ergodic capacity, affected area and GASE of wireless ad hoc network. Besides, we analyze the effect of transmitter coordination on the network performance. We find that in sparse network, non CSMA/CA network achieves better ergodic capacity. However, in dense network, CSMA/CA network can ameliorate the increase of aggregate interference level and achieve the same amount of ergodic capacity with fewer transmitters than non CSMA/CA network. We also analyze the effect of transmission power on the performance of wireless ad hoc network and provide a new perspective on the transmission power optimization. Finally, we propose a new cognitive radio scheme to explore spatial spectrum resource of wireless network. We analyze the effect of this scheme in terms of ergodic capacity, affected area and GASE of two-tier cognitive network. We find that although it deteriorates GASE performance of two-tier cognitive network, secondary network is able to increase ergodic capacity as well as exploit spatial spectrum resource of wireless network. However, numerical examples show that the network performance

is sensitive to the number of secondary transmitters and their transmission power. Moreover, GASE metric offers a new perspective on transmitter intensity selection and transmission power optimization.

5.1 System Model and Interference Statistics

5.1.1 System Model

We consider a wireless network in two-dimensional homogeneous space $\mathbb{R}^2$. The transmitters in the network are distributed according to Poisson point process $\Pi = \{r_i\}$ of intensity λ, where r_i's are the random distances between the transmitters and the origin of the space. We assume all the transmitters are equipped with omni-directional antennas and share the same frequency bandwidth. Each transmitter communicates with one and only one receiver. For each transmitter-receiver pair, the distance between transmitter and receiver d is uniformly distributed in the region (d_l, d_h), whose PDF is given by

$$f(d) = \frac{2(d - d_l)}{(d_h - d_l)^2}, \qquad d_l < d < d_h. \tag{5.1}$$

The transmitted signal will experience path loss and multipath fading effect. For the sake of clarity, we ignore the shadowing effect.

5.1.2 Interference Statistics

With homogeneous assumption, the interference statistics at the reference node R_0 located at the origin of $\mathbb{R}^2$ is applicable to any other locations in $\mathbb{R}^2$. As such, the interference analysis in the following section is generic and applicable to any points in $\mathbb{R}^2$. The aggregate interference experienced by the origin is given, under the assumption of non-coherent addition of interference power, by

$$I = \sum_{i \in \Pi} \overline{\gamma}_i \cdot z_i, \tag{5.2}$$

where $\overline{\gamma}_i = P_t / r_i^a$ and z_i is the fading power gain for the i^{th} transmitter. Note that the individual interference signal is assumed to follow the same power decaying law. In addition, the random locations of the transmitters are distributed in $\mathbb{R}^2$ according to Poisson point process $\Pi = \{r_i\}$ of intensity λ. Therefore, the aggregate interference power I can be modeled as shot noise [38]. It follows that the MGF of the aggregate

interference power I from the area of $r_l \leq r_i \leq r_h$ is given by [35]

$$\Phi_I(s) = \exp\Big\{ -\pi\lambda\Psi_I(s)\Big\}, \tag{5.3}$$

where $\Psi_I(s)$ is given by

$$\begin{aligned}\Psi_I(s) =& \underbrace{r_h^2\,\mathrm{E}_Z\big[1-e^{-\overline{\gamma}_h zs}\big]+(P_t s)^{\frac{2}{a}}\,\mathrm{E}_Z\Big[z^{\frac{2}{a}}\Gamma\big(1-\frac{2}{a},\overline{\gamma}_h zs\big)\Big]}_{\Psi_h(s)} \\ &- \underbrace{\Big\{r_l^2\,\mathrm{E}_Z\left[1-e^{-\overline{\gamma}_l zs}\right]+(P_t s)^{\frac{2}{a}}\,\mathrm{E}_Z\left[z^{\frac{2}{a}}\Gamma\big(1-\frac{2}{a},\overline{\gamma}_l zs\big)\right]\Big\}}_{\Psi_l(s)},\end{aligned} \tag{5.4}$$

where $\mathrm{E}_Z[\cdot]$ is the expectation with respect to Z, and $\Gamma(\alpha,x)=\int_x^\infty e^{-t}t^{\alpha-1}\,\mathrm{d}t$ is the incomplete gamma function defined in [67, 8.350]. Over Rayleigh fading channels, Z is an exponential RV with unit mean. It can be shown that

$$\mathrm{E}_Z\left[1-e^{-\overline{\gamma}_h zs}\right]=\frac{\overline{\gamma}_h s}{1+\overline{\gamma}_h s}. \tag{5.5}$$

Applying [67, 6.455.1], we can further show that

$$\mathrm{E}_Z\left[z^{\frac{2}{a}}\,\Gamma\left(1-\frac{2}{a},\overline{\gamma}_h zs\right)\right]=\frac{\big(\overline{\gamma}_h s\big)^{1-\frac{2}{a}}}{(1+\frac{2}{a})(1+\overline{\gamma}_h s)^2}\,F\left(1,2;2+\frac{2}{a};\frac{1}{1+\overline{\gamma}_h s}\right), \tag{5.6}$$

where $F(\mu_1,\mu_2;\nu;t)$ is the Gauss hypergeometric function defined in [67, 9.111]. Substituting (5.5), (5.6) into (5.4) and applying [67, 9.137.4], $\Psi_I(s)$ can be simplified to

$$\Psi_I(s)=\frac{\overline{\gamma}_h r_h^2 s}{1+\overline{\gamma}_h s}\,F\left(1,1;1+\frac{2}{a};\frac{1}{1+\overline{\gamma}_h s}\right)-\frac{\overline{\gamma}_l r_l^2 s}{1+\overline{\gamma}_l s}\,F\left(1,1;1+\frac{2}{a};\frac{1}{1+\overline{\gamma}_l s}\right). \tag{5.7}$$

Finally, after substituting (5.7) into (5.3), we can obtain the MGF of the aggregate interference power I over Rayleigh fading channels, as

$$\Phi_I(s)=\exp\left\{-\pi\lambda\left[\frac{\overline{\gamma}_h r_h^2 s}{1+\overline{\gamma}_h s}\,F\big(1,1;1+\frac{2}{a};\frac{1}{1+\overline{\gamma}_h s}\big)-\frac{\overline{\gamma}_l r_l^2 s}{1+\overline{\gamma}_l s}\,F\big(1,1;1+\frac{2}{a};\frac{1}{1+\overline{\gamma}_l s}\big)\right]\right\}. \tag{5.8}$$

From (5.4), we can also derive MGF of the aggregate interference for several special cases as follows.

Infinite space

When $r_h \to \infty$, the transmitters are distributed in an infinite space. It can be shown that $\Psi_h^{\infty}(s) = k(sP_t)^{\frac{2}{a}}$, where $k = \frac{2\pi/a}{\sin(2\pi/a)}$. MGF of the aggregate interference in infinite area is given by

$$\Phi_{\infty}(s) = \exp\left\{ -\pi\lambda\left[k(sP_t)^{\frac{2}{a}} - \frac{\overline{\gamma}_l r_l^2 s}{1+\overline{\gamma}_l s}\, F\big(1,1;1+\frac{2}{a};\frac{1}{1+\overline{\gamma}_l s}\big)\right]\right\}. \tag{5.9}$$

Continuous space

When $r_l = 0$, the space is continuous without singular point at the origin. It can be obtained that $\Psi_l^0(s) = 0$, and MGF of aggregate interference in continuous area is given by

$$\Phi_0(s) = \exp\left\{ -\pi\lambda\frac{\overline{\gamma}_h r_h^2 s}{1+\overline{\gamma}_h s}\, F\big(1,1;1+\frac{2}{a};\frac{1}{1+\overline{\gamma}_h s}\big)\right\}. \tag{5.10}$$

Continuous infinite space

For nodes distributed in continuous infinite space, its aggregate interference MGF is given by

$$\Phi_{(0,\infty)}(s) = \exp\Big\{ -\pi\lambda k(sP_t)^{\frac{2}{a}}\Big\}. \tag{5.11}$$

The PDF of the aggregate interference I, $f_I(x)$, can be derived by applying the inverse Laplace transform on $\Phi_I(s)$, i.e. $f_I(x) = \mathfrak{L}^{-1}\big\{\Phi_I(s)\big\}$. Due to the complexity of $\Phi_I(s)$, no generic closed-form expression is known for $f_I(x)$. However, for special case ($r_l = 0, r_h \to \infty$, and $a = 4$), its PDF can be derived from (5.11), and is given by

$$f_I(x) = \frac{\lambda}{4}\left(\frac{\pi P_t}{x}\right)^{\frac{3}{2}} \exp\left\{-\frac{P_t\pi^4\lambda^2}{16x}\right\}, \tag{5.12}$$

which is equivalent to [35, eq. 11]. Correspondingly, its CDF expression, $F_I(x)$, is given by

$$F_I(x) = \operatorname{erfc}\left(\frac{\sqrt{P_t}\lambda\pi^2}{4\sqrt{x}}\right). \tag{5.13}$$

5.2 GASE Analysis for Wireless Ad Hoc Networks

GASE is defined as the ratio of overall effective ergodic capacity of the transmission link over the affected area of the transmission, where a significant amount of transmission power is observed and parallel transmissions over the same frequency will suffer high interference level [69]. In this dissertation, we extend the GASE analysis to network level. Specifically, we analyze GASE performance of wireless ad hoc network in Poisson field over Rayleigh fading channels. We first derive the total ergodic capacity and affected area of wireless ad hoc network by applying the statistics of aggregate interference obtained in the above section. Then GASE of such network is given by the ergodic capacity over the affected area. This network-level GASE analysis not only considers the transmission power of individual node in the network, but also the node intensity and co-channel interference among them. Furthermore, we employ CSMA/CA mechanism in wireless ad hoc network and analyze the impact of node coordination on system GASE performance. Through mathematical analysis and numerical examples, we compare the system performance of wireless network with and without CSMA/CA in terms of ergodic capacity, affected area and GASE.

5.2.1 Ergodic Capacity Analysis

The total ergodic capacity of wireless network is given by

$$C_{\text{total}} = \sum_{i=1}^{\lambda\Omega} C_i(d_i), \tag{5.14}$$

where λ is the intensity of the transmitters, Ω is the total area of $\mathbb{R}^2$, $d_i \in [d_l, d_h]$ is the distance among the ith transmitter-receiver pair, and $C_i(d_i)$ is the ergodic capacity of individual transmitter-receiver pair. It follows that the ergodic capacity $C_i(d_i)$ can be calculated by averaging the instantaneous capacity, $\mathcal{C} = \log_2(1 + \mathbf{\Gamma}_i)$, over the distribution of the received signal-to-interference-plus-noise ratio (SINR), $\mathbf{\Gamma}_i$, as

$$C_i(d_i) = \int_0^\infty \log_2(1 + \mathbf{\Gamma}_i)\, \mathrm{d}F_{\mathbf{\Gamma}_i}(\gamma), \tag{5.15}$$

where $\mathbf{\Gamma}_i = \frac{\mathbf{P}_i}{\mathbf{I}+N}$, $\mathbf{P}_i$ is the received signal power, $\mathbf{I}$ is the aggregate interference power, N is the noise power, and $F_{\mathbf{\Gamma}_i}(\gamma)$ is the CDF of $\mathbf{\Gamma}_i$. Over Rayleigh fading channels, the received signal power $\mathbf{P}_i$ follows exponential distribution with average received

signal power determined by the path loss, i.e. $\mathbf{P}_i \sim \mathcal{E}(d_i^a/P_t)$. It can be shown that the CDF of the SINR at the receiver is given by

$$F_{\mathbf{\Gamma}_i}(\gamma) = P\left\{\frac{\mathbf{P}_i}{\mathbf{I}+N} < \gamma\right\} = 1 - \exp\left(-\frac{Nd_i^a}{P_t}\gamma\right)\Phi_I\left(\frac{d_i^a}{P_t}\gamma\right), \tag{5.16}$$

where $\Phi_I(\cdot)$ is the MGF of the aggregate interference given by (5.8). Substitute (5.16) into (5.15) and make some manipulations, the ergodic capacity of individual transmitter-receiver pair can be written as

$$C_i(d_i) = \frac{1}{\ln 2}\int_0^\infty \frac{e^{-\frac{Nd_i^a}{P_t}\gamma}}{1+\gamma}\Phi_I\left(\frac{d_i^a}{P_t}\gamma\right)\mathrm{d}\gamma. \tag{5.17}$$

When $\lambda\Omega$ is sufficiently large, C_{total} can be approximately calculated as

$$C_{\text{total}} = \lambda\Omega\int_{d_l}^{d_h} C(d)f(d)\,\mathrm{d}d, \tag{5.18}$$

where $f(d)$ is the PDF of the distance d among a pair of transmitter-receiver given by (5.1). Substitute (5.1) and (5.17) into (5.18), we can arrive at

$$C_{\text{total}} = \kappa\int_{d_l}^{d_h}\int_0^\infty \lambda e^{-\frac{Nd^a}{P_t}\gamma}\Phi_I\left(\frac{d^a}{P_t}\gamma\right)\frac{d-d_l}{1+\gamma}\,\mathrm{d}\gamma\,\mathrm{d}d, \tag{5.19}$$

where $\kappa = \frac{2\Omega}{\ln 2\cdot(d_h-d_l)^2}$. For continuous infinite space, substituting (5.11) into (5.19), we can arrive at

$$C_{(0,\infty)} = \kappa\int_{d_l}^{d_h}\int_0^\infty \lambda\underbrace{\exp(-\pi\lambda k d^2\gamma^{\frac{2}{a}})}_{\mathfrak{F}_I}\times\underbrace{\exp(-Nd^a\gamma/P_t)}_{\mathfrak{F}_N}(d-d_l)/(1+\gamma)\,\mathrm{d}\gamma\,\mathrm{d}d, \tag{5.20}$$

where $\mathfrak{F}_N = \exp(-Nd^a\gamma/P_t)$ presents the effect of transmission and noise power on ergodic capacity, and $\mathfrak{F}_I = \exp(-\pi\lambda k d^2\gamma^{\frac{2}{a}})$ presents the effect of aggregate interference on ergodic capacity. Note that when $N/P_t \to 0$, $\mathfrak{F}_N \to 1$.

5.2.2 GASE Result

The affected area is defined as the area where the aggregate interference power is greater than a threshold value I_{th}. Mathematically speaking, the affected area can

be calculated as

$$\mathrm{A}_{\mathrm{aff}} = \oint_{\mathbb{R}^2} \Pr[I > I_{\mathrm{th}}] \mathrm{d}\mathbf{S}. \tag{5.21}$$

As we assume the interference statistics is identical on the homogeneous space $\mathbb{R}^2$, the affected area can be written as

$$\mathrm{A}_{\mathrm{aff}} = \Big(1 - F_I(I_{\mathrm{th}})\Big)\Omega, \tag{5.22}$$

where $F_I(I_{\mathrm{th}})$ is the CDF of the aggregate interference. Finally, with (5.18) and (5.22), the overall GASE is given by

$$\eta = \frac{C_{\mathrm{total}}}{\mathrm{A}_{\mathrm{aff}}} = \frac{\lambda \int_{d_l}^{d_h} C(d) f(d)\, \mathrm{d}d}{1 - F_I(I_{\mathrm{th}})}. \tag{5.23}$$

5.2.3 Effect of CSMA/CA

The above section considered the transmitters in wireless ad hoc networks distributed according to Poisson point process, which implies that the transmitters' locations are independent with each other. However, this strong assumption is not valid in most practical wireless ad hoc networks. Medium Access Control (MAC) protocol ensures that two close transmitters cannot transmit simultaneously by implementing the CSMA/CA mechanism. Before establishing a successful connection with the target receiver, the transmitter broadcasts a Request-to-Send (RTS) signal with power P_{RTS}. Other transmitters that receive the RTS signaling will postpone their transmissions. If only considering the path loss effect, the transmitter defines a guard zone with radius R_{RTS}, proportional to P_{RTS}. As such, the distance between two active transmitters should be larger than R_{RTS}. Poisson point process does not take this constraint into account and leads to inaccuracy in the distribution of active transmitters in wireless ad hoc network that implements CSMA/CA mechanism. Alternatively, we introduce Matèrn point process [44] to model the spatial distribution of active transmitters in CSMA/CA network.

Matèrn point process can be obtained by thinning an underlying Poisson point process. Specifically, we consider a collection of potential transmitters $\{X_i\}_{i=1,\ldots,K}$ independently and uniformly distributed in $\mathbb{R}^2$, where K is an RV describing the total potential transmitters in $\mathbb{R}^2$ and follows a discrete Poisson Law. The K potential transmitters constitute the underlying Poisson point process Π_0 with intensity λ_0. To

build Matèrn point process $\Theta(K)$, the transmitters X_1 is first selected into the active transmitters set $\mathcal{X}$. At the i^{th} step, the transmitters X_i is selected into $\mathcal{X}$ if and only if none of the previous $i-1$ transmitters lies in a circle centered at X_i with radius R_{RTS}. The procedure stops when all the K transmitters have been considered. As such, the transmitters $\{X_j\}_{j=1,\ldots,N(K)}$ constitute a Matèrn point process $\Theta(K)$, where $N(K)$ is a RV describing the number of active transmitters selected into $\Theta(K)$ from the total K potential transmitters in Π_0. Without considering the boundary effect, the active transmitter intensity of Matèrn point process λ_m can be calculated as

$$\lambda_m = \frac{1 - e^{-\lambda\pi R_{\text{RTS}}^2}}{\pi R_{\text{RTS}}^2}. \tag{5.24}$$

We can follow the same procedure as previous sections to determine the statistics of aggregate interference as well as the ergodic capacity by substituting λ with λ_m.

The affected area of wireless ad hoc network that implements CSMA/CA mechanism is given by

$$\text{A}_{\text{CSMA/CA}} = \bigcup_{X_i\in\Theta} \mathcal{B}_{X_i} + \oint_{\mathbb{R}^2\setminus\bigcup_{X_i\in\Theta}\mathcal{B}_{X_i}} \Pr\{I > I_{\text{th}}\}\text{d}\mathbf{S}. \tag{5.25}$$

The first part, $\bigcup_{X_i\in\Theta}\mathcal{B}_{X_i}$, represents the union area of circles $\mathcal{B}_{X_i}$'s centered at the active transmitters, X_i's, with radius R_{RTS}. According to [44], it approximates to

$$\bigcup_{X_i\in\Theta} \mathcal{B}_{X_i} \approx (1-e^{-\lambda\pi R_{\text{RTS}}^2})\Omega - \frac{\Omega}{\pi R_{\text{RTS}}^2}\int_{R_{\text{RTS}}}^{2R_{\text{RTS}}} \mathfrak{F}_1(y)\left(\frac{1-e^{-\lambda\mathfrak{F}_2(y)}}{\mathfrak{F}_2(y)} - \frac{e^{-\lambda\pi R_{\text{RTS}}^2} - e^{-\lambda\mathfrak{F}_1(y)}}{\mathfrak{F}_2(y) - \pi R_{\text{RTS}}^2}\right)2\pi y\text{d}y, \tag{5.26}$$

where

$$\begin{cases} \mathfrak{F}_1(y) = \nu(\mathcal{B}_o \cap \mathcal{B}_y) = 2R_{\text{RTS}}^2\cos^{-1}(\frac{y}{2R_{\text{RTS}}}) - \frac{1}{2}y\sqrt{4R_{\text{RTS}}^2 - y^2}, \\ \mathfrak{F}_2(y) = \nu(\mathcal{B}_o \cup \mathcal{B}_y) = 2\pi R_{\text{RTS}}^2 - \nu(\mathcal{B}_o \cap \mathcal{B}_y). \end{cases} \tag{5.27}$$

The second part represents the area outside $\bigcup_{X_i\in\Theta}\mathcal{B}_{X_i}$ and the aggregate interference power of which is greater than I_{th}. Under homogeneous assumption, it can be written as

$$\oint_{\mathbb{R}^2\setminus\bigcup_{X_i\in\Theta}\mathcal{B}_{X_i}} \Pr\{I > I_{\text{th}}\}\text{d}\mathbf{S} = \left(\Omega - \bigcup_{X_i\in\Theta}\mathcal{B}_{X_i}\right)\left(1 - F_I(I_{\text{th}})\right). \tag{5.28}$$

Substituting (5.28) into (5.25), we can arrive at the affected area of CSMA/CA net-

work, as

$$\mathrm{A}_{\mathrm{CSMA/CA}} = \bigcup_{X_i \in \Theta} \mathcal{B}_{X_i} \cdot F_I(I_{\mathrm{th}}) + \Big(1 - F_I(I_{\mathrm{th}})\Big)\Omega. \tag{5.29}$$

Finally, GASE of the wireless network with CSMA/CA is given by

$$\eta = \frac{\lambda_m \Omega C}{\bigcup_{X_i \in \Theta} \mathcal{B}_{X_i} \cdot F_I(I_{\mathrm{th}}) + \Big(1 - F_I(I_{\mathrm{th}})\Big)\Omega}. \tag{5.30}$$

5.2.4 Numerical Examples

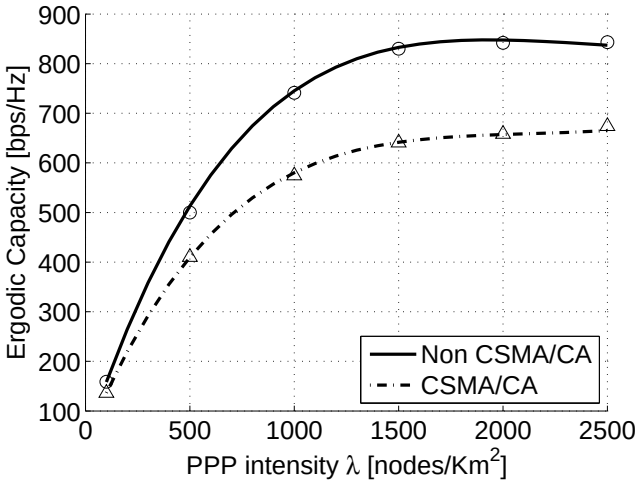

(a) Ergodic capacity

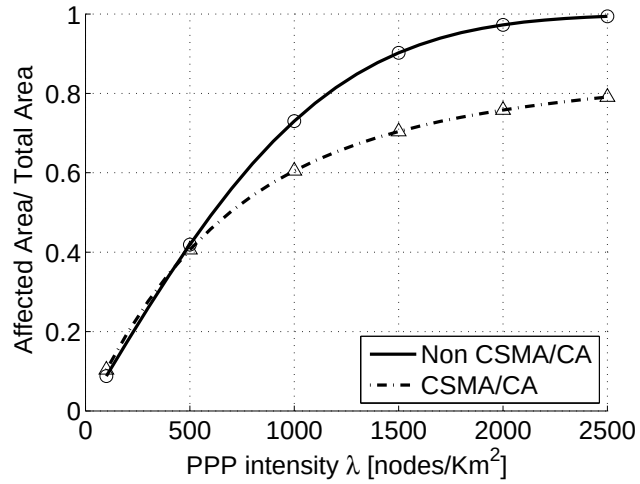

(b) Affected area

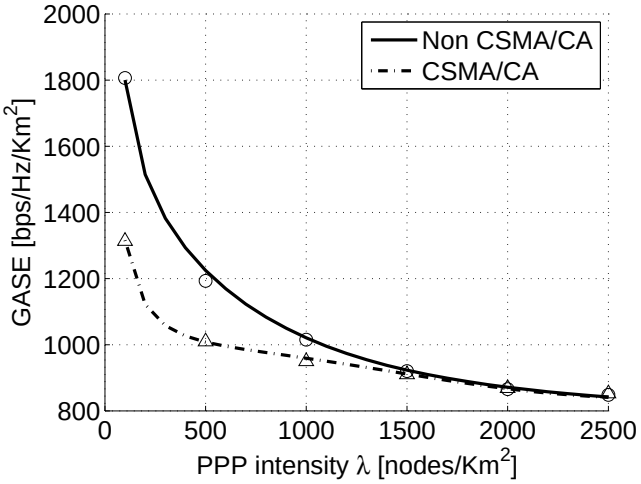

(c) GASE

Figure 5.1: Ergodic capacity, affected ratio and GASE as function of the node intensity λ.

We consider a wireless ad hoc network in continuous infinite area of $\Omega = 1000 \times 1000\ \mathrm{m}^2$, $a = 4$, $N = -40$ dBm, $R_{\mathrm{RTS}} = 40$ m. The transmission power $P_t = 10$ dBm, the interference threshold $I_{\mathrm{th}} = -20$ dBm. The average number of transmitters is given by $\lambda\Omega$. The receivers are assumed to be uniformly distributed in an annulus of radius $d_l = 1$m and $d_h = 20$m centered at the transmitter. The simulation results are shown as discrete dots, which match well with the analytical results. In Fig. 5.1, we plot the ergodic capacity, affected ratio as well as GASE of wireless ad hoc network as function of the Poisson point process intensity λ.

Fig. 5.1a shows that there exists a maximal value of ergodic capacity with respect to the intensity λ, which implies the ergodic capacity does not always increase with λ. As λ increases, the average number of transmitters increases correspondingly. The increasing number of transmitters has two effects on the network performance. For one thing, it increases network aggregate interference level. For another thing, more transmitter-receiver pair means more capacity is taken into account of the total ergodic capacity of wireless ad hoc network. In sparse network, i.e. λ is small, the benefit on capacity incurred by increasing λ is more significant than the negative effect incurred by the increasing interference level. Therefore, the ergodic capacity is an increasing function of λ in sparse network. On the contrary, in dense network, the interference effect dominates and thus the ergodic capacity decreases with respect to λ. Fig. 5.1a also shows that for small value of λ, the ergodic capacity in CSMA/CA network is smaller than that in non CSMA/CA network, which tells that prohibiting close transmitters from simultaneous transmitting decreases the overall system ergodic capacity. However, when λ goes large, without CSMA/CA mechanism, the ergodic capacity decreases dramatically after achieving a maximal value, while the network with CSMA/CA mechanism decreases slightly. This is due to in non CSMA/CA network, the transmitters in the network can be activated without restriction. In dense network, too many transmitters will greatly increase the interference level and thus decrease the total ergodic capacity of the network. However, CSMA/CA mechanism prevents excessive transmitters to be activated in dense network. Therefore, when the network distribution area is saturated, no more transmitters are allowed to transmit and thus the ergodic capacity only slightly decreases after achieving the maximal value. This phenomenon implies that CSMA/CA mechanism effectively ameliorates the increase of aggregate interference level in dense network. Note that in CSMA/CA network, we use Matèrn point process to model the distribution of active transmitters. As Matèrn point process is a thinning progress of the

Poisson point process, the active transmitters in CSMA/CA network is no greater than its underlying non CSMA/CA network. This means in dense wireless ad hoc network, CSMA/CA network requires fewer transmitters to achieve the same amount of ergodic capacity as in non CSMA/CA network.

Fig. 5.1b shows that the affected area is an increasing function of λ. Meanwhile, the affected area of CSMA/CA network increases slower than that of non CSMA/CA network. This is due to for the same value of λ, CSMA/CA network has fewer active transmitters than that of non CSMA/CA network. Finally, Fig. 5.1c shows that in sparse network, non CSMA/CA network enjoys better GASE performance than that of CSMA/CA network. However, as the number of simultaneous transmitters increases, the latter outperforms the former. Meanwhile, GASE of CSMA/CA and non CSMA/CA network are both monotonically decreasing function of λ. This is due to GASE not only considers the negative effect of co-channel interference incurred by simultaneous transmissions, but also takes into account the spatial effect of wireless transmission in terms of affected area.

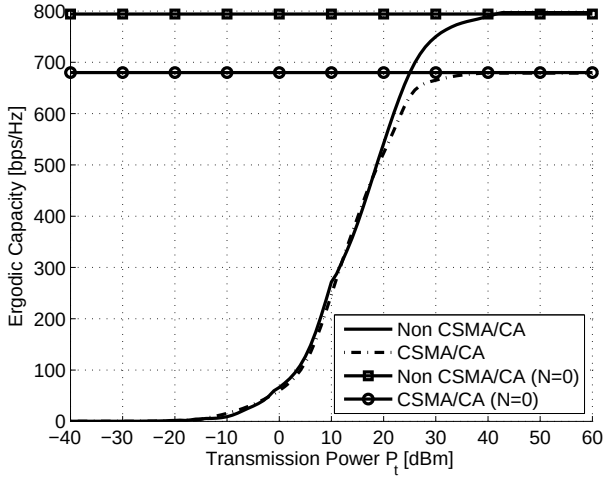

(a) Ergodic capacity

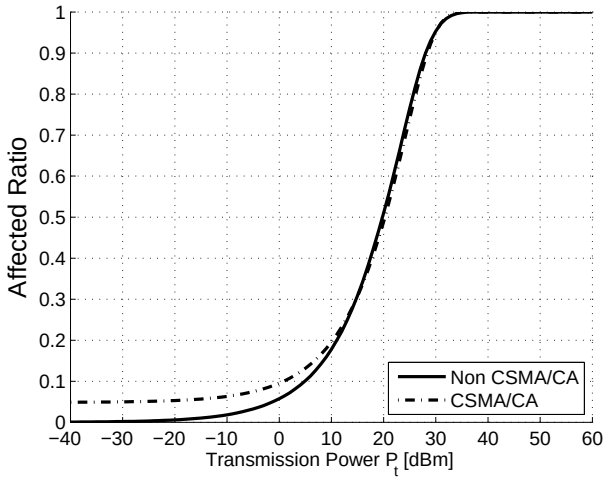

(b) Affected area

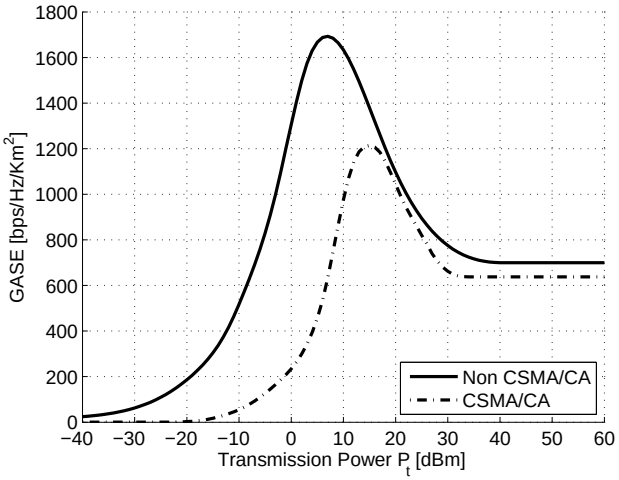

(c) GASE

Figure 5.2: Ergodic capacity, affected ratio and GASE as function of the transmission power P_t.

In Fig. 5.2, we analyze the effect of transmission power P_t on network performance. The node intensity $\lambda_p = 200$ nodes/Km^2. From (5.20), we can see that if $P_t \gg N$, i.e. the transmission power P_t is sufficiently larger than the noise power N, then $\mathfrak{F}_N = \lim_{N/P_t \to 0} \exp(-Nd^a\gamma/P_t) \to 1$. Under this circumstance, the network ergodic capacity is function of transmitter intensity λ and path loss exponent a, irrelevant to individual transmission power P_t, which means even we continue increase P_t, we cannot achieve higher network ergodic capacity. This observation can be justified by Fig. 5.2a. It shows that the ergodic capacity of wireless ad hoc network is an increasing function of P_t. However, when $P_t \gg N$, the ergodic capacity converges to a constant value, which equals to the value calculated from (5.20) with $\mathfrak{F}_N = 1$.

The affected area of CSMA/CA network is calculated by (5.22), as $\mathrm{A}_{\mathrm{aff}} = (1 - F_I(I_{\mathrm{th}}))\cdot \Omega$. For the special case $a = 4$, $F_I(I_{\mathrm{th}}) = \mathrm{erfc}\left(\frac{\lambda\pi^2}{4}\sqrt{\frac{P_t}{I_{\mathrm{th}}}}\right)$, which is function of transmitter intensity λ, transmission power P_t and aggregate interference threshold I_{th}. If $P_t \gg I_{\mathrm{th}}$, $F_I(I_{\mathrm{th}}) = 0$, then the affected area $\mathrm{A}_{\mathrm{aff}} = \Omega$, which means all $\mathbb{R}^2$ is affected. Fig. 5.2b justifies this observation. With Fig. 5.2a and Fig. 5.2b, we conclude that too large P_t saturates the network distribution area without help in increasing the system ergodic capacity. On the other hand, too small P_t leads to small ergodic capacity and insufficient utilization of the network spatial spectrum resource.

Fig. 5.2c shows an maximum GASE value with respect to transmission power P_t. By considering ergodic capacity and affected area together, GASE measures the relationships between P_t, N and I_{th} with one generic performance metric, and provides a new perspective on the transmission power optimization.

5.3 GASE Analysis for Two-Tier Cognitive Network

In the above sections, we investigated the GASE performance of wireless ad hoc networks with and without implementing CSMA/CA mechanism. From mathematical analysis and numerical examples, we found that as the number of transmitter increases, ergodic capacity does not necessarily increase correspondingly, but the affected area does. Besides, the overall GASE performance of wireless ad hoc network is a decreasing function of transmitter intensity λ. From this perspective, we cannot fully utilize the spatial spectrum resource and achieve high ergodic capacity at the same time. In this section, we utilize secondary cognitive network to exploit the

spatial spectrum potential of CSMA/CA network. We also examine the impact of secondary cognitive network on system overall GASE.

We consider a two-tier cognitive network distributed in continuous infinite space $\mathbb{R}^2$. In particular, the primary network is the CSMA/CA network described in section 5.2.3. The transmitter intensity of primary network is λ_p, and the transmission power is P_p. These primary transmitters define the primary affected area $\mathrm{A_p}$ given by (5.29). The MGF of aggregate interference generated by primary network is given by

$$\Phi_p(s) = \exp\left\{-\pi\lambda_p k(sP_p)^{\frac{2}{a}}\right\}. \tag{5.31}$$

The secondary network is distributed in $\mathbb{R}^2$ according to Poisson point process Π_{ps} with λ_{ps}, independent from the primary network. However, only those secondary transmitters located outside the primary affected area $\mathrm{A_p}$ can transmit with power P_s. The active secondary transmitters constitute a new Poisson point process with intensity $\lambda_s = (1 - \frac{\mathrm{A_p}}{\Omega})\lambda_{ps}$. The MGF of aggregate interference generated by active secondary transmitters is given by

$$\Phi_s(s) = \exp\left\{-\pi\lambda_s k(sP_s)^{\frac{2}{a}}\right\}. \tag{5.32}$$

The total interference of the two-tier cognitive network I_c is the summation of the interference generated by both primary and secondary network, i.e. $I_c = I_p + I_s$. As we assume that primary and secondary network are independently distributed, the MGF of the total interference of two-tier cognitive network is given by $\Phi_c(s) = \Phi_p(s)\cdot\Phi_s(s)$. With (5.31) and (5.32), we can arrive at

$$\Phi_c(s) = \exp\left\{-\pi k\left(\lambda_p P_p^{\frac{2}{a}} + \lambda_s P_s^{\frac{2}{a}}\right)s^{\frac{2}{a}}\right\}. \tag{5.33}$$

The total ergodic capacity of two-tier cognitive network is given by

$$C_{\mathrm{c}} = \kappa\int_{d_l}^{d_h}\int_0^{\infty}\left\{\lambda_p e^{-\frac{Nd^a}{P_p}\gamma}\cdot\Phi_c\left(\frac{d^a}{P_p}\gamma\right) + \lambda_s e^{-\frac{Nd^a}{P_s}\gamma}\cdot\Phi_c\left(\frac{d^a}{P_s}\gamma\right)\right\}\frac{d-d_l}{1+\gamma}\,\mathrm{d}\gamma\,\mathrm{d}d. \tag{5.34}$$

The affected area of two-tier cognitive network is given by

$$\mathrm{A_{cog}} = \bigcup_{X_i\in\Theta}\mathcal{B}_{X_i}\cdot F_{I_c}(I_{\mathrm{th}}) + \Big(1 - F_{I_c}(I_{\mathrm{th}})\Big)\Omega. \tag{5.35}$$

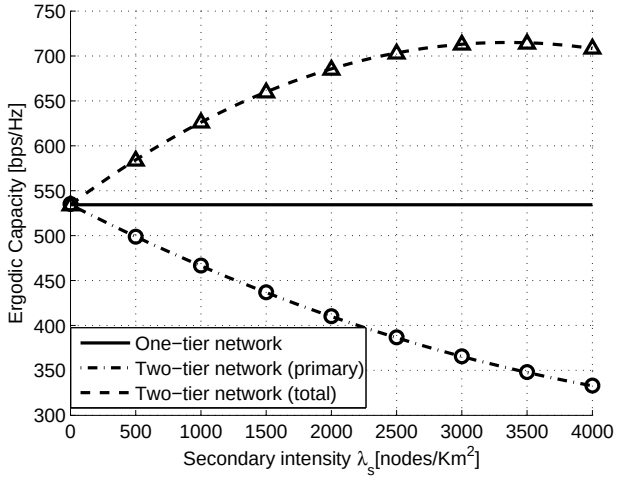

(a) Ergodic capacity

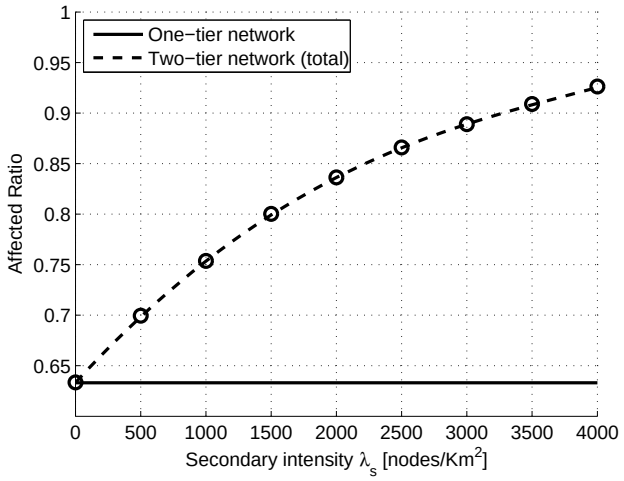

(b) Affected area

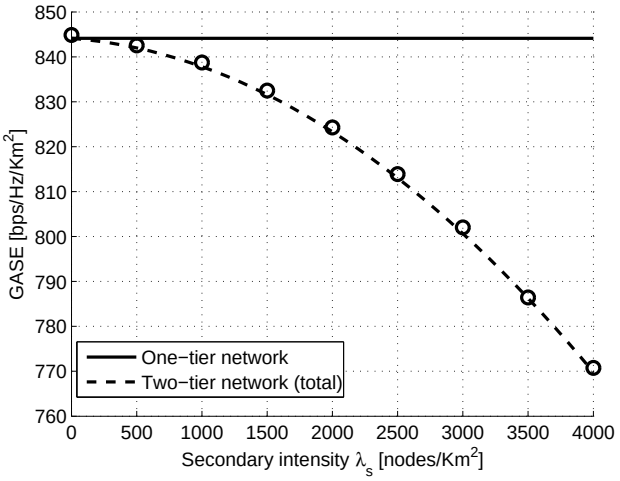

(c) GASE

Figure 5.3: Ergodic capacity, affected ratio and GASE as function of the secondary transmitter intensity λ_s.

In Fig. 5.3, we plot ergodic capacity, affected area and GASE of two-tier cognitive network as function of the secondary intensity λ_s. The primary transmitter intensity $\lambda_p = 1000$ nodes/Km^2 with transmission power $P_p = 10$ dBm. The secondary transmission power $P_s = 5$ dBm. For comparison, we also include these values of one-tier network that has the same system parameters as in primary network. Fig. 5.3a shows that secondary transmitters may degrade the ergodic capacity of existing primary network. The more secondary transmitters there are, the severe degradation there exists. On the other hand, secondary transmitters can improve the total ergodic capacity of two-tier cognitive network, but this improvement on ergodic capacity shrinks as the intensity of secondary transmitters increases. Excessive secondary transmitters even decrease ergodic capacity of two-tier network. This is due to secondary transmitters can elevate the interference level of two-tier cognitive network, and thus cause negative effect on the ergodic capacity of existing primary network and the two-tier network. Fig. 5.3b shows that secondary network increases the affected ratio of two-tier cognitive network. As the active secondary transmitters are located outside the primary affected area, this observation implies that cognitive secondary network can exploit the spatial spectrum resources in primary network. However, secondary transmitters have less effect on increasing total ergodic capacity than on increasing the affected area. As such, GASE is a decreasing function with respect to secondary transmitter intensity λ_s, as shown in Fig. 5.3c. Although cognitive secondary network deteriorates GASE performance of two-tier network, it may increase the total ergodic capacity as well as exploit the spatial spectrum resources of wireless network when the number of secondary transmitters is in a proper range.

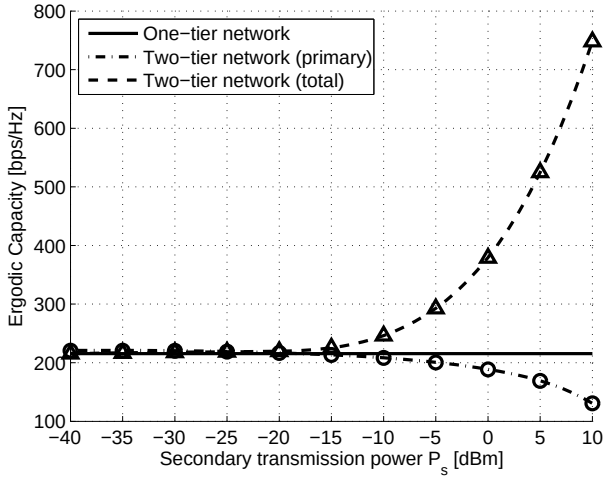

(a) Ergodic capacity

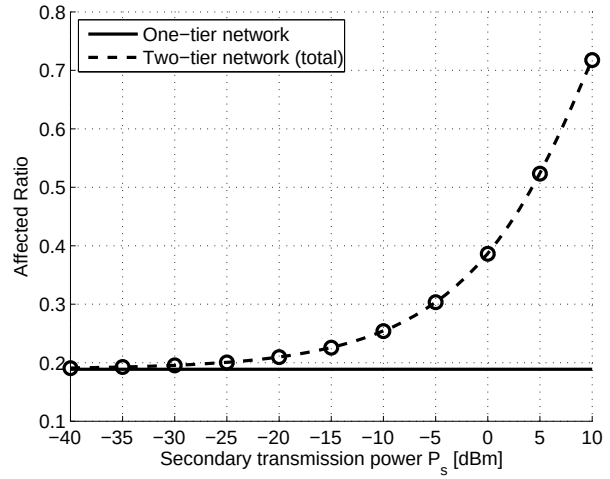

(b) Affected area

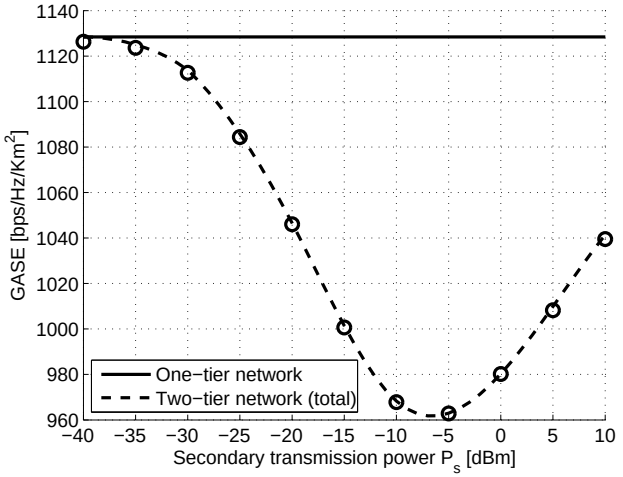

(c) GASE

Figure 5.4: Ergodic capacity, affected ratio and GASE as function of the secondary transmission power P_s.

In Fig. 5.4, we plot the ergodic capacity, affected ratio and GASE as function of the secondary transmission power P_s. For practical reason, we assume P_s is not larger than $P_p = 10$ dBm. The primary and secondary transmitter intensity are $\lambda_p = 200$ nodes/Km^2, $\lambda_s = 1000$ nodes/Km^2, respectively. In small P_s region, secondary network has negligible effect on ergodic capacity, as shown in Fig. 5.4a; but the affected area slightly increases with P_s, as shown in Fig. 5.4b. As such, GASE is a decreasing function in small P_s region. However, when P_s is the same order of magnitude as primary transmission power P_p, both ergodic capacity and affected area significantly increase. Moreover, GASE is an increasing function of P_s in this region, which implies ergodic capacity increases faster than affected area. Therefore, there exists a minimum GASE value with respect to P_s, as shown in Fig. 5.4c. In order to achieve higher ergodic capacity as well as more effectively utilize the spatial spectrum resource of wireless network, the secondary transmission power P_s should be larger than the value where GASE arrives at its minimum.

5.4 Conclusion

In this chapter, we analyzed the performance of wireless ad hoc network in Poisson field over Rayleigh fading channels. We derived the generic closed-form MGF expression of aggregate interference of such wireless network. We then applied the statistics into the calculation of ergodic capacity, affected area and GASE metrics. We also analyzed the effect of CSMA/CA mechanism on network performance. Through mathematical analysis and numerical examples, we found that in sparse scenario, non CSMA/CA network shows better performance than CSMA/CA network; however, in dense scenario, CSMA/CA network can ameliorate the increase of aggregate interference, and achieve same amount of ergodic capacity with fewer transmitters. Finally, we proposed a new cognitive scheme, which only allows the secondary transmitters located outside the primary affected area to transmit. Numerical examples show that the number of secondary transmitters and their transmission power are essential to the network performance in terms of ergodic capacity and affected area. Meanwhile, we found that GASE provides a new perspective on transmission power selection and secondary network optimization.

Chapter 6

Conclusion and Future Work

6.1 Conclusion

In this dissertation, we studied the spatial spectral utilization efficiency of wireless communication. We carried out the analysis in different wireless communication scenarios.

In Chapter 2, we applied the concept of ASE to studying the spatial spectral efficiency performance of single-cell wireless relay system. We derived the closed-form expression of ASE of the relay-enhanced single-cell system and the conventional system, which captures the small spacial footprint of relay transmission. In Chapter 3, we investigated the ASE performance of multi-cell wireless relay system. We analyzed the total interference from the dominant co-channel cells operating either in direct or relay mode over Rayleigh fading channels, based on which we obtained the statistics of the SINR of an arbitrary MS in the target cell. We then derived the exact analytical expressions of ergodic capacity and ASE of the relay enhanced cellular systems with and without in-cell frequency reuse.

In Chapter 4, we generalized the conventional ASE performance metric to study the performance of arbitrary wireless transmissions while considering the spatial effect of wireless transmissions. We carried out a comprehensive study on the resulting GASE performance metric by considering point-to-point transmission, dual-hop relay transmission, cooperative relay transmission, two-user X channels as well as cognitive radio transmission.

In Chapter 5, we analyzed the performance of wireless ad hoc network in Poisson field over Rayleigh fading channels. We derived the generic closed-form MGF

expression of aggregate interference of such wireless network. We then applied the statistics to the calculation of ergodic capacity, affected area and GASE metrics. We also analyzed the effect of CSMA/CA mechanism on network performance.

Through analytical research and numerical examples, we showed that

- Relay transmission is power efficient and can greatly improve the greenness of wireless transmissions. However, both the RSs position and BS-RS links should be properly selected in order to obtain better ASE performance than the conventional systems without relays.
- Both ASE and GASE provide a new perspective on the design, evaluation and optimization of arbitrary wireless transmissions, especially with respect to the transmission power selection.
- GASE performance metric can be used to exploit the space-spectrum resources of wireless networks, especially with the help of secondary cognitive radio transmission. However, the secondary transmitters and their transmission power are essential the network performance in terms of GASE.

6.2 Future Work

In our future work, we will analyze the spatial spectral efficiency performance of wireless networks using adaptive transmission techniques. Adaptive transmission enables robust and spectrally efficient transmission over time-varying channels. The basic premise is that the receivers estimate the channel and then feed this estimation back to the transmitters. The transmitters then can adapt their transmission scheme based on the channel characteristics. Adaptive transmission techniques can increase average throughput and transmission link reliability, or reduce required transmit power. Specifically, under favorable channel conditions, the transmitters can either send data at higher data rates or use lower power; on the other hand, as the channel degrades, the transmitters can either reduce the data rate or increasing transmission power to guarantee the average probability of bit error. There are many parameters that can be varied at the transmitter relative to the channel conditions, e.g. data rate, transmission power, coding schemes, error probability, and etc. In our research, we will focus on the transmission power adaptation. In particular, as the channel gain varies, the transmitters adapt their transmission power to adjust to this variation. As such,

the interference "pollution" they generate to surrounding environment is varying as well, leading to a time-varying "affected area" of wireless transmission. Therefore, there will be a tradeoff between transmission power, data rate and the affected area. We will use GASE performance metric to quantify this tradeoff in wireless networks using adaptive power transmission techniques.

Appendix A

List of Publications

A.1 Conference Paper

- Lei Zhang, Hong-Chuan Yang, and Mazen O. Hasna, "Area spectral efficiency of infrastructure-relay enhanced single-cell wireless systems," in *Proc. 2011 IEEE Pacific Rim Conf. on Commun., Computers and Signal Process.,* pp. 786-790, Aug. 2011.

- Lei Zhang, Hong-Chuan Yang, and Mazen O. Hasna, "Analysis of cell spectral efficiency of infrastructure relay-enhanced cellular system," in *Proc. 2011 Int. Conf. on Wireless Commun. and Signal Process.,* pp. 1-6, Nov. 2011.

- Lei Zhang, M. O. Hasna, and Hong-Chuan Yang, "Area spectral efficiency of cooperative network with opportunistic relaying," in *Proc. 2012 IEEE 75th Veh. Tech. Conf.* pp. 1-5, May 2012.

- Lei Zhang, Hong-Chuan Yang, and Mazen O. Hasna, "Area spectral efficiency of cooperative network with DF and AF relaying," in *Proc. 2012 Asia-Pacific Signal & Inf. Process. Association Annual Summit and Conf.,* pp. 1-6, Dec. 2012.

- Lei Zhang, Hong-Chuan Yang, and Mazen O. Hasna, "Generalized area spectral efficiency: An effective performance metric for green wireless communications," in *Proc. 2013 IEEE Int. Conf. on Commun.,* pp. 5376-5380, Jun. 2013.

- Lei Zhang, Hong-Chuan Yang, and Mazen O. Hasna, "On ergodic capacity of wireless transmission subject to Poisson distributed interferers over rayleigh

fading channels," in *Proc. 2013 IEEE 77th Veh. Tech. Conf.,* pp. 1-6, Jun. 2013.

- Lei Zhang, Hong-Chuan Yang, and Mazen O. Hasna, "Area spectral efficiency of underlay cognitive radio transmission over rayleigh fading channels," in *Proc. 2013 IEEE Wireless Commun. and Networking Conf.,* pp. 2988-2992, Apr. 2013.

A.2 Journal Paper

- Lei Zhang, Hong-Chuan Yang, and Mazen O. Hasna, "Generalized area spectral efficiency: an effective performance metric for green wireless communications," *IEEE Trans. Commun.,* vol. 62, no. 2, pp. 747-757, Feb. 2014.

A.3 Submitted Journal Paper

- Lei Zhang, Hong-Chuan Yang, and Mazen O. Hasna, "Coverage and spectral efficiency analysis for infrastructure relay enhanced cellular systems," submitted to *IEEE Trans. Wireless Commun.*.

- Lei Zhang, Hong-Chuan Yang, and Mazen O. Hasna, "Generalized area spectral efficiency of wireless networks in Poisson field over rayleigh fading channels," submitted to *Wireless Commun. and Mobile Computing.*

Bibliography

[1] D. Soldani and S. Dixit, "Wireless relays for broadband access," *IEEE Commun. Mag.*, vol. 46, pp. 58–66, Mar. 2008.

[2] R. Pabst, B. H. Walke, D. C. Schultz, P. Herhold, H. Yanikomeroglu, S. Mukherjee, H. Viswanathan, M. Lott, W. Zirwas, M. Dohler, H. Aghvami, D. D. Falconer, and G. P. Fettweis, "Relay-based deployment concepts for wireless and mobile broadband radio," *IEEE Commun. Mag.*, vol. 42, pp. 80–89, Sep. 2004.

[3] J. Sydir and R. Taori, "An evolved cellular system architecture incorporating relay stations," *IEEE Commun. Mag.*, vol. 47, pp. 115–121, Jun. 2009.

[4] V. Genc, S. Murphy, Y. Yu, and J. Murphy, "IEEE 802.16J relay-based wireless access networks: an overview," *IEEE Wireless Commun.*, vol. 15, pp. 56–63, Oct. 2008.

[5] D. R. Basgeet and Y. C. Chow, "Uplink performance analysis for a relay based cellular system," in *Proc. IEEE 63rd Veh. Techn. Conf.*, vol. 1, pp. 132–136, May 2006.

[6] E. Weiss, S. Max, O. Klein, G. Hiertz, and B. Walke, "Relay-based vs. conventional wireless networks: capacity and spectrum efficiency," in *Proc. IEEE 18th Int. Symp. on Personal, Indoor and Mobile Radio Commun.*, pp. 1–5, Sep. 2007.

[7] O. Oyman, "Opportunistic scheduling and spectrum reuse in relay-based cellular networks," *IEEE Trans. Wireless Commun.*, vol. 9, pp. 1074–1085, Mar. 2010.

[8] W. Nam, W. Chang, S. Y. Chung, and Y. Lee, "Transmit optimization for relay-based cellular OFDM systems," in *Proc. 2007 IEEE Int. Conf. on Commun.*, pp. 5714–5719, Jun. 2007.

[9] N. Devroye, M. Vu, and V. Tarokh, "Cognitive radio networks," *IEEE Signal Process. Mag.*, vol. 25, pp. 12–23, Nov. 2008.

[10] M. S. Alouini and A. J. Goldsmith, "Area spectral efficiency of cellular mobile radio systems," *IEEE Trans. on Veh. Techn.*, vol. 48, pp. 1047–1066, Jul. 1999.

[11] A. Goldsmith, *Wireless communications*. Cambridge University Press, 2005.

[12] Y. Zhuang and J. Pan, "Random distances associated with hexagons," tech. rep., 2011.

[13] Y. Kim, T. Kwon, and D. Hong, "Area spectral efficiency of shared spectrum hierarchical cell structure networks," *IEEE Trans. Veh. Techn.*, vol. 59, pp. 4145–4151, Oct. 2010.

[14] V. Chandrasekhar and J. Andrews, "Spectrum allocation in tiered cellular networks," *IEEE Trans. Commun.*, vol. 57, pp. 3059–3068, Oct. 2009.

[15] R. Bendlin, V. Chandrasekhar, R. Chen, A. Ekpenyong, and E. Onggosanusi, "From homogeneous to heterogeneous networks: A 3GPP Long Term Evolution rel. 8/9 case study," in *Proc. 2011 45th Annual Conf. on Inf. Sci. and Systems*, pp. 1–5, Mar. 2011.

[16] B. Niu, C. Wu, M. Kountouris, and Y. Li, "Distributed opportunistic medium access control in two-tier femtocell networks," in *Proc. 2012 IEEE Wireless Commun. and Networking Conf. Workshops*, pp. 93–97, Apr. 2012.

[17] K. Son, E. Oh, and B. Krishnamachari, "Energy-aware hierarchical cell configuration: From deployment to operation," in *Proc. 2011 IEEE Conf. on Computer Commun. Workshops*, pp. 289–294, Apr. 2011.

[18] L. Zhao, J. Cai, and H. Zhang, "Radio-efficient adaptive modulation and coding: green communication perspective," in *Proc. 2011 IEEE 73rd Veh. Techn. Conf.*, pp. 1–5, May 2011.

[19] M. W. Arshad, A. Vastberg, and T. Edler, "Energy efficiency improvement through pico base stations for a green field operator," in *Proc. 2012 IEEE Wireless Commun. and Networking Conf.*, pp. 2197–2202, Apr. 2012.

[20] M. Usman, A. Vastberg, and T. Edler, "Energy efficient high capacity HETNET by offloading high QoS users through femto," in *Proc. 2011 17th IEEE Int. Conf. on Networks*, pp. 19–24, Dec. 2011.

[21] S. Verdú, "Spectral efficiency in the wideband regime," *IEEE Trans. Inf. Theory*, vol. 48, pp. 1319–1343, Jun. 2002.

[22] J. Wu, N. B. Mehta, A. F. Molisch, and J. Zhang, "Unified spectral efficiency analysis of cellular systems with channel-aware schedulers," *IEEE Trans. Commun.*, vol. 59, pp. 3463–3474, Dec. 2011.

[23] T. Chen, H. Kim, and Y. Yang, "Energy efficiency metrics for green wireless communications," in *Proc. Int. Conf. on Wireless Commun. and Signal Process.*, pp. 1–6, Oct. 2010.

[24] F. Richter, A. J. Fehske, and G. P. Fettweis, "Energy efficiency aspects of base station deployment strategies for cellular networks," in *Proc. 2009 IEEE 70th Veh. Techn. Conf.*, pp. 1–5, Sept. 2009.

[25] C. Xiong, G. Li, S. Zhang, Y. Chen, and S. Xu, "Energy- and spectral-efficiency tradeoff in downlink ofdma networks," *IEEE Trans. Wireless Commun.*, vol. 10, pp. 3874–3886, Nov. 2011.

[26] Y. Chen, S. Zhang, S. Xu, and G. Y. Li, "Fundamental trade-offs on green wireless networks," *IEEE Commun. Mag.*, vol. 49, pp. 30–37, Jun. 2011.

[27] A. J. Fehske, P. Marsch, and G. P. Fettweis, "Bit per joule efficiency of cooperating base stations in cellular networks," in *Proc. 2010 IEEE GLOBECOM Workshops*, pp. 1406–1411, Dec. 2010.

[28] J. Lorincz, N. Dimitrov, and T. Matijevic, "Bit per joule and area energy-efficiency of heterogeneous macro base station sites," in *Proc. 2012 20th Int. Conf. on Software, Telecommun. and Computer Networks*, pp. 1–6, Sept. 2012.

[29] S. N. Chiu, D. Stoyan, W. S. Kendall, and J. Mecke, *Stochastic geometry and its applications*. John Wiley & Sons, 2013.

[30] J. F. C. Kingman, *Poisson processes*, vol. 3. Oxford University Press, 1992.

[31] E. Salbaroli and A. Zanella, "Interference analysis in a poisson field of nodes of finite area," *IEEE Trans. Veh. Techn.*, vol. 58, pp. 1776–1783, May 2009.

[32] E. Salbaroli and A. Zanella, "A connectivity model for the analysis of a wireless ad hoc network in a circular area," in *Proc. IEEE Int. Conf. on Commun.*, pp. 4937–4942, Jun. 2007.

[33] T. Q. S. Quek, D. Dardari, and M. Z. Win, "Energy efficiency of dense wireless sensor networks: to cooperate or not to cooperate," *IEEE J. Selected Areas in Commun.*, vol. 25, pp. 459–470, Feb. 2007.

[34] J. Venkataraman, M. Haenggi, and O. Collins, "Shot noise models for the dual problems of cooperative coverage and outage in random networks," in *Proc. Allerton Conf. on Comm., Control, and Computing*, 2006.

[35] J. Venkataraman, M. Haenggi, and O. Collins, "Shot noise models for outage and throughput analyses in wireless ad hoc networks," in *Proc. 2006 IEEE Military Commun. Conf.*, pp. 1–7, Oct. 2006.

[36] E. S. Sousa, "Performance of a spread spectrum packet radio network link in a poisson field of interferers," *IEEE Trans. on Inf. Theory*, vol. 38, pp. 1743–1754, Nov. 1992.

[37] S. Govindasamy, F. Antic, D. W. Bliss, and D. H. Staelin, "The performance of linear multiple-antenna receivers with interferers distributed on a plane," in *Proc. 2005 IEEE 6th Workshop on Signal Process. Advances in Wireless Commun.*, pp. 880–884, Jun. 2005.

[38] S. B. Lowen and M. C. Teich, "Power-law shot noise," *IEEE Trans. Inf. Theory,*, vol. 36, pp. 1302–1318, Nov. 1990.

[39] J. Wang, E. E. Kuruoglu, and T. Zhou, "Alpha-stable channel capacity," *IEEE Commun. Lett.*, vol. 15, pp. 1107–1109, Oct. 2011.

[40] X. Ge, K. Huang, C. X. Wang, X. Hong, and X. Yang, "Capacity analysis of a multi-cell multi-antenna cooperative cellular network with co-channel interference," *IEEE Trans. Wireless Commun.*, vol. 10, pp. 3298–3309, Oct. 2011.

[41] X. Yang and A. P. Petropulu, "Co-channel interference modeling and analysis in a poisson field of interferers in wireless communications," *IEEE Trans. on Signal Process.*, vol. 51, pp. 64–76, Jan. 2003.

[42] K. Gulati, B. L. Evans, J. G. Andrews, and K. R. Tinsley, "Statistics of co-channel interference in a field of poisson and poisson-poisson clustered interferers," *IEEE Trans. Signal Process.*, vol. 58, pp. 6207–6222, Dec. 2010.

[43] M. Z. Win, P. C. Pinto, and L. A. Shepp, "A mathematical theory of network interference and its applications," *Proc. of the IEEE*, vol. 97, pp. 205–230, Feb. 2009.

[44] A. Busson, G. Chelius, J. M. Gorce, *et al.*, "Interference modeling in csma multi-hop wireless networks," 2009.

[45] T. A. Weiss and F. K. Jondral, "Spectrum pooling: an innovative strategy for the enhancement of spectrum efficiency," *IEEE Commun. Mag.*, vol. 42, pp. 8–14, Mar. 2004.

[46] A. Goldsmith, S. A. Jafar, I. Maric, and S. Srinivasa, "Breaking spectrum gridlock with cognitive radios: an information theoretic perspective," *Proc. of the IEEE*, vol. 97, pp. 894–914, May 2009.

[47] N. Devroye, P. Mitran, and V. Tarokh, "Achievable rates in cognitive radio channels," *IEEE Trans. Inf. Theory*, vol. 52, pp. 1813–1827, May 2006.

[48] S. Haykin, "Cognitive radio: brain-empowered wireless communications," *IEEE J. Selected Areas in Commun.*, vol. 23, pp. 201–220, Feb. 2005.

[49] M. Gastpar, "On capacity under receive and spatial spectrum-sharing constraints," *IEEE Trans. Inf. Theory,*, vol. 53, pp. 471–487, Feb. 2007.

[50] E. C. Van Der Meulen, "Three-terminal communication channels," *Advances in Applied Prob.*, pp. 120–154, 1971.

[51] T. Cover and A. E. Gamal, "Capacity theorems for the relay channel," *IEEE Trans. on Inf. Theory*, vol. 25, pp. 572–584, Sep. 1979.

[52] R. U. Nabar, H. Bolcskei, and F. W. Kneubuhler, "Fading relay channels: performance limits and space-time signal design," *IEEE J. Selected Areas in Commun.*, vol. 22, pp. 1099–1109, Aug. 2004.

[53] J. N. Laneman, D. N. C. Tse, and G. W. Wornell, "Cooperative diversity in wireless networks: Efficient protocols and outage behavior," *IEEE Trans. Inf. Theory*, vol. 50, pp. 3062–3080, Dec. 2004.

[54] T. Huynh, N. T. Pham, W. J. Hwang, and F. Theoleyre, "Stochastic optimization for minimum outage in cooperative ad-hoc network," in *Proc. 2012 IEEE 26th Int. Conf. on Advanced Inf. Networking and Applications*, pp. 898–905, Mar. 2012.

[55] L. Song and D. Hatzinakos, "Cooperative transmission in poisson distributed wireless sensor networks: protocol and outage probability," *IEEE Trans. Wireless Commun.*, vol. 5, pp. 2834–2843, Oct. 2006.

[56] B. Li, W. Wang, Q. Yin, R. Yang, Y. Li, and C. Wang, "A new cooperative transmission metric in wireless sensor networks to minimize energy consumption per unit transmit distance," *IEEE Commun. Lett.*, vol. 16, pp. 626–629, May 2012.

[57] K. Adachi, S. Sun, and C. K. Ho, "Power minimization of cooperative relay transmission with relay's private information," *IEEE Trans. on Wireless Commun.*, vol. 11, pp. 2520–2530, Jul. 2012.

[58] D. R. Brown and F. Fazel, "A game theoretic study of energy efficient cooperative wireless networks," *J. Commun. and Networks*, vol. 13, pp. 266–276, Jun. 2011.

[59] Q. Gao, Y. Zuo, J. Zhang, and X. H. Peng, "Improving energy efficiency in a wireless sensor network by combining cooperative mimo with data aggregation," *IEEE Trans. Veh. Techn.*, vol. 59, pp. 3956–3965, Oct. 2010.

[60] S. A. Jafar and S. Shamai, "Degrees of freedom region of the MIMO X channel," *IEEE Trans. Inf. Theory*, vol. 54, pp. 151–170, Jan. 2008.

[61] M. A. Maddah-Ali, A. S. Motahari, and A. K. Khandani, "Communication over mimo x channels: interference alignment, decomposition, and performance analysis," *IEEE Trans. Inf. Theory*, vol. 54, pp. 3457–3470, Aug. 2008.

[62] F. Li and H. Jafarkhani, "Space-time processing for x channels using precoders," *IEEE Trans. Signal Process.*, vol. 60, pp. 1849–1861, Apr. 2012.

[63] A. Ghasemi and E. S. Sousa, "Fundamental limits of spectrum-sharing in fading environments," *IEEE Trans. Wireless Commun.*, vol. 6, pp. 649–658, Feb. 2007.

[64] L. Musavian and S. Aissa, "Capacity and power allocation for spectrum-sharing communications in fading channels," *IEEE Trans. Wireless Commun.*, vol. 8, pp. 148–156, Jan. 2009.

[65] R. Zhang, "On peak versus average interference power constraints for protecting primary users in cognitive radio networks," *IEEE Trans. Wireless Commun.*, vol. 8, pp. 2112–2120, Apr. 2009.

[66] C. X. Wang, X. Hong, H. H. Chen, and J. Thompson, "On capacity of cognitive radio networks with average interference power constraints," *IEEE Trans. Wireless Commun.*, vol. 8, pp. 1620–1625, Apr. 2009.

[67] I. S. Gradshteyn and I. M. Ryzhik, *Table of Integrals, Series, and Products 7th edition*. San Diego, CA: Academic Press, 2007.

[68] M. O. Hasna and M. S. Alouini, "Performance analysis of two-hop relayed transmissions over Rayleigh fading channels," in *Proc. 2002 IEEE 56th Veh. Techn. Conf.*, vol. 4, pp. 1992–1996, 2002.

[69] L. Zhang, H. C. Yang, and M. O. Hasna, "Generalized area spectral efficiency: an effective performance metric for green wireless communications," *IEEE Trans. Commun.*, vol. 62, pp. 747–757, Feb. 2014.